



Universidade do Minho

Escola de Ciências

Pedro José Pereira da Silva

Pathogenic potential characterization of two distinct *Pseudomonas aeruginosa* strains

Dissertação de Mestrado em Bioquímica Aplicada
Área de especialização em Biomedicina

Trabalho efetuado sob orientação de
Professora Doutora Andreia Gomes
Professor Doutor Pedro Santos
Professora Doutora Isabel Alcobia

Janeiro de 2016

Declaração

Nome

Pedro José Pereira da Silva

Endereço eletrónico: pedro01010000@gmail.com**Telefone:** 00351915201755**Número de identificação civil:** 13758599**Título da dissertação de mestrado:**

“Pathogenic potential characterization of two distinct *Pseudomonas aeruginosa* strains”

“Caracterização do potencial patogénico de duas estirpes distintas de *Pseudomonas aeruginosa*”

Orientadores:

Professora Doutora Andreia Gomes

Co-orientadores:

Professor Doutor Pedro Santos

Professora Doutora Isabel Alcobia

Ano de conclusão: 2016**Designação do Mestrado ou do Ramo de Conhecimento do Doutoramento:**

Ciências – Mestrado em Bioquímica Aplicada – Área de especialização em Biomedicina

1. É AUTORIZADA A REPRODUÇÃO INTEGRAL DESTA DISSERTAÇÃO APENAS PARA EFEITOS DE INVESTIGAÇÃO, MEDIANTE DECLARAÇÃO ESCRITA, QUE A TAL SE COMPROMETE.

Universidade do Minho, 29 de Janeiro de 2016

Assinatura: _____

To Hugo,
my friend and little brother.

Para sempre o rapaz que sempre sorriu.

Acknowledgments

First of all, I would like to sincerely and gratefully acknowledge my supervisors Professor Andreia Gomes and Professor Pedro Santos, for their closely guidance, orientation and patience through the development of this thesis work. Their mentorship was exceedingly significant to my person as a scientist, in providing me a well-rounded experience in scientific research and stimulated me to grow as a critic biochemist and independent thinker. A special and honest thanks to Professor Isabel Alcobia who also took part in the supervision of this thesis work.

Immensely, I want to acknowledge my parents. There is no one who deserves a greater “thank you” than they deserve. They always stood by my side, supporting my academic course, and even in spite of not being easy, they fought for me and they deprive from many comforts, sacrificing them just to fulfil their biggest dream: give their children the education and opportunities that they weren't allowed to achieve.

To my little sister, Rita, I want to thank for her support and for her thoughtfulness towards my thesis work period. I have much pride on her and I know she will be a great woman.

And to all my family who supported me during this period of my academic life.

To all people and co-works from the Biotechnology Molecular Lab and the Animal Biology Lab I want to thank. And among them all, a special and merited acknowledgement to Artur who motivated me and guided me through the experimental work.

To Liliana, a very special person in my life, who in spite of accompanied me only in the last part of this thesis work, always cheered me up and motivated me to pursuit the objective until the end and never give up, to that I most thankful.

To my great and good friends, Eduardo, Ivo, Júnio and Nelson, for their support and friendship that always make the most of everything. Also, I want to acknowledge my friend Eva, for her support and concern.

To all my colleagues from the Bachelor of Science in Biochemistry and Master of Science in Applied Biochemistry. Especially, to my dear friend Rubén that since the begging of my academic course he proved to be a respectable companion and a loyal friend.

I want to acknowledge, also, the Portuguese Red Cross and the Portuguese Youth Red Cross that has been part of my life, which contributed to the building my character and personality, and motivated me to succeed in my academic course.

Finally, I want to acknowledge someone that cannot share, anymore, from my joys and sorrows, from my achievements and failures. Someone simple in is way of being, but always with something to learn from him. He managed always to come out from the difficult times with a smile in his face. And he taught me so much, so much... For all of that, thank you Hugo, always.

Resumo

“Caracterização do potencial patogénico de duas estirpes distintas de *Pseudomonas aeruginosa*”

A *Pseudomonas aeruginosa* é um patógeno oportunista e ubíquo, exibindo altos níveis de resistência a antibióticos e proliferando em muitos ambientes, incluindo unidades de saúde. A alta infecciosidade deste patógeno em pacientes debilitados e imunocomprometidos, especialmente em pacientes com fibrose cística, está associada a altas taxas de morbidade e mortalidade. Não é de estranhar que esta bactéria se tenha tornado numa das principais preocupações em termos de infeções hospitalares, e por conseguinte, motivado vários trabalhos de caracterização deste patógeno.

Uma colaboração entre o Centro de Biologia Molecular e Ambiental da Universidade do Minho e o Hospital de Braga permitiu o acesso a dois diferentes isolados clínicos do muco pulmonar dos pacientes infetados com *Pseudomonas aeruginosa*, designados como HB13 e HB15. A estirpe HB13 não produz pigmentos e evidenciou resistência a uma ampla gama de antibióticos. Por outro lado, a estirpe HB15 produz uma quantidade significativa de piocianina e é suscetível a antibióticos. A estirpe PAO1 da *Pseudomonas aeruginosa* foi utilizada neste trabalho de tese como estirpe de referência. Estas estirpes foram selecionadas para avaliar os seus níveis de citotoxicidade nas linhas celulares L929 e A549, por incubação com os fatores de virulência segregados. As alterações morfológicas e stress oxidativo induzido nestas linhas celulares foram também consideradas neste trabalho de tese.

Os resultados do estudo de citotoxicidade mostraram que as estirpes de *Pseudomonas aeruginosa* quando proliferando fora de um contexto de infeção, continuam capazes de produzir um conjunto de fatores de virulência segregados que induziram altos níveis de inviabilidade celular nas células L929 e A549. De acordo com a literatura, estabeleceu-se que a estirpe HB15 é mais patogénica do que a estirpe HB13, demonstrando um padrão de patogenidade semelhante ao da estirpe PAO1. A análise da morfologia das células L929 e A549, incubadas com os fatores de virulência das estirpes, por microscopia de contraste de fase e microscopia de fluorescência, revelou várias alterações na morfologia celular, tais como aglutinação celular, alteração da morfologia celular, formação de corpos apoptóticos, desorganização do citoesqueleto e fragmentação nuclear. Os resultados do estudo de stress oxidativo mostraram que, nas fases iniciais de incubação com os fatores de virulência das estirpes, as linhas celulares aumentaram a produção de espécies reativas de oxigénio, conduzindo a uma intensificação do stress oxidativo, apontado como uma das causas da citotoxicidade das estirpes testadas da *Pseudomonas aeruginosa*.

Este trabalho de tese abriu caminho para uma melhor compreensão do potencial patogénico destas estirpes e trabalhos futuros devem ser direcionados a fim de conseguir-se uma avaliação mais completa dos mecanismos e processos celulares subjacentes à patogenidade destas estirpes.

Abstract

“Pathogenic potential characterization of two distinct *Pseudomonas aeruginosa* strains”

Pseudomonas aeruginosa is an opportunist and ubiquitous pathogen, displaying high levels of antibiotic resistance and proliferating in many environments, including healthcare facilities. The high infectivity of this pathogen in impaired and immunocompromised patients, especially cystic fibrosis patients, leads to high rates of morbidity and mortality. It is no surprise that this bacterium became one of the main concerns regarding nosocomial infections, and so forth driven the attention of many researchers to study and characterize this pathogen.

A collaboration between the Molecular and Environment Biology Centre of the University of Minho and the Hospital of Braga, provided two different clinical isolates from the sputum of the patients infected with *Pseudomonas aeruginosa*, classified as HB13 and HB15. The strain HB13 does not produce pigments and evidenced resistance to a wide range of antibiotics. On the other hand, the strain HB15 produces a significant quantity of pyocyanin pigments and is susceptible to antibiotics. The *Pseudomonas aeruginosa* strain PAO1 was used in this thesis work as a reference strain. These strains were selected to assess their levels of cytotoxicity, in the L929 and A549 cell lines by incubation with the strains' secreted virulence factors. Morphological changes and oxidative stress induced in these cell lines were also considered in this thesis work.

The cytotoxicity study outcomes showed that the *Pseudomonas aeruginosa* strains when growing out of an infection context, were still able to produce a set of secreted virulence factors that induced high levels of cellular death on L929 and A549 cells. Previous literature established that the HB15 strain is more pathogenic than the HB13 strain, demonstrating a pathogenic pattern close to the PAO1 strain. The analysis of the morphology of the L929 and A549 cells, incubated with the strains' virulence factors, by contrast phase microscopy and fluorescence microscopy, unveiled several cellular morphology alterations, such as cell agglutination, loss of cellular shape, cellular blebbing, evidences of apoptotic bodies, cytoskeleton disorganization and nuclear fragmentation. The results of the oxidative stress study showed that in the early stages of incubation with the strains' virulence factors, the cell lines increased the production of reactive oxygen species, leading to an intensification of oxidative stress, pointed out as one of the causes of the *Pseudomonas aeruginosa* strains cytotoxicity.

This thesis work paved the way for perceiving and understanding the pathogenic potential of these strains, and future work should be directed in order to achieve a more complete assessment of the mechanisms and cellular processes underlying the pathogenicity of these strains.

Table of contents

| | |
|--|------|
| Declaração | ii |
| Acknowledgments..... | v |
| Resumo | vii |
| Abstract | ix |
| Table of contents..... | xi |
| Glossary of abbreviations | xv |
| List of Figures..... | xvii |
| List of Tables..... | xxv |
| 1. Introduction | 1 |
| 1.1. Bacterial Pathogenesis: an actual and worldwide serious concern | 3 |
| 1.2. <i>Pseudomonas aeruginosa</i> , the bacterium and the pathogen..... | 7 |
| 1.2.1. Pathogenicity..... | 8 |
| 1.2.1.1. Virulence factors | 9 |
| 1.2.1.1.1. Cell-associated virulence factors | 9 |
| 1.2.1.1.2. Secreted virulence factors | 11 |
| 1.2.1.2. Biofilms | 14 |
| 1.2.1.3. Quorum sensing | 16 |
| 1.2.1.4. Antibiotic resistance | 16 |
| 1.3. Bacterial Strains..... | 21 |
| 1.3.1. <i>Pseudomonas aeruginosa</i> strains..... | 21 |
| 1.3.1.1. Clinical isolates HB13 and HB15 | 25 |
| 1.4. Bacterial infection mechanisms and host models..... | 27 |
| 1.4.1. Infection host models | 30 |
| 1.4.1.1 Cell lines host models..... | 34 |
| 1.4.1.1.1 L929 and A549 cell lines | 35 |
| 1.5. Objectives | 38 |
| 2. Material and Methods | 39 |
| 2.1. Biological Material..... | 41 |
| 2.1.1. Bacterial species and strains..... | 41 |
| 2.1.2. Bacterial culture media..... | 41 |
| 2.1.3. Animal cell lines maintenance..... | 41 |
| 2.1.4. Animal cell culture media..... | 42 |

| | | |
|----------|---|----|
| 2.2. | <i>Pseudomonas aeruginosa</i> virulence factors..... | 43 |
| 2.2.1. | Growth conditions of <i>Pseudomonas aeruginosa</i> strains..... | 43 |
| 2.2.2. | Bacterial culture supernatants extraction..... | 43 |
| 2.2.3. | Total protein quantification..... | 43 |
| 2.3. | Virulence studies..... | 44 |
| 2.3.1. | <i>Pseudomonas aeruginosa</i> virulent factors testing concentrations..... | 44 |
| 2.3.2. | pH tests..... | 44 |
| 2.3.3. | Cell lines growth conditions..... | 44 |
| 2.3.4. | Cytotoxicity tests..... | 44 |
| 2.3.4.1. | Incubations with virulent factors..... | 45 |
| 2.3.4.2. | MTT assay..... | 45 |
| 2.3.5. | Cellular morphology observations..... | 46 |
| 2.3.5.1. | Sample preparation for fluorescence microscopy..... | 46 |
| 2.3.5.2. | Incubation with virulent factors..... | 46 |
| 2.3.5.3. | Cytoskeleton and nucleus staining..... | 46 |
| 2.3.6. | Oxidative stress tests..... | 47 |
| 2.3.6.1. | Sample preparation..... | 47 |
| 2.3.6.2. | Incubation with virulent factors..... | 47 |
| 2.3.6.3. | DCF assay..... | 47 |
| 2.4. | Statistical Analysis..... | 48 |
| 3. | Results and Discussion..... | 49 |
| 3.1. | Bacterial culture growth..... | 51 |
| 3.2. | Virulence factors extraction..... | 51 |
| 3.3. | Protein quantification of the supernatants..... | 52 |
| 3.4. | pH measurements of the supernatants concentrations of the <i>Pseudomonas aeruginosa</i> strains.... | 53 |
| 3.5. | Cytotoxicity tests..... | 54 |
| 3.5.1. | Cytotoxicity of culture supernatants of the <i>Pseudomonas aeruginosa</i> strains in the L929 and A549 cell lines..... | 54 |
| 3.5.2. | Comparison of cytotoxicity in L929 and A549 cell lines exposed to culture supernatants from the <i>P. aeruginosa</i> strains..... | 61 |
| 3.6. | Morphology alteration studies..... | 63 |
| 3.6.1. | Cellular morphological changes in L929 cell line..... | 63 |
| 3.6.2. | Cellular morphological changes in A549 cell line..... | 69 |
| 3.7. | Final considerations and future perspectives..... | 74 |
| 4. | References..... | 79 |
| 5. | Appendix..... | 97 |

| | |
|---|-----|
| 5.1. Appendix 1 – pH measurements of the supernatant concentrations of the <i>Pseudomonas aeruginosa</i> strains | 99 |
| 5.2. Annex 2 – Cytotoxicity of <i>Pseudomonas aeruginosa</i> strains in L929 cell availed in all concentrations tested..... | 100 |
| 5.3. Annex 3 – Cytotoxicity of <i>Pseudomonas aeruginosa</i> strains in A549 cell availed in all concentrations tested..... | 103 |
| 5.4. Annex 4 - L929 and A549 cell line culture growth through time | 106 |
| 5.5. Annex 5 - Oxidative stress induced by <i>Pseudomonas aeruginosa</i> strains culture supernatants | 107 |

Glossary of abbreviations

| | |
|----------------|---|
| AHL | N-acyl homoserine lactone |
| AprA | Alkaline protease |
| AQ | 2-alkyl-4-quinolone |
| ATCC | American Type Culture Collection |
| cAMP | Cyclic adenosine monophosphate |
| CDC | Centers for Disease Control and Prevention |
| CF | Cystic fibrosis |
| CFU | Colony forming-unit |
| DCF | Dichlorofluorescein |
| DCFH-DA | 2',7' -dichlorofluorescein diacetate |
| DMEM | Dulbecco's Modified Eagle Medium |
| DMSO | Dimethyl sulfoxide |
| DNA | Deoxyribonucleic acid |
| ECDC | European Centre for Disease Prevention and Control |
| EDTA | Ethylenediaminetetraacetic acid |
| EF2 | Elongation factor 2 |
| ESBL | Extended spectrum beta-lactamase |
| ETA | Exotoxin A |
| ExoS | Exoenzyme S |
| ExoT | Exoenzyme T |
| ExoU | Exoenzyme U |
| ExoY | Exoenzyme Y |
| FBS | Fetal bovine serum |
| FliD | Flagellar cap protein |
| CG | Guanine-Cytosine |
| GI | Genomic island |
| HAI | Healthcare acquired infections |
| HB13 | Hospital Braga 13 |
| HB15 | Hospital Braga 15 |
| HEPES | 2-[4-(2-hydroxyethyl)piperazin-1-yl]ethanesulfonic acid |
| HHQ | 2-heptyl-4-quinolone |
| IC50 | Half maximal inhibitory concentration |
| IgG | Immunoglobulin G |
| LasA | <i>Pseudomonas aeruginosa</i> staphylolysin |
| LasB | Elastase B |
| LB | Lysogeny broth |
| LESB58 | Liverpool Epidemic Strain B58 |
| LPS | Lipopolysaccharide |
| MBL | Metallo-beta-lactamase |
| MDR | Multidrug-resistance |
| MRBA | Multidrug-resistant <i>Acinetobacter baumannii</i> |

| | |
|----------------|---|
| MRSA | Methicillin-resistant <i>Staphylococcus aureus</i> |
| MTT | (3-(4,5-dimethylthiazol-2-yl)-2,5-diphenyltetrazolium bromide |
| NAD(P)H | Nicotinamide adenine dinucleotide phosphate-oxidase |
| NK | Natural Killer |
| OD | Optical density |
| ORF | Open reading frame |
| PA | <i>Pseudomonas aeruginosa</i> |
| PA7 | <i>Pseudomonas aeruginosa</i> 7 |
| PA14 | <i>Pseudomonas aeruginosa</i> 14 |
| PAI-1 | <i>Pseudomonas aeruginosa</i> autoinducer 1 |
| PAI-2 | <i>Pseudomonas aeruginosa</i> autoinducer 2 |
| PA01 | <i>Pseudomonas aeruginosa</i> strain O1 |
| PAPI-1 | <i>Pseudomonas aeruginosa</i> pathogenic islands 1 |
| PAPI-2 | <i>Pseudomonas aeruginosa</i> pathogenic islands 2 |
| PBS | Phosphate-buffered saline |
| PQS | <i>Pseudomonas</i> quinolone signal |
| QS | Quorum sensing |
| Rhl | Rhamnolipid |
| RND | Resistance-nodulation-division |
| Tfp | Type IV pili |
| TLR5 | Toll-like receptor 5 |
| TTSS | Type III secretion system |
| VISA | Vancomycin-intermediate <i>Staphylococcus aureus</i> |
| VRE | Vancomycin-resistant <i>Enterococci</i> |
| WHO | World Health Organization |

List of Figures

- Figure 1 - Top leading causes of death in the world 2012.** In the bar graphic, it is represent the main leading causes of death worldwide, in the year 2012. The first cause is ischaemic heart disease (7.4 million deaths), second it is stroke also known as cerebrovascular accident (6.7 million deaths), third it is chronic obstructive pulmonary disease (3.1 million deaths), fourth it is lower respiratory infectious (3.1 million deaths), fifth it is trachea, bronchus, lungs cancer (1.6 million deaths), sixth it is HIV/AIDS (1.5 million deaths), seventh it is diarrhoeal diseases (1.5 million deaths), eighth it is diabetes mellitus (1.5 million deaths), ninth it is road injury (1.3 million deaths) and tenth it is hypertensive heart disease (1.1 million deaths). Adapted from World Health Organization, Fact Sheet n° 310 (2014) [2]. 3
- Figure 2 - Percentage (%) of MDR *Pseudomonas aeruginosa* isolates by country in Europe, in 2012.** Adapted from ECDC surveillance report (2013) [12]. 5
- Figure 3 – Scanning electron microscopy images of *Pseudomonas aeruginosa* bacteria.** Image of adherent isolate of *Pseudomonas aeruginosa* forming clumps of cells. White bar indicates the image scale (1 µm). Adapted from Deligianni (2010) [20]. 7
- Figure 4 - Model of *Pseudomonas aeruginosa* pathogenicity in an immunocompromised host's infection.** The figure represents the pathogenic features of *P. aeruginosa* following a context of infection in a cystic fibrosis patient airways. Pathogenic features such as arranged colonization, cell-associated virulence factors, secreted virulence factors, production of biofilms and antibiotic resistance are illustrated in the figure enhancing the infection development in the debilitated host. Adapted from Cohen (2012) [27]. 9
- Figure 5 - Type IV pilli.** Illustrate representation of the type IV pilus mechanism. In the inner membrane the pilin monomer is embedded with its hydrophilic head placed in the periplasm. The pillin signal sequence is cleaved by a pre-pilin peptidase (PilD). The pilus is extended aided by supplementary assembly proteins. After extension is done, the retraction starts by action of PilT. Adapted from Kaiser (2000) [32]. 10
- Figure 6 - Schematic representation of *Pseudomonas aeruginosa* flagellum.** Structure of the *P. aeruginosa* flagellum embedded in the cell wall and membrane and its components. Adapted from EMBL-EBI BioModels Database (2012) [35]. 11
- Figure 7 - Model of type III secretion system (TTSS) function.** The figure represents the TTSS divided into 5 components: the regulatory proteins, the effector proteins, the chaperones, the needle complex and the translocation apparatus. The aseemble of this 5 components makes the TTSS function and allows the injection of effector proteins into the host cells. Adapted from Hauser (2009) [42]. 13
- Figure 8 - *Pseudomonas aeruginosa* culture in agar plate displaying pyocyanin production.** Adapted from Mavrodi (2001) [46]. 14
- Figure 9 - Biofilm development.** The figure represent the 5 stages of the biofilm development. (1) First stage of biofilm development, the initial attachment. (2) Second stage of biofilm development, the irreversible attachment. (3) Third stage of biofilm development, the initial phase of maturation. (4) Fourth stage of biofilm development, the definitive phase of maturation. (5) Fifth stage of biofilm development, the dispersion. Adapted from Monroe (2007) [51]. 15
- Figure 10 - Bacterial population variations induced by antibiotic action.** Bacteria with acquired antibiotic resistance (red coloured) compete with the susceptible counterparts in their population niche. (1) When in absence of antibiotic administration, the resistant bacteria will not predominate unless they have a higher inherent biological fitness. Plus, the acquirement of resistance to antibiotics generally represents a loss of biological fitness. (2) When there's an administration of antibiotic the susceptible bacteria growth is inhibited which turns in an ecological opportunity for the resistant bacteria to thrive. (3) Under this conditions the resistant bacteria will proliferate and dominate the bacterial population. After the population is absent from the antibiotic action the bacterial population may return to its original scenario and the dominance of the resistant bacteria

disappear. (4) Alternatively the resistant bacteria may acquire compensatory mutations which will maintain a noticeable occurrence of the resistant bacteria among the bacterial population. Adapted from Martínez (2007) [61]..... 17

Figure 11 - Genome representation of PAO1. The outer circle is a base pair scale (each tick equivalent to 100,000 bp) that represents the chromosomal location. The colour distribution of the central circle represents genes according to its functional category. The arrow in the representation stands for the direction of transcription (the inner band represents the minus strand, the outer band represents the plus strand). Green arrow represents the inverted region resulting from homologous recombination event between *rrnA* and *rrnB*. Red arrows represent transcription direction and locations of rRNA genes. Blue arrows represents locations containing probable bacteriophages. The inner black band represents the G+C percentage schemed as the average for non-overlapping 1000 bp windows spanning one strand for the entire *P. aeruginosa* genome. Yellow bars represents genome regions of ≥ 3000 bp with G+C content of two standard deviations ($<58.8\%$) below the mean (66.6%). Adapted from Stover (2000) [19]..... 22

Figure 12 - *Pseudomonas aeruginosa* strains phylogenetic tree. The tree presented is an unrooted maximum likelihood tree representing 389 genomes of *P. aeruginosa* strains, based on SNPs within the core genome, using Harvest method (100 bootstraps). The tree is divided into three major groups of strains (group 1: blue, group 2: orange/pink, group 3: green). The strains distributed for each group are presented in circles. Black circles represent the strains already sequenced before the *Freschi et al.* study [76]; White circles represent one or more strains sequenced during *Freschi et al.* study [76]. The group 3 true appearance was contracted for visual proposes, the miniature of the tree true appearance is displayed in a framed miniature. Adapted from *Freschi et al.*, 2015 [76]..... 24

Figure 13 – Summary of the bacterial mechanisms for pathogenicity. (A) Bacterial pathogens finding a human host may induce a set of host responses and counter with several host defence evading mechanisms. The components from the pathogen that interact with the host include: (I) the capsule, which “frustrate” the phagocytic function and protect the pathogen from neutrophil and macrophage engulfment; (II) lipopolysaccharides (LPS) and cell wall components which may lead to septic shock; (III) toxins responsible for host cell damage and aiding in invasion; and (IV) adhesins that eases the binding of the pathogen with the host surface. In what level these mechanisms intervene in the pathogenesis of the infection is dependent of some factors such as bacterial species and strains, immune status of the host and pathogen entry site. (B) When the bacterial pathogen adheres to the host surface it can break into cell tissue by expressing and secreting proteases and glycanases that destroy the extracellular matrix. Furthermore, the pathogen invading cell tissue is also able to access intracellular domain. This process can be aided by action of natural phagocytosis mechanisms of macrophages and neutrophils or by action of an induced uptake where pathogen induce the host cell to engulf the adhered bacteria. One of the most common methods of the pathogens to induce uptakes is the type III secretion system which injects bacterial signalling proteins into the host cells. When inside the host cell, the pathogen can reside in the cell host cytosol or as a phagosome or even as a phagolysome (a lysosome fused with hagosome). Adapted from Wilson *et al.*, 2002 [1]. 28

Figure 14 – L929 cells. Contrast phase microscope shot of L929 cell culture grown in 96 well plate at 24h endpoint. The image show abundant distinguishable fibroblasts with spindle and stellate shape. The scale bar is set for 200 μm 36

Figure 15 - A549 cells. Contrast phase microscope shot of A549 cell culture grown in 96 well plate at 24h endpoint. The image show abundant distinguishable fibroblasts with spindle and stellate shape. The scale bar is set for 200 μm 37

Figure 16 – Comparison between cellular viabilities from two time points of bacterial growth of *Pseudomonas aeruginosa* culture supernatant in L929 cells. The graphic displays the comparison of the cellular viabilities results in L929 cells from the MTT assay for each *Pseudomonas aeruginosa* strains (PAO1,

HB15 and HB13) culture supernatants at the concentration 3.42 µg/ml, in all the 3 end times of incubation (24h, 48h, 72), between the bacterial growth periods t₁ (24 hours of bacterial growth) and t₂ (48 hours of bacterial growth). The resulting data was statistically analysed by a One-way ANOVA with Tukey test where the P value was set for: P <0.05. Significant values comparing cellular viabilities between t₁ and t₂ were represented in the graphic as, * for P <0.05, ** for P <0.01 and *** for P <0.001..... 55

Figure 17 - Cytotoxicity of the *Pseudomonas aeruginosa* strains culture supernatants on L929 cells. The graphic displays the results of the MTT assay performed on L929 cells submitted to two total protein concentrations (3.42 µg/ml and 20.50 µg/ml) of the culture supernatants of the *Pseudomonas aeruginosa* strains (PAO1, HB15 and HB13) in cell viability percentage represented by bars with the respective standard deviation represented by vertical lines for a number of replicas n=2. The bar legend represents the end times of incubation (24h, 48h and 72h) with the supernatants. The full data is available in the appendix section of the thesis. The controls are presented in the graphic represented as "CONTROL". The negative control has the constant value of 100% of viability for each end times of incubation and not shown in the graphic. The positive control is represented as "+" on the graphic. The controls of the bacterial culture media (LB) are represented on the graphic as "LB 25%" and "LB 7.5%". The resulting data was statistically analysed by a One-way ANOVA with Tukey test where P value was set for: P <0.05. Significant values comparing to the negative control were represented in the graphic as, * for P <0.05, ** for P <0.01 and *** for P <0.001..... 57

Figure 18 – Comparison between cellular viabilities from two periods of bacterial growth of *Pseudomonas aeruginosa* culture supernatant in A549 cells. The graphic displays the comparison of the cellular viabilities results in A549 cells from the MTT assay for each *Pseudomonas aeruginosa* strains (PAO1, HB15 and HB13) culture supernatants at the concentration 3.42 µg/ml, in all the 3 end times of incubation (24h, 48h, 72), between the bacterial growth periods t₁ (24 hours of bacterial growth) and t₂ (48 hours of bacterial growth). The resulting data was statistically analysed by a One-way ANOVA with Tukey test where P value was set for: P <0.05. Significant values comparing cellular viabilities between t₁ and t₂ were represented in the graphic as, * for P <0.05, ** for P <0.01 and *** for P <0.001..... 59

Figure 19 - Cytotoxicity of the *Pseudomonas aeruginosa* strains culture supernatants on A549 cells. The graphic displays the results of the MTT assay performed on A549 cells submitted to two total protein concentrations (3.42 µg/ml and 20.50 µg/ml) of the culture supernatants of the *Pseudomonas aeruginosa* strains (PAO1, HB15 and HB13) in cell viability percentage represented by bars with the respective standard deviation represented by vertical lines for a number of replicas n=2. The bar legend represents the end times of incubation (24h, 48h and 72h) with the supernatants. The full data is available in the appendix section of the thesis. The controls are presented in the graphic represented as "CONTROL". The negative control has the constant value of 100% of viability for each end times of incubation and not shown in the graphic. The positive control is represented as "+" on the graphic. The controls of the bacterial culture media (LB) are represented on the graphic as "LB 25%" and "LB 7.5%". The resulting data was statistically analysed by a One-way ANOVA with Tukey test where P value was set for: P <0.05. Significant values comparing to the negative control were represented in the graphic as, * for P <0.05, ** for P <0.01 and *** for P <0.001..... 60

Figure 20 – Cellular viability comparison of the L929 and A549 cell lines incubated with the supernatants from the *Pseudomonas aeruginosa* strains. The graphic displays the comparison of the cellular viabilities results of the MTT assays performed between the two cell lines L929 and A549 incubated with two concentrations (3.42 µg/ml and 20.50 µg/ml) of culture supernatants of the *Pseudomonas aeruginosa* strains where the viability variance between cell lines were highest. The cellular viabilities are represented for all end time points of incubation with the supernatants. The full data is available in the appendix of the thesis. The graphic bars represents the cellular viability percentage and the respective vertical lines represents the standard deviation, for a number of replicas n=2. The resulting data was statistically analysed by a One-way ANOVA with

Tukey test where p value was set for: $P < 0.05$. Significant values comparing cellular viabilities of L929 cells and A549 cells were represented in the graphic as, * for $P < 0.05$, ** for $P < 0.01$ and *** for $P < 0.001$ 61

Figure 21 - Morphologic alterations in L929 cells induced by *Pseudomonas aeruginosa* strains culture supernatants. The figure shows the L929 cells morphology alterations induced by *Pseudomonas aeruginosa* strains culture supernatants, cultured in 96 well plate, using phase contrast microscopy. The figure is divided in two sections, referring to morphologic alterations at 3.42 $\mu\text{g}/\text{ml}$ and 20.50 $\mu\text{g}/\text{ml}$. The images of the cells are displayed by incubation times (24, 48 and 72 hours) horizontally and by *P. aeruginosa* strain (PA01, HB15 and HB13) vertically. The scale bars represents 100 μm length. Cytotoxicity data from previous results are shown to make relation between cellular viability and cellular morphology observations. Data represents the means \pm SD, n=2 independent experiments. * for $P < 0.05$, ** for $P < 0.01$ and *** for $P < 0.001$ 65

Figure 22 - Fluorescence microscopy of L929 cells to study morphological features induced by *Pseudomonas aeruginosa* strains. The cytoskeleton of the L929 cells are stained with the probe Phalloidin Alexa Fluor 568 (red) and the nucleus of the L929 cells are stained with the bisbenzimidazole dye Hoechst 34580 (blue). The merging of the individual stained components provides a composite image refining the cellular morphology observation. The L929 control cells cultured in DMEM medium, grown for 24h and transferred in cover slips for prior microscopy observation are represented as "Control (-)". The L929 cells incubated with the supernatants of the *P. aeruginosa* strains are represented as "PA01", "HB15" and "HB13". All cells were incubated with 3.42 $\mu\text{g}/\text{ml}$ of *P. aeruginosa* strains supernatants during 24h, respectively and transferred in cover slips for prior microscopy observation. The white arrows points to noteworthy morphological features, in the up row (Phalloidin Alexa Fluor 568) indicates a visible cellular blebbing and in the middle row (Hoechst 34580) indicates a visible nuclear fragmentation. The scale bar represents 25 μm length. 68

Figure 23 - Morphologic alterations in A549 cells induced by *Pseudomonas aeruginosa* strains culture supernatants. The figure shows the A549 cells morphology alterations induced by *Pseudomonas aeruginosa* strains culture supernatants, cultured in 96 well plate, using phase contrast microscopy. The figure is divided in two sections, referring to morphologic alterations at 3.42 $\mu\text{g}/\text{ml}$ and 20.50 $\mu\text{g}/\text{ml}$. The images of the cells are displayed by incubation times (24, 48 and 72 hours) horizontally and by *P. aeruginosa* strain (PA01, HB15 and HB13) vertically. The scale bars represents 100 μm length. Cytotoxicity data from previous results are shown to make relation between cellular viability and cellular morphology observations. Data represents the means \pm SD, n=2 independent experiments. * for $P < 0.05$, ** for $P < 0.01$ and *** for $P < 0.001$ 70

Figure 24 - Fluorescence microscopy of A549 cells to study morphological features induced by *Pseudomonas aeruginosa* strains. The cytoskeleton of the A549 cells are stained with the probe Phalloidin Alexa Fluor 568 (red) and the nucleus of the L929 cells are stained with the bisbenzimidazole dye Hoechst 34580 (blue). The merging of the individual stained components provides a composite image refining the cellular morphology observation. The A549 control cells cultured in DMEM medium, grown for 24h and transferred in cover slips for prior microscopy observation are represented as "Control (-)". The A549 cells incubated with the supernatants of the *P. aeruginosa* strains are represented as "PA01", "HB15" and "HB13". All cells were incubated with 3.42 $\mu\text{g}/\text{ml}$ of *P. aeruginosa* strains supernatants during 24h, respectively and transferred in cover slips for prior microscopy observation. The white arrows points to noteworthy morphological features, in the up row (Phalloidin Alexa Fluor 568) indicates a visible cellular blebbing and in the middle row (Hoechst 34580) indicates a visible nuclear fragmentation. The scale bar represents 25 μm length. 72

Figure A 1 - pH measurements of the supernatant concentrations of the *Pseudomonas aeruginosa* strains. The graphic exhibits pH measurements of the highest and lowest concentration of the supernatants of the *P. aeruginosa* strains, PA01, HB15 and HB13, from the two time points of bacterial growth ($t_1 = 24\text{h}$, $t_2 =$

48h) from the serial dilutions made. Grey bars represent the supernatant *P. aeruginosa* strains dilution concentrations, light grey for the t_1 and hard grey for the t_2). The pH measurements for the DMEM medium and LB medium are also shown represent by the white bars. The resulting data was statistically analysed by a One-way ANOVA with Tukey test where P value was set for: $P < 0.05$. Significant values comparing to the negative control were represented in the graphic as, * for $P < 0.05$, ** for $P < 0.01$ and *** for $P < 0.001$ 99

Figure A 2 - Cytotoxicity of the *Pseudomonas aeruginosa* HB15 strain culture supernatant on L929 cells.

The graphic displays the results of the MTT assay performed on L929 cells submitted to a range of total protein concentrations of the culture supernatants of the *Pseudomonas aeruginosa* HB15 strain, grown in two different time setups, represented in the graphic as t_1 and t_2 , respectively 24 hours of bacterial culture growth and 48 hours of bacterial culture growth, in cell viability percentage represented by bars with the respective standard deviation represented by vertical lines for a number of replicas $n=2$. The bar legend represents the end times of incubation (24h, 48h and 72h) with the supernatants. The controls are presented in the graphic represented as "CONTROL". The negative control has the constant value of 100% of viability for each end times of incubation and not shown in the graphic. The positive control is represented as "+" on the graphic. The controls of the bacterial culture media (LB) are represented on the graphic as "LB 25%" and "LB 7.5%". The resulting data was statistically analysed by a One-way ANOVA with Tukey test where P value was set for: $P < 0.05$. Significant values comparing to the negative control were represented in the graphic as, * for $P < 0.05$, ** for $P < 0.01$ and *** for $P < 0.001$ 100

Figure A 3 - Cytotoxicity of the *Pseudomonas aeruginosa* HB13 strain culture supernatant on L929 cells.

The graphic displays the results of the MTT assay performed on L929 cells submitted to a range of total protein concentrations of the culture supernatants of the *Pseudomonas aeruginosa* HB13 strain, grown in two different time setups, represented in the graphic as t_1 and t_2 , respectively 24 hours of bacterial culture growth and 48 hours of bacterial culture growth, in cell viability percentage represented by bars with the respective standard deviation represented by vertical lines for a number of replicas $n=2$. The bar legend represents the end times of incubation (24h, 48h and 72h) with the supernatants. The controls are presented in the graphic represented as "CONTROL". The negative control has the constant value of 100% of viability for each end times of incubation and not shown in the graphic. The positive control is represented as "+" on the graphic. The controls of the bacterial culture media (LB) are represented on the graphic as "LB 25%" and "LB 7.5%". The resulting data was statistically analysed by a One-way ANOVA with Tukey test where P value was set for: $P < 0.05$. Significant values comparing to the negative control were represented in the graphic as, * for $P < 0.05$, ** for $P < 0.01$ and *** for $P < 0.001$ 101

Figure A 4 - Cytotoxicity of the *Pseudomonas aeruginosa* PA01 strain culture supernatant on L929 cells.

The graphic displays the results of the MTT assay performed on L929 cells submitted to a range of total protein concentrations of the culture supernatants of the *Pseudomonas aeruginosa* PA01 strain, grown in two different time setups, represented in the graphic as t_1 and t_2 , respectively 24 hours of bacterial culture growth and 48 hours of bacterial culture growth, in cell viability percentage represented by bars with the respective standard deviation represented by vertical lines for a number of replicas $n=2$. The bar legend represents the end times of incubation (24h, 48h and 72h) with the supernatants. The controls are presented in the graphic represented as "CONTROL". The negative control has the constant value of 100% of viability for each end times of incubation and not shown in the graphic. The positive control is represented as "+" on the graphic. The controls of the bacterial culture media (LB) are represented on the graphic as "LB 25%" and "LB 7.5%". The resulting data was statistically analysed by a One-way ANOVA with Tukey test where P value was set for: $P < 0.05$. Significant values comparing to the negative control were represented in the graphic as, * for $P < 0.05$, ** for $P < 0.01$ and *** for $P < 0.001$ 102

Figure A 5 - Cytotoxicity of the *Pseudomonas aeruginosa* HB15 strain culture supernatant on A549 cells.

The graphic displays the results of the MTT assay performed on A549 cells submitted to a range

of total protein concentrations of the culture supernatants of the *Pseudomonas aeruginosa* HB15 strain, grown in two different time setups, represented in the graphic as t_1 and t_2 , respectively 24 hours of bacterial culture growth and 48 hours of bacterial culture growth, in cell viability percentage represented by bars with the respective standard deviation represented by vertical lines for a number of replicas $n=2$. The bar legend represents the end times of incubation (24h, 48h and 72h) with the supernatants. The controls are presented in the graphic represented as "CONTROL". The negative control has the constant value of 100% of viability for each end times of incubation and not shown in the graphic. The positive control is represented as "+" on the graphic. The controls of the bacterial culture media (LB) are represented on the graphic as "LB 25%" and "LB 7.5%". The resulting data was statistically analysed by a One-way ANOVA with Tukey test where P value was set for: $P < 0.05$. Significant values comparing to the negative control were represented in the graphic as, * for $P < 0.05$, ** for $P < 0.01$ and *** for $P < 0.001$ 103

Figure A 6 - Cytotoxicity of the *Pseudomonas aeruginosa* HB13 strain culture supernatant on A549 cells. The graphic displays the results of the MTT assay performed on A549 cells submitted to a range of total protein concentrations of the culture supernatants of the *Pseudomonas aeruginosa* HB13 strain, grown in two different time setups, represented in the graphic as t_1 and t_2 , respectively 24 hours of bacterial culture growth and 48 hours of bacterial culture growth, in cell viability percentage represented by bars with the respective standard deviation represented by vertical lines for a number of replicas $n=2$. The bar legend represents the end times of incubation (24h, 48h and 72h) with the supernatants. The controls are presented in the graphic represented as "CONTROL". The negative control has the constant value of 100% of viability for each end times of incubation and not shown in the graphic. The positive control is represented as "+" on the graphic. The controls of the bacterial culture media (LB) are represented on the graphic as "LB 25%" and "LB 7.5%". The resulting data was statistically analysed by a One-way ANOVA with Tukey test where P value was set for: $P < 0.05$. Significant values comparing to the negative control were represented in the graphic as, * for $P < 0.05$, ** for $P < 0.01$ and *** for $P < 0.001$ 104

Figure A 7 - Cytotoxicity of the *Pseudomonas aeruginosa* PA01 strain culture supernatant on A549 cells. The graphic displays the results of the MTT assay performed on A549 cells submitted to a range of total protein concentrations of the culture supernatants of the *Pseudomonas aeruginosa* PA01 strain, grown in two different time setups, represented in the graphic as t_1 and t_2 , respectively 24 hours of bacterial culture growth and 48 hours of bacterial culture growth, in cell viability percentage represented by bars with the respective standard deviation represented by vertical lines for a number of replicas $n=2$. The bar legend represents the end times of incubation (24h, 48h and 72h) with the supernatants. The controls are presented in the graphic represented as "CONTROL". The negative control has the constant value of 100% of viability for each end times of incubation and not shown in the graphic. The positive control is represented as "+" on the graphic. The controls of the bacterial culture media (LB) are represented on the graphic as "LB 25%" and "LB 7.5%". The resulting data was statistically analysed by a One-way ANOVA with Tukey test where P value was set for: $P < 0.05$. Significant values comparing to the negative control were represented in the graphic as, * for $P < 0.05$, ** for $P < 0.01$ and *** for $P < 0.001$ 105

Figure A 8 - L929 cell line culture growth through time. Contrast phase microscope shot of L929 cell culture grown in 96 well plate at 24h, 48h and 72h. The image show abundant distinguishable fibroblasts with spindle and stellate shape and some round shape fibroblast. The scale bar is set for 200 μm 106

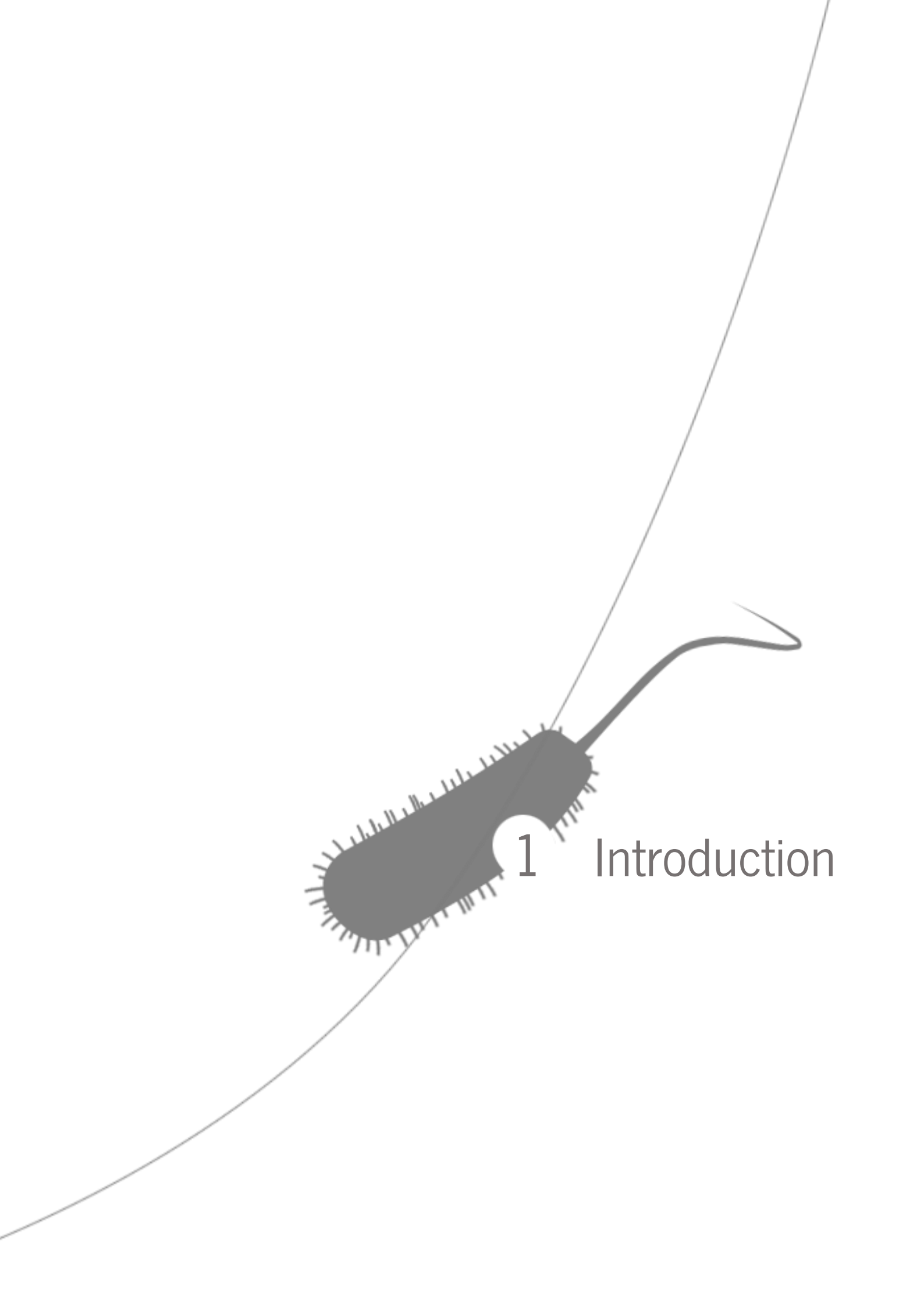
Figure A 9 – A549 cell line culture growth through time. Contrast phase microscope shot of A549 cell culture grown in 96 well plate at 24h, 48h and 72h. The image show abundant distinguishable fibroblasts with spindle and stellate shape and some round shape fibroblast. The scale bar is set for 200 μm 106

Figure A 10 – Oxidative stress induced by *Pseudomonas aeruginosa* strains culture supernatant in A549 cells. The graphic displays the results of the DCF assay performed on A549 cells submitted 3.42 $\mu\text{g/ml}$ total protein of the culture supernatants of the *Pseudomonas aeruginosa* strains (PA01, HB15 and HB13)

in fluorescence intensity (absolute units) obtained from fluorimetry using an emission wavelength of 538nm and excitation wavelength of 485nm, with the respective standard deviation represented by vertical lines for a number of replicas n=2. The bar legend represents the end times of incubation (white bar = 1h and grey bar = 4h) with the supernatants. The controls are presented in the graphic represented as "CONTROL". The negative control represents the fluorescence intensity from the oxidative stress of the cells growing with only DMEM medium. The H₂O₂- control represent represents the fluorescence intensity from the oxidative stress of the cells growing with 2mM H₂O₂. The resulting data was statistically analysed by a One-way ANOVA with Tukey test where P value was set for: P <0.05, for n=2 independent experiments 107

List of Tables

| | |
|---|----|
| Table 1 - Major resistance mechanisms to antipseudomonal antibiotics. Adapted from Hancock (2000) [64]. | 20 |
| Table 2 - <i>Pseudomonas aeruginosa</i> fully sequenced genomes. | 23 |
| Table 3 – Comparison summary of general features between the two clinical isolates HB13 and HB15. | 26 |
| Table 4 - Comparison between different animal host model features for studying infection mechanisms. | 31 |
| Table 5 - List of bacteria strains used in this thesis work. | 41 |
| Table 6 - Generic properties of the animal cell lines used in this work thesis. | 42 |
| Table 7 - L929 and A549 cell culture medium formulation. | 42 |
| Table 8 – Table of supernatant culture protein concentration gradient. | 44 |
| Table 9 – Optical densities of the culture growth and total protein determinations of the culture supernatants from the <i>Pseudomonas aeruginosa</i> strains. The table shows the optical densities (OD) of 24h and 48h bacterial culture growth from <i>P. aeruginosa</i> strains, and the subsequent protein concentration from its culture supernatants. | 52 |



1

Introduction

1.1. Bacterial Pathogenesis: an actual and worldwide serious concern

One of the main afflictions nowadays regarding worldwide public health is the pathogenesis associated to the onset of a widespread infectious bacteria. Bacteria causing infectious diseases are one of the major leads of worldwide mortality [1]. The World Health Organization (WHO) published statistic data from the leading causes of death in the world at the year 2012, where lower respiratory tract infections, majorly caused by pathogenic bacteria, was responsible for more than 3 million deaths worldwide, which represents one of the main global health threats (Figure 1). Moreover, bacteria pathogenesis are implicated in other main leading causes of death, such as diarrhoeal diseases [2]. Another study from WHO stated that infectious diseases are the main cause for worldwide deaths of children and young adults. In developing countries, infectious diseases were responsible for 45% of all deaths and 63% of all deaths in early infants [3]. These statistic facts enlighten the affect that pathogenic bacteria has in global health and why it is an established field of study among researchers and regarded under careful surveillance of governments and non-governmental organizations.

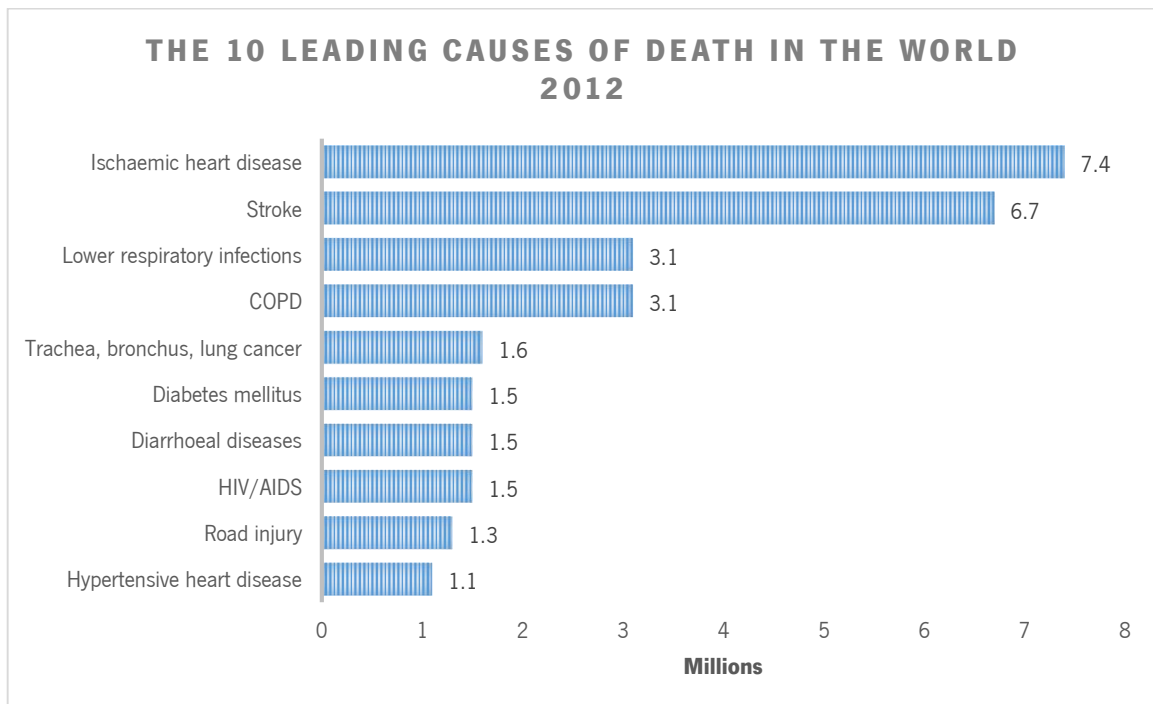


Figure 1 - Top leading causes of death in the world 2012. In the bar graphic, it is represent the main leading causes of death worldwide, in the year 2012. The first cause is ischaemic heart disease (7.4 million deaths), second it is stroke also known as cerebrovascular accident (6.7 million deaths), third it is chronic obstructive pulmonary disease (3.1 million deaths), fourth it is lower respiratory infectious (3.1 million deaths), fifth it is trachea, bronchus, lungs cancer (1.6 million deaths), sixth it is HIV/AIDS (1.5 million deaths), seventh it is diarrhoeal diseases (1.5 million deaths), eighth it is diabetes mellitus (1.5 million deaths), ninth it is road injury (1.3 million deaths) and tenth it is hypertensive heart disease (1.1 million deaths). Adapted from World Health Organization, Fact Sheet n° 310 (2014) [2].

The impact of bacterial pathogenesis, not only lies in the occurrence of new infectious diseases, but also in the re-emergence of lethal infectious diseases and in the increasing prevalence of antibiotic resistant bacteria strains [1].

The emergence of antibiotic resistant bacteria strains has been established as a main concern in general bacterial infections and as an actual and predominant threat to global health. These pathogens are identified as multidrug-resistant (MDR) bacteria, also informally known as “superbugs”. These microorganisms are able to survive to a generality of antibiotics, at least non-susceptible to 1 or more drugs in 3 or more classes of antibiotics, precluding treatment of infectious diseases that culminate in high numbers of morbidity and mortality, which make them a serious public health threat, concerning several governments and organizations [4], [5]. The world health organization (WHO) has recognized the potential of the impact of these bacteria in public health, in its first global report release on antibiotic resistance, shouting that antibiotic resistance problem is no longer an issue of the future because it is taking place at the moment all over the world. The WHO assistant director-general for health security, Dr. Keiji Fukuda, stated that if there isn't a synchronized and hurried response to the MDR pathogens progress, the world will enter in a “post-antibiotic era” where common illnesses will be fatal again. The relevance of this problem of public health has led most of the global microbial research to an extensive study of these organisms [6].

The emergence of prevalent MDR bacteria has led to outbreaks, generally common in close environment, such as hospitals and residual care facilities. In hospitals, the emergence of MDR bacteria is a regular occurrence and take the major role concerning the outbreak threat. The disseminated administration of antibiotic is a propeller for resistance acquirement and the plentiful vehicles of bacteria dissemination are ideal for antibiotic-resistant bacteria to thrive in these environments [7]. Nosocomial infections are infections acquired by patients under medical care, also known as healthcare/hospital associated/acquired infections (HAI). These kind of infections caused by MDR pathogens turn out to be a major concern in the hospital environment given its high prevalence and the increasing rates of morbidity and mortality. Currently, resistant bacteria such as methicillin-resistant *Staphylococcus aureus* (MRSA), vancomycin-resistant *Enterococci* (VRE), vancomycin-intermediate *Staphylococcus aureus* (VISA), multidrug-resistant *Acinetobacter baumannii* (MRBA) and extended spectrum beta-lactamase (ESBL) bacteria, as also multidrug-resistant Gram-negative *bacilli* like *Pseudomonas aeruginosa*, became common and regular terms of the hospital environment vocabulary. The prevalence of these pathogens causing nosocomial infections have become a serious concern. The resistant form of *S. aureus* (MRSA) has had an increasing incidence in the number of hospitalizations in Europe and the United States (US). The rates of incidence in the United States of MRSA has already exceed 50% and in some Asian countries the rate of incidence came close to 90% [8]. Plus, the WHO shouted that people infected with the resistant form of *S. aureus* (MRSA) are estimated to be 64% more susceptible to decease than people infected with the non-resistant form [6].

The vancomycin-resistant *Enterococci* (VRE) is one of the currently concerning antibiotic resistant pathogen. Data from Centers for Disease Control and Prevention (CDC) in the year of 2004 show that in US the VRE caused about 1/3 of the infections in hospital intensive care units [4].

Furthermore data from National Nosocomial Infections Surveillance system reported that infections by *P. aeruginosa* was the second most common cause of pneumonia (18.1%), the third most common cause of urinary tract infections (16.3%) and the eighth most frequently isolated pathogen from the bloodstream (3,4%) [13].

As the antibiotic resistance in *P. aeruginosa* is on the increase and given their opportunistic and resilient characteristics this bacteria became one of the most concerning issues in pathogenesis at the present time and turn the attention of many researchers into getting more knowledge and understanding of this pathogen [10].

1.2. *Pseudomonas aeruginosa*, the bacterium and the pathogen

The *Pseudomonas aeruginosa* species was described for the first time in 1872 by Schroeter. Years later, in 1882, Gessard isolated in pure culture these bacteria from the surface of wound exacerbations in a form of a “blue-green pus”. Afterwards, this bacterium species was continuously studied [14], [15].

The *Pseudomonas aeruginosa* is a bacillus shaped gram-negative bacterium with an aerobic metabolism, having mostly only one flagellum (Figure 3). These bacteria have a remarkable and versatile metabolism which allows it to survive and proliferate in numerous environments, from soil to the human organism [16]–[18]. This biological success of *Pseudomonas aeruginosa* has taken advantage from its huge genomic and metabolic potential. The first sequenced *Pseudomonas aeruginosa* strain, PAO1, revealed 6.3 million base pairs, including 5,570 predicted open reading frames (ORF), which contains a large fraction of transcriptional regulators or two-component regulatory systems (about 10%), that engender a facilitated adaptive physiological response [19].

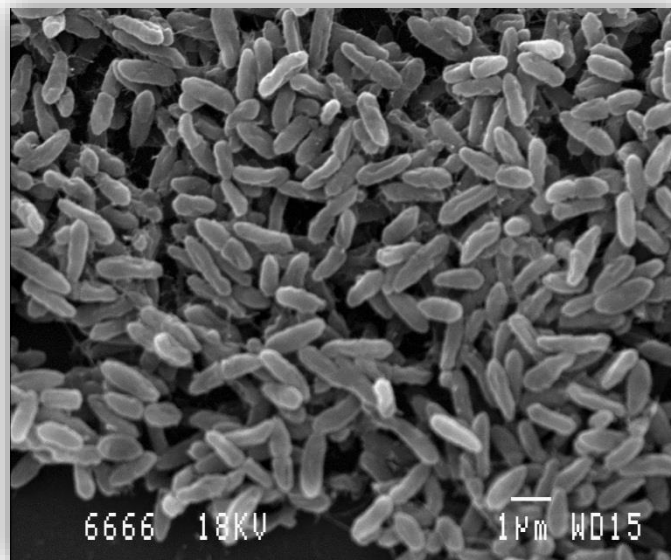


Figure 3 – Scanning electron microscopy images of *Pseudomonas aeruginosa* bacteria. Image of adherent isolate of *Pseudomonas aeruginosa* forming clumps of cells. White bar indicates the image scale (1 µm). Adapted from Deligianni (2010) [20].

Metabolically, this bacterium can utilize a variety of different carbon sources to survive. Despite of its characterized aerobic metabolism, *Pseudomonas aeruginosa* can respire under anaerobic conditions using nitrogen as an alternative carbon source. It can also subsist with minimal nutrient requirement and can keep growing through temperatures up to 42° C [21].

This bacterium belongs to the *Proteobacteria* phylum the large bacteria phylum that includes a large variety of known pathogens. In this group, *Pseudomonas aeruginosa* appears as a ubiquitous and opportunistic pathogen that infects several organisms including the human organism. In the era of antimicrobial research, *P. aeruginosa* turns to be one of the main agents of nosocomial infections causing morbidity and mortality in the

hospital infected patients [22]. The way of infecting of this bacterium is the great example of an opportunistic agent action rarely infecting healthy patients, waiting for the moment when the host organism becomes feeble to attack [23]. This is observable in several clinical cases like pneumonia, urinary tract infections, surgical wound infections, bloodstream infections. Immunocompromised patients, like in cases of bone marrow transplants, neutropenic cancer, burns and AIDS, are also susceptible to this pathogen infection action. In patients suffering from cystic fibrosis, *P. aeruginosa* represents the most common pathogen that leads to the progression of this disease and death [24].

Pseudomonas infections can be classified into chronic and acute infections. In chronic infections the pathogen lives inside the host during long periods of time. On the other hand, the acute infections like pneumonia and urinary tract infections are categorized by a quick bacterial progression and growth, leading in some cases to septicaemias and to host death [22].

The versatility of the *P. aeruginosa* as an opportunistic and resistant pathogen supports the interest of scientific research about this bacteria potentialities and their large field of applications ranging from their associated pathogenicity and clinical concern to biotechnological and biomedical applications. Within this range, the most prominent point of focus in *P. aeruginosa* research interests is its infectiousness [25].

1.2.1. Pathogenicity

P. aeruginosa is an opportunistic pathogen that leads to much discussion and concern as it became one of the most dangerous and recurrent agent of infection in hospital environments [22]. Its status as a major opportunistic human pathogen is due to its antibiotic and disinfectant resistance that eradicates other environmental bacteria [19]. The immune condition of the host and the given environment influence the attack mechanism of *Pseudomonas aeruginosa* which can behave as quiescent colonizer, a highly virulent invader during acute infection or cause of chronic infection (Figure 4) [25]. In some human cases have been described the colonization in chronic obstructive pulmonary disease by *P. aeruginosa*, the abrupt and acute ventilator-associated pneumonia in respiratory tract of patients and also chronic infections in cystic fibrosis patients that lead to a progressive and deteriorating lung function [26]. Its infectivity potential comes in part from a large sort of virulence factors derived from *P. aeruginosa* versatile and flexible genome, where 10% of its genes are organized in "pathogenic genomic islands" [21].

This fact triggers a combined effort between extensive molecular, biologic, clinical and therapeutic research to better understand the pathogenicity potential of *P. aeruginosa* [22].

There is a large set of pathogenic features underlying the overall infectious capacity of *P. aeruginosa*. The combination of the several pathogenic determinants of the *P. aeruginosa* is assumed to be more relevant to the infectious success than the effect of one given infectious element, and the mechanisms of the combined action of the different pathogenic features is very relevant to research [21].

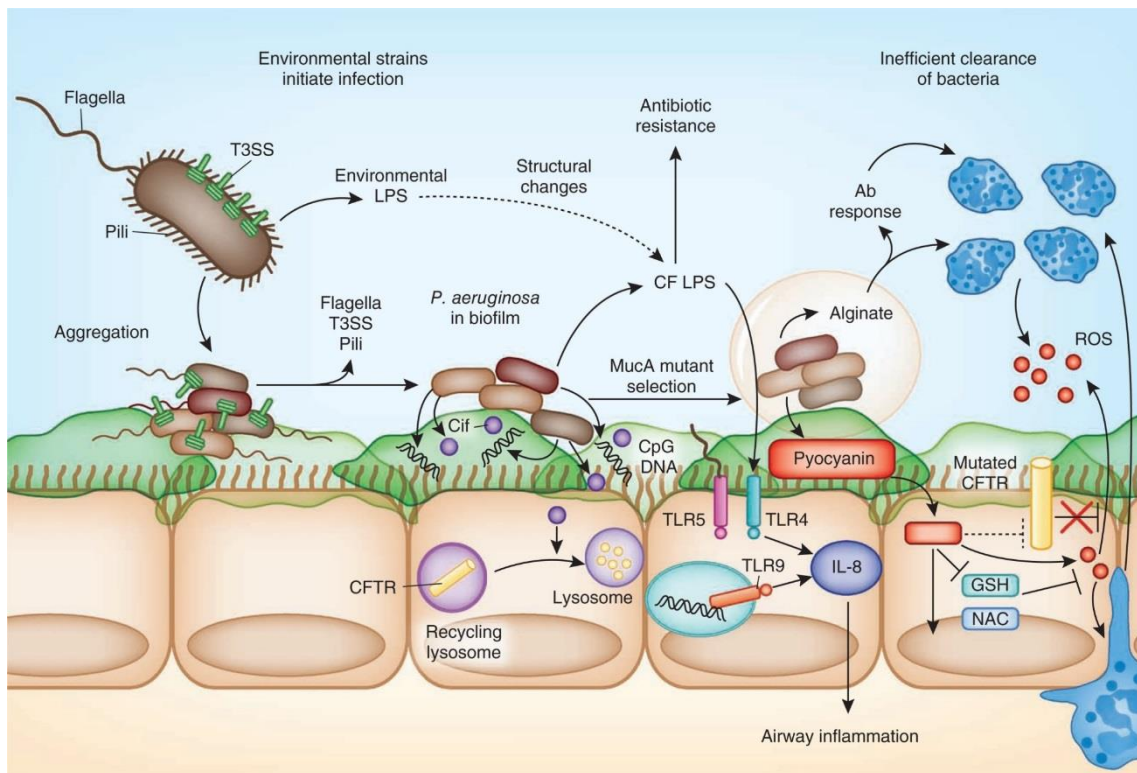


Figure 4 - Model of *Pseudomonas aeruginosa* pathogenicity in an immunocompromised host's infection. The figure represents the pathogenic features of *P. aeruginosa* following a context of infection in a cystic fibrosis patient airways. Pathogenic features such as arranged colonization, cell-associated virulence factors, secreted virulence factors, production of biofilms and antibiotic resistance are illustrated in the figure enhancing the infection development in the debilitated host. Adapted from Cohen (2012) [27].

1.2.1.1. Virulence factors

One of the most infectious characteristics of *P. aeruginosa* is its associated virulence factors. Factors such as bacterial surface components and lipopolysaccharide (LPS), as well as secreted toxins and enzymes, enhance the impact of *P. aeruginosa* in infections [26].

These factors can be categorized into secreted virulence factors or cell-associated virulence factors [24].

1.2.1.1.1. Cell-associated virulence factors

The several cell-associated virulence factors of *P. aeruginosa* are essential for the bacterial colonization process. The components of the cell structure of *P. aeruginosa* that have virulence potential include motility promoters such as pili and flagella, delivery systems that carry effector proteins into the host cells and LPS which has capacity to block the host immune response and also contribute to the maintenance of persistent infections [28], [29].

Type IV pili (Tfp) are polarity localized *P. aeruginosa* cell appendages constituted by pili polymers having the capacity of reversible assemblage and disassembling, providing to *P. aeruginosa* movement across solid surfaces, process called twitching motility (Figure 5). This feature confers *P. aeruginosa* the ability to move or glide through nutritional and environment signals and enables biofilm formation as well fast colonization on surfaces [30]. Tfp

can act as a phage receptor playing roles in early biofilm formation and adhesion to mammalian cells. In many studies was found glycosphingolipids as host receptors for Tfp, in bacteria binding to the apical surface of host polarized cells, though the binding mechanism is not yet totally clear [31]. The connexion of *P. aeruginosa* with host cells seems to modulate the Tfp expression, when the bacteria binds to the host cell the expression of pili proteins is instantly annulled [29].

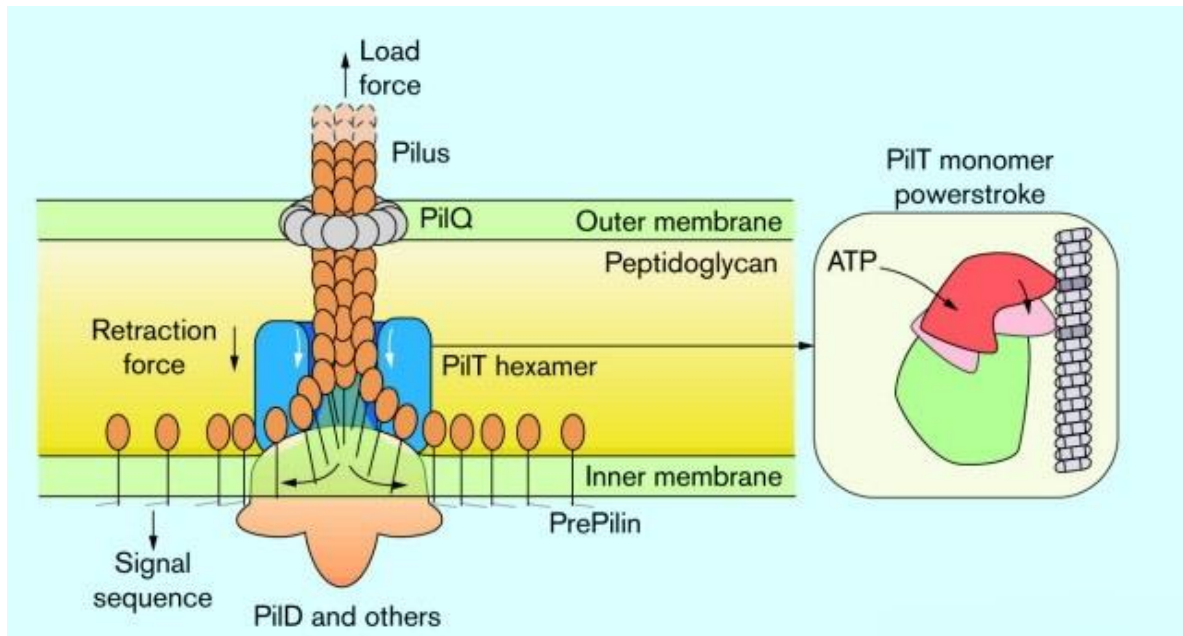


Figure 5 - Type IV pili. Illustrate representation of the type IV pilus mechanism. In the inner membrane the pilin monomer is embedded with its hydrophilic head placed in the periplasm. The pilin signal sequence is cleaved by a pre-pilin peptidase (PilD). The pilus is extended aided by supplementary assembly proteins. After extension is done, the retraction starts by action of PiT. Adapted from Kaiser (2000) [32].

The bacterial flagellum is a polymer composed of flagellin, often presented in *P. aeruginosa* as a single polar unit [31]. It is a product of the *fljC* gene, though other genes products are necessary to the flagellar self-construct [33]. Structurally is an organelle consisting in a filament with a connecting hook, bond to the cell surface by a basal body embedded in it (Figure 6) [24], [30]. *P. aeruginosa* flagella are essential for cell swimming and swarming motility, adhesion to cells and biofilm formation. Also the flagella constituent, monomeric flagelin, is detected by the innate immune system, either by recognition of individual subunits by intracellular cytosolic sensors or by ligation to Toll-like receptor 5 (TLR5) at the cell surface [31].

There is still incomplete understanding about the mechanistic and structural details of the interaction of flagella with the host epithelium. The flagellar cap protein (FlhD) of the *P. aeruginosa* strain O1 (PAO1), but not other strains, demonstrated to be involved in bacterial adherence to mucin on the respiratory tract, by binding to LewisX oligosaccharides and glycolipids receptors [24], [31].

LPS are key cell-associated factors in virulence and both innate and acquired host responses to infection. In outer-membrane of *P. aeruginosa* LPS is a main component composed by Lipid A, a hydrophobic domain, and a hydrophilic tail of core polysaccharides and O-specific polysaccharide coming out from the cell surface [24], [34].

In summary, these cell-associated virulence factors aid *P. aeruginosa* in colonization of host organisms, helping the bacteria to adhere and invade breaking the host immune responses and blocking the antibiotic's action [21].

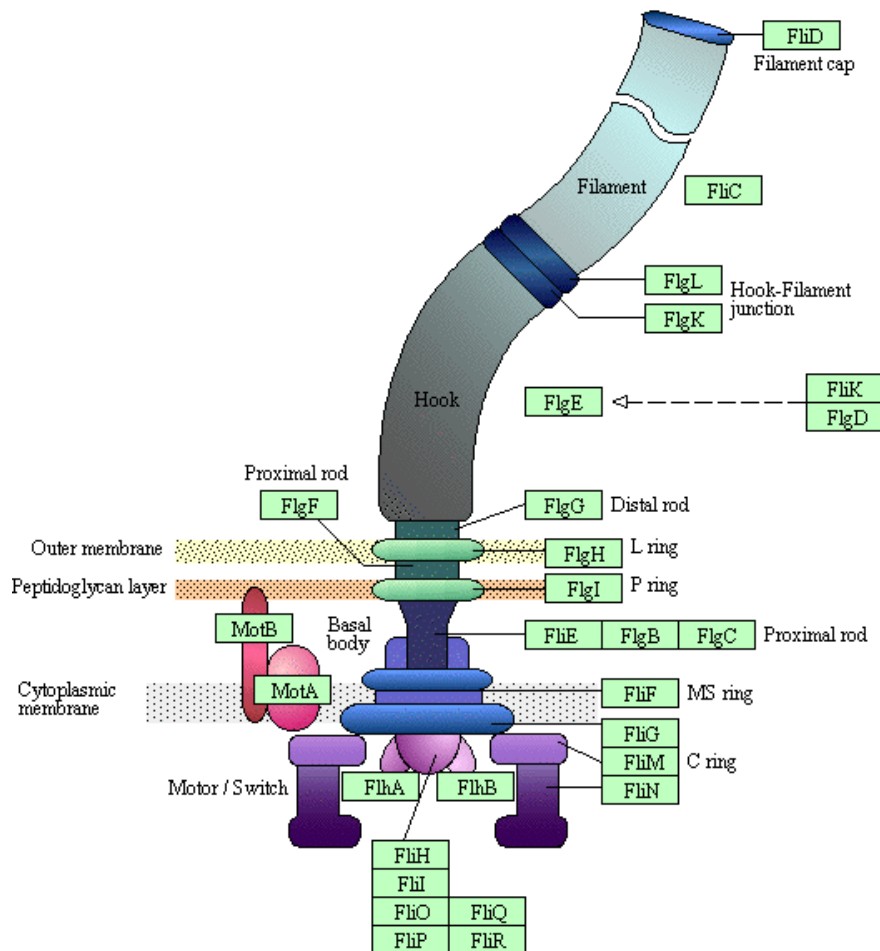


Figure 6 - Schematic representation of *Pseudomonas aeruginosa* flagellum. Structure of the *P. aeruginosa* flagellum embedded in the cell wall and membrane and its components. Adapted from EMBL-EBI BioModels Database (2012) [35].

In terms of pathogenicity conferred by virulence factors, there are other *P. aeruginosa* features that have special relevance in the mechanisms of infection which are related with the bacterial population activity and interactions.

1.2.1.1.2. Secreted virulence factors

Several extracellular factors are secreted by *P. aeruginosa* after colonization with the potential to cause extensive tissue damage, bloodstream invasion and dissemination. The type of infection may vary with the given factor contribution, associated to systems involving cell-to-cell signalling [21].

Proteases among other virulence factors play a major role in acute infection. There are four types of proteases currently known to be secreted: protease IV, alkaline protease, LasA elastase and LasB elastase

(staphylolysin). These secreted proteases improve the capacity of the *P. aeruginosa* to invade cellular tissues and block mechanisms of defence [21], [36].

The destruction of elastin is a major virulence feature of the *P. aeruginosa* in acute infections. This protein is one of the main components of the cell tissues of the lungs responsible for the organ expansion and contraction. This protein is also an essential component responsible for blood vessels' resilience [21].

The two proteases LasA and LasB give a defined elastolytic activity when acting together. This lytic action is acknowledged to destroy elastin-containing human lung tissue and cause pulmonary haemorrhages. LasA elastase is a zinc metalloendopeptidase, also known as staphylolysin. This elastase is one of the most abundant secreted virulence factors of *P. aeruginosa*. Its action consists in cleaving the elastin, turning it susceptible to degradation by other proteases, like LasB and neutrophil elastase, and alkaline protease. LasB elastase is a zinc metalloprotease acts in many other proteins besides elastin. This enzyme is highly effective, with about ten times of the alkaline protease lytic activity and an activity against casein four times that of trypsin [37]. These two proteases, LasA and LasB, were found in the mucus of the lungs of cystic fibrosis (CF) patients. The role of one of these elastases, LasB, in tissue destruction of cystic fibrosis remains less understood. The wide range of action of this enzyme permits not only to destroy tissue structures but also disturbing the infected organism defense mechanisms. In animal study models, *P. aeruginosa* mutants of LasB elastase are less pathogenic than the parental strains, sustaining the LasB crucial function as a virulence factor [25], [38].

The alkaline protease (AprA) also called aeruginolysin belongs to the subfamily B of the M10 peptidase family, included in the metzincin superfamily. This enzyme is a zinc-dependent metallo-endopeptidase secreted by *P. aeruginosa* [38]. One of the AprA targets is laminin which is an essential component of the basal lamina of cellular tissues. AprA and LasB have the capacity of inactivate human γ -interferon and human necrosis factor- α responsible for effective host immune response [38].

Also, AprA and LasB can inhibit neutrophils' function affecting their chemotaxis providing bacteria with more chances to escape by affecting the phagocytic activity of leucocytes, through cleavage of cell receptors. Natural killer (NK) cells are also affected by inhibition of the effector/target cell conjugate formation. Furthermore the alkaline protease can inactivate different human protease inhibitors and degrade cytokines such as interleukin-6 [38].

The protease IV, also called lysyl endopeptidase or iron-regulated protein PrpL, is a serine protease secreted by *P. aeruginosa*, belonging to the chymotrypsin family S1. This protease has the capacity of cleavage of bovine fibrinogen, a large biopolymer and part of the blood coagulation system. Disruption on the fibrinogen integrity leads to haemorrhages in the host. Plasminogen, immunoglobulin G (IgG), complement components 3 and C1q are also degradation targets for protease IV that interferes with the host immune system [38].

One of the known secreted virulence factors is Exotoxin A (ETA). This toxin has the ability to blockade protein synthesis and lead to cell death, via ADP-ribosylation and inhibition of the elongation factor 2 (EF2). Local tissue damage is one of the consequences of ETA action, from renal-necrosis and liver cell-necrosis to lung haemorrhage. In CF patients, this exotoxin has its main role in bacterial invasion and immunosuppression [39].

P. aeruginosa has a delivery mechanism for virulence factors, the type III secretion system (TTSS or T3SS) that transports exoenzymes to the host cells (Figure 7). These are four enzymes: exoenzyme S (ExoS), exoenzyme T (ExoT), exoenzyme U (ExoU) and exoenzyme Y (ExoY) which they are expressed inequality in different isolates [40]. In a study conducted by Feltman *et al.*, it was concluded that all isolates contained ExoT whereas the presence of other exoenzymes seemed to be reciprocally exclusive [41].

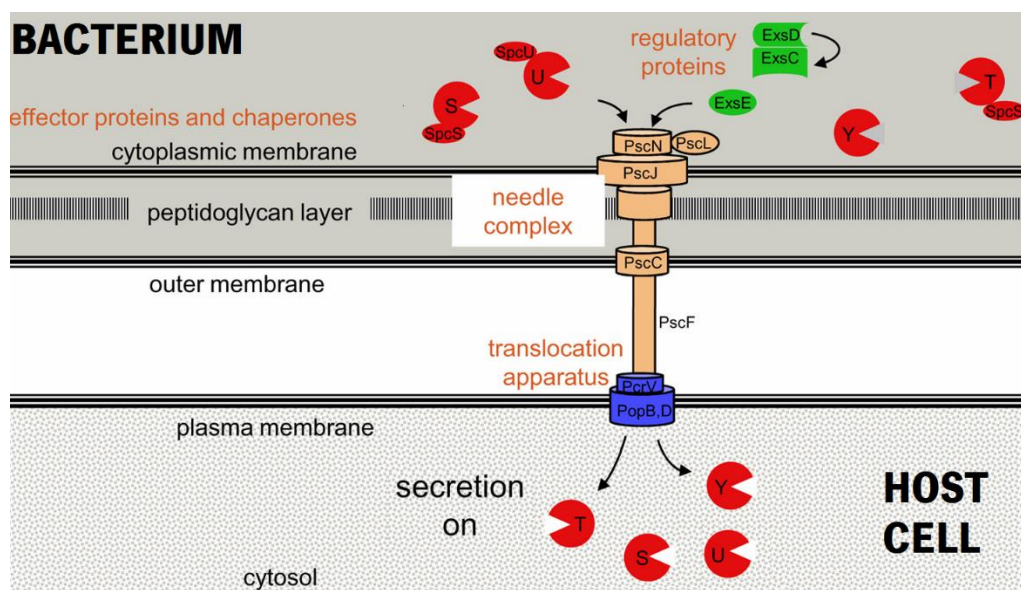


Figure 7 - Model of type III secretion system (TTSS) function. The figure represents the TTSS divided into 5 components: the regulatory proteins, the effector proteins, the chaperones, the needle complex and the translocation apparatus. The assemble of this 5 components makes the TTSS function and allows the injection of effector proteins into the host cells. Adapted from Hauser (2009) [42]

The virulence mechanisms of these exoenzymes are distinct. While the ExoS and ExoT acts in the damage of the cytoskeleton of the host cells by disrupting the actin assemblage, leading to programmed cell death, the ExoU make host sensible to secondary infections. ExoY raises the levels of intracellular cyclic AMP (cAMP) which in turn damages the actin cytoskeleton, indirectly [24].

The bacterial surfactants named rhamnolipids are virulence factors frequently secreted by *P. aeruginosa*. Their action is related to the development and maintenance of biofilms and in *ex-vivo* studies showed to interfere with cell-to-cell communication, by modulating and disrupting tight junctions of respiratory epithelial cells [43].

Pyoverdinin and Pyochelin are two secreted siderophores responsible for the recruitment of iron by the *P. aeruginosa*. Iron is necessary for bacterial growth and an increase in its intracellular accumulation enhances the persistence of infections [44].

Pyocyanin is a blue greenish, chloroform-soluble pigment synthesized by *P. aeruginosa* responsible for the typical blue colour in wound pus. Apart from the colour feature of this pigment, it possesses virulence potential causing the inhibition of epidermal cell growth, cell respiration in mammalian and prokaryotic cells, and plays a central role in lung infections and in iron acquisition. Also, catalase expression is repressed by pyocyanin [45].

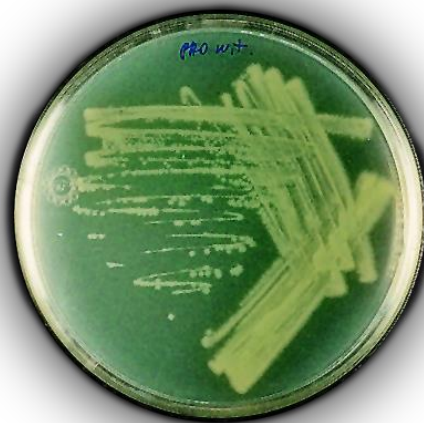


Figure 8 - *Pseudomonas aeruginosa* culture in agar plate displaying pyocyanin production. Adapted from Mavrodi (2001) [46].

It was demonstrated in *P. aeruginosa* pyocyanin-mutant isolates that it has minor virulence aptitude than the wild type strains using mice models as hosts. Despite the reduced pathogenic potential compared to the wild type strains, the mutant strains were still capable of causing local inflammation, to the significance of the infectious capacity of other virulence factors [45], [47].

Other virulence factors secreted by *P. aeruginosa* contribute to its pathogenicity capability, such as phospholipase C, histamine and leukocidin, although few information is available [24].

Besides the wide panoply of virulence factors, *P. aeruginosa* have other characteristics that confer very unique pathogenicity to this bacterium. Among them, the best known are the capacity of producing biofilms and quorum sensing, a special extracellular communication.

1.2.1.2. Biofilms

Biofilm assemblage is a remarkable feature of *P. aeruginosa* that boost survival capacity and adaptation of this bacteria. The formation of biofilms is included in stages of the bacterial life of *P. aeruginosa*, committed to some substrate or surface, or in a planktonic form, as a single organism, actively swimming using its motility

organs. These surface communities are organized in cell agglomerates involved by its self-produced polymeric matrix which give adherent properties to a variety of surfaces [24], [48].

P. aeruginosa biofilm physiology has a complex structure whereas cells show a heterogeneous physiological status determined by the position of each individual cell inside the different layers of cells composing the biofilm. In the surface layers of the biofilm, cells have more easy access to nutrients and oxygen and, as they are metabolically active, they have reduced concerns with the release of metabolic waste products [49].

The development of *P. aeruginosa* biofilms is divided in five stages (Figure 9) [50], [51]. The first stage is the reversible attachment, where planktonic cells attach to the substratum by flagella. *P. aeruginosa* is able of freely attachment and disattachment to the substratum [50]. The second stage is the irreversible attachment, in this step bacteria cells can lose its flagella due to a reorientation of the cell axis and so ending the motility ability. Afterwards, bacteria agglomerate and form microcolonies. In this phase, type IV pili plays an important role by preserving the twitching motility. Upon definitive attachment, *P. aeruginosa* initiates protein expression of the genes *algC*, *algD* and *algU* responsible for the synthesis of alginate's extracellular matrix component [52]. The third stage is early maturation, when there is an exponential upregulation of genes and the involvement of proteins responsible for anaerobic processes [52]. The fourth stage is the definitive maturation where the biofilm has its maximum thickness and structurally adopts a multicellular mushroom-shaped assembly, depending on the medium existent nutrients [24], [53]. The last stage is the detachment phase where single or grouped cells can detach from the biofilm and leave to form new biofilms. The swimming ability of *P. aeruginosa* and the matrix enzyme degradation are important factors for the dispersion and detachment of bacteria cells from the biofilm [52].

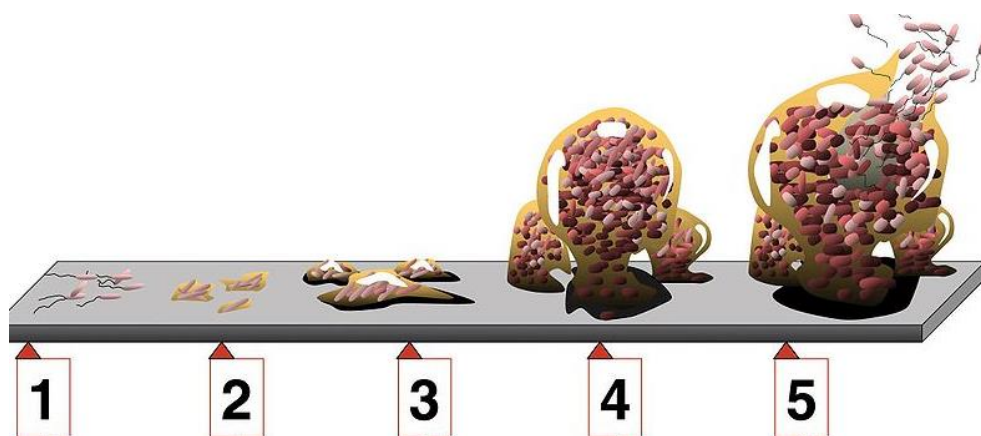


Figure 9 - Biofilm development. The figure represent the 5 stages of the biofilm development. (1) First stage of biofilm development, the initial attachment. (2) Second stage of biofilm development, the irreversible attachment. (3) Third stage of biofilm development, the initial phase of maturation. (4) Fourth stage of biofilm development, the definitive phase of maturation. (5) Fifth stage of biofilm development, the dispersion. Adapted from Monroe (2007) [51].

Bacteria can thrive in a roll of nutrient-sufficient environment when organized in biofilms that enhance the capacity to resist to antibiotics and disinfectants, beyond this biopolymer coats such as exopolysaccharide

(EPS) matrix that encase the *P. aeruginosa* biofilms confers protection from host immune mechanisms. In summary, biofilm structures are inherent to *P. aeruginosa* survival even under stringent conditions [54].

1.2.1.3. Quorum sensing

Several bacteria cells developed a system of stimulus and response to the presence of other same cells recognized as quorum sensing (QS). By this system, bacteria cells are able to communicate with each other and regulate gene expression [55]. Autoinducers are signal molecules self-generated by bacteria involved in QS that allow monitoring of the cell population density. When a maximum concentration of autoinducers is reached, target genes expression is altered by specific receptor binding. Therefore population density will control the induction or repression of defined genes, while affecting the cell population behavior [45]. Beyond the population density monitoring, QS signal molecules can regulate the expression of several secreted virulence factors as also control the formation of *Pseudomonas aeruginosa* biofilms [55].

Three distinct quorum sensing systems have been described up to now. The rhl and las are two N-acyl homoserine lactone (AHL)-dependent QS system, each one involving respectively the autoinducers N-butyryl-L-homoserine lactone (PAI-2) and the N-(3-oxo-dodecanoyl)-L-homoserine lactone (PAI-1). These two systems are organized in an established hierarchy, and more than 10% of the *P. aeruginosa* genome is regulated by their signal pathways [45], [55], [56]. The third QS system is a 2-alkyl-4-quinolone (AQ)-dependent system, related with the signal systems such as *Pseudomonas* quinolone signal (PQS) and the HHQ precursor. Other factors are susceptible to manipulate the activity of the QS systems like GacA/GacS and PhoB/PhoR two component system and transcriptional factors such as PqsR and Vfr [45], [55].

The pathogenic features of *P. aeruginosa* hereby presented cannot be effective if the pathogen is not able to survive under counter procedures. In the clinical environment, the bacterial pathogenicity is often contended with antibiotic administration. However, the given pathogenicity of *P. aeruginosa* is complemented with a persevering resistance against several antibiotics that make these bacteria so hazardous.

1.2.1.4. Antibiotic resistance

Antibiotics have been the main weapon against pathogenic microorganisms since the early 1940s after the advent of penicillin discovery [57]. Administration of antibiotics as treatment of infectious diseases proved to be a clinical success, although researchers stated that this success came out with the price of drug-resistance [58]. The acquisition of drug-resistance by these microorganisms may have different origins. The direct cause of drug-resistance induction bases in the own microorganism exposure to the antibiotic that causes a natural selection of the individuals with genes for resistance, which leads to a dissemination of these resistance genes through the bacteria population. The plasticity of the bacteria genome also represents a main factor for acquisition of drug-resistance caused by spontaneous or induced mutations. Also, bacteria can acquire

resistance genes from other bacteria by either horizontal gene transfer or transmissible plasmids. Most of these plasmids contain genes conferring multiple resistance to several antibiotics [59].

The extensive use of antibiotics for infection treatments induced a selective pressure on bacterial populations that allowed resistant individuals to thrive (Figure 10). Generalized resistance induced over antibiotic administration became worryingly common, demanding alternatives and different treatment approaches. Nevertheless, the continuous administration of antibiotics ultimately resulted in even more resistant strains [60].

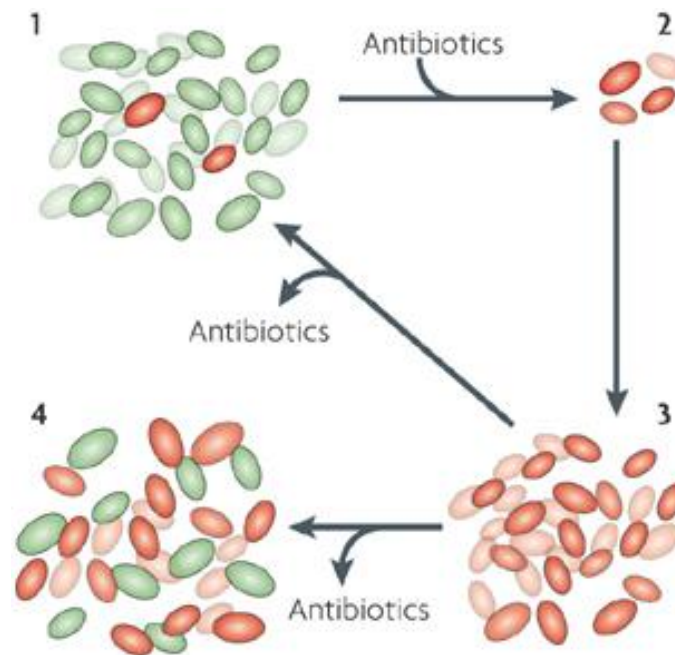


Figure 10 - Bacterial population variations induced by antibiotic action. Bacteria with acquired antibiotic resistance (red coloured) compete with the susceptible counterparts in their population niche. (1) When in absence of antibiotic administration, the resistant bacteria will not predominate unless they have a higher inherent biological fitness. Plus, the acquirement of resistance to antibiotics generally represents a loss of biological fitness. (2) When there's an administration of antibiotic the susceptible bacteria growth is inhibited which turns in an ecological opportunity for the resistant bacteria to thrive. (3) Under this conditions the resistant bacteria will proliferate and dominate the bacterial population. After the population is absent from the antibiotic action the bacterial population may return to its original scenario and the dominance of the resistant bacteria disappear. (4) Alternatively the resistant bacteria may acquire compensatory mutations which will maintain a noticeable occurrence of the resistant bacteria among the bacterial population. Adapted from Martinez (2007) [61].

As it is already known, *P. aeruginosa* is one of the main pathogens responsible for nosocomial infections. This status is in large part due to its antibiotic resistance or also called multidrug-resistance phenotype [29]. The broad resistance of *P. aeruginosa* it is associated with a combinatorial factors such as the innate resistance to antibiotic agents due to outer-membrane low permeability, the genetic capacity to express an expansive stock of resistance mechanisms, the acquisition of mutation in chromosomal genes regulating resistance genes and the acquirement of additional resistance genes from other organisms via plasmids, bacteriophages and transposons [62].

P. aeruginosa's associated resistance is frequently categorized into intrinsic/innate resistance and acquired or mutational resistance [29], [63]. The innate resistance is related to general adaptive processes which is independent of the category of antibiotic [64]. On the other hand, the acquired resistance mechanism

is a feature of the *P. aeruginosa* obtained by mutations in the genomic material content such as addition of new DNA, as also by incorporation of transposons, integrons and plasmids [64]. Internal changes in the regulatory systems of the bacteria could also play a role in the resistance to antibiotics [65].

There are three main antibiotic resistance mechanisms associated to *P. aeruginosa*: drug inactivation, restricted uptake and efflux and changes in targets [62].

One of the intrinsic resistance features of the *P. aeruginosa* is the capability of producing an AmpC-like inducible chromosomal β -lactamase that hydrolyse β -lactams, inactivating it. The β -lactams, such as ceftazidime, meropenem, piperacillin, aztreonam and imipenem, disrupt the assemblage of the bacterial cell wall by inhibiting the peptidoglycan-assembling transpeptidases in the outer layer of the cytoplasmic membrane. The bacterium cell exposure to some β -lactams will induce production of β -lactamases, which ultimately will result in an increased resistance to the inducing β -lactams and other β -lactams. The chromosomal AmpC β -lactamase is normally regulated by induction, although mutations may alter its mechanism of induction. It is a common case of mutation resistance of *P. aeruginosa* strains, the derepression of β -lactamases associated with the inactivation of the *ampD* gene, which in clinical context is the most common case of β -lactams resistance in these bacteria [62], [63].

The distinctive structure of the *P. aeruginosa*'s outer-membrane is one of the main features of its intrinsic resistance. The combination of restricted uptake through the outer-membrane with energy-dependent efflux systems represents a barrier to the inflowing of a range of antimicrobials in the pathogenic cell. The low permeable outer-membrane play a major role in antibiotic resistance because agents that break down the outer-membrane make the cells more susceptible to antibiotics. The structure of the outer-membrane in gram-negative cells is composed by a phospholipid bilayer that contains porins forming water-filled channels as the major path for diffusion of hydrophilic molecules. In *P. aeruginosa*, the OprF is the major porin that allows the efflux of large compounds such as tri-saccharides and tetra-saccharides, and possibly some antibiotics, however it forms majorly small channels that reject the efflux of the molecules referred above [63].

The low permeability of the outer-membrane alone does not confer a proper resistance mechanism, in fact its main function is decreasing the rate of antibiotic uptake keeping a slow efflux despite the external antibiotic concentration and therefore the secondary resistance mechanisms, such as antibiotic efflux or degradation, can work more efficiently. It has been described that two efflux systems play an important role in intrinsic antibiotic resistance given their constitutive expression and influence of inhibitors and knockout mutations. The first system described was the MexAB-OprM system, a RND (resistance-nodulation-division) system with 3 constituent proteins, the MexB, a cytoplasmic pump protein, the MexA a periplasmic linker protein and the OprM an outer-membrane protein. This pump system is capable to efflux a broad range of antibiotics such as chloramphenicol, tetracyclines, sulfamethoxazole, trimethoprim, quinolones and some β -lactams, although it is ineffective against other antibiotics such as erythromycin, aminoglycosides, polymyxins or

imipenem and other β -lactams. The second efflux system described is the MexX-MexY conjoining with OprM. The wide analysis of this system reveals that many substrates of the MexAB-OprM are extruded by MexX-MexY, although with a main role in the intrinsic resistance to erythromycin and aminoglycosides [63]. After these two efflux pumps, much more were identified and described playing important roles in the extrusion of antimicrobials [63], [66]. Regulatory mutations on *nalB* (*mexR*) lead to overexpression in the MexAB-Opr efflux system, other regulatory mutations lead also to overexpression to other efflux systems. The up-regulation of these efflux pumps are one of the main mutational resistance of *P. aeruginosa* and confer resistance to fluoroquinolones, cephalosporins, some β -lactams and also aminoglycosides [63], [67].

The most common resistance mechanism of *P. aeruginosa* by changes in the target are structural modification in the enzyme DNA gyrase, thwarting the action of quinolones. The majority of the reported cases describe a missense in the *gyrA* subunit (*gyrA*) of the DNA gyrase at codon 83 (quinolone target). Other mutations are occasionally noticed, by instance in higher levels of resistance its observable mutations in the DNA gyrase subunit B (*gyrB*) or in the topoisomerase IV (*parC*), which are target sites that alter susceptibility to all quinolones [63], [67].

As it is mentioned above, these resistance mechanisms, especially involving mutational resistance mechanisms, opposes to several frequently administered anti-*Pseudomonas* antibiotics, precluding clinical treatments and increasing morbidity and mortality rates (Table 1) [62].

Alongside the resistance mechanisms already described, *P. aeruginosa*'s biofilm structure is referred as a resistance mechanism by itself. Once a population of *P. aeruginosa* aggregates assemble into a biofilm structure, the encased cells are protected by an alginate polysaccharide, which confers to the population a recalcitrant property against physical and biochemical aggressions, including antibiotics. On the other hand, studies demonstrate that specific compounds present in the biofilm have a more specific interaction with antibiotics. Findings of Man *et al.*, demonstrated that periplasmic glucans produced in the biofilm are responsible for sequestering antimicrobial agents in the periplasm avoiding it to reach its active sites [62], [68].

Through the years, the established pathogenicity of *P. aeruginosa* has been the focus of several studies about infectious mechanisms, virulence factors and antibiotics resistance. The research, up to now, performed on bacteria pathogenicity has recurred to the use of selected biological models in order to evaluate the associated infectiveness and potential lethality, which open various paths to reach a more complete understanding of the *P. aeruginosa* pathogenic mechanism.

Table 1 - Major resistance mechanisms to antipseudomonal antibiotics. Adapted from Hancock (2000) [63].

| Class | Agents | Resistance Mechanisms/Comments |
|-----------------------|--|--|
| Penicillin | Ticarcillin Carbenicillin Piperacillin | Derepression of chromosomal b-lactamase. Overexpression of the MexAB-OprM multidrug efflux pump due to a NalB mutation. Specific plasmid-mediated b-lactamases. |
| Cephalosporin | Ceftazidime Cefoperazone Cefepime Cefpirome | Derepression of chromosomal b-lactamase. Overexpression of the MexAB-OprM multidrug efflux pump due to a NalB mutation. For the fourth generation cephalosporins cefepime and cefpirome, overexpression of the MexCD-OprJ multidrug efflux pump due to an NfxB mutation. |
| Aminoglycoside | Gentamicin Tobramycin Amikacin | Overexpression of the MexXY efflux pump in impermeability type-resistance due to a mutation in the regulatory gene MexZ. Plasmid-mediated production of modifying enzymes. |
| Quinolone | Ciprofloxacin | Target site mutations in the GyrA (or sometimes the GyrB) topoisomerase subunit; Overexpression of multidrug efflux pumps due to NalB, NfxB or NfxC mutations. |
| Polymyxin | Colistin | Outer membrane LPS changes due to PhoP/PhoQ regulatory mutations. No evidence this occurs in the clinic. |
| Carbapenem | Imipenem Meropenem | Loss of specific outer membrane porin channel, OprD; Reduction in levels of OprD due to an NfxC mutation that also upregulates multidrug resistance due to MexEF-OprN; For meropenem overexpression of the MexAB-OprM multidrug efflux pump due to a NalB mutation. |

1.3. Bacterial Strains

The term “bacterial strain” has been used to classify a subset population of bacterial species, which differs from other bacteria species in minor identifiable characteristics and features. Literature references such from Staley *et al.* [69], defined strain as “...made up of the descendants of a single isolation in pure culture and usually is made up of a succession of cultures ultimately derived from initial single colony” and Tenover *et al.* [70], which defined strain as “...an isolate or a group of isolates that can be distinguished from other isolates of the same genus and species by phenotypic characteristics or genotypic characteristics or both”. Strains can be of natural occurrence or created in laboratory by mutagenizing the wild-type existing bacteria species. The upsurge of strains, may lead to having, inside the same species, populations of bacteria displaying particular different functions from its counterparts, such as having a pathogenic population vs. a non-pathogenic population [71].

At present day, there are hundreds of identified and characterized strains of *Pseudomonas aeruginosa*. The adaptability and plasticity of its genome is one of the main features responsible for the dissemination and proliferation of numerous different strains [72]–[75]. It is no surprise that is found in the *P. aeruginosa* species such divergent strains in genomic and phenotypic features. Within the *P. aeruginosa* species it is verified highly pathogenic strains as PA14 strain, moderate pathogenic strains as PAO1 and non-pathogenic strains as ATCC 15442 [76], [77].

1.3.1. *Pseudomonas aeruginosa* strains

Through the genomic era, bacterial characterization such identifying bacteria at the strain level or bacterial strain typing, became a main issue due to the importance for diagnosis, treatment and epidemiological surveillance of bacterial infections. This level of bacterial characterization is significant for bacteria strain classification and expose the genetic diversity undiscovered in important phenotypic features [78].

In the year 2000, the first *Pseudomonas aeruginosa* genome was completely sequenced using the strain PAO1. This strain is regarded as the *P. aeruginosa* common reference strain, initially a spontaneous chloramphenicol-resistant mutant of the original PAO strain (previously called “*Pseudomonas aeruginosa* strain 1”) isolated from an infected burn wound of a patient in Melbourne, Australia in 1954 (ATCC 15692). Since then, this strain from Bruce Holloway’s laboratory was the main work strain for *Pseudomonas* genetics and functional analyses [79], [80].

At the time, the genome of PAO1 was the largest bacterial genome sequenced with 6.3 million base pairs (Figure 11). The genome sequence of PAO1 enlightened our knowledge in *Pseudomonas aeruginosa* bacterial versatility, pathogenicity and its inherent antibiotic resistance, such is the revealing of outer membrane proteins (OMPs) and efflux systems genes involved in transport of antibiotics [19].

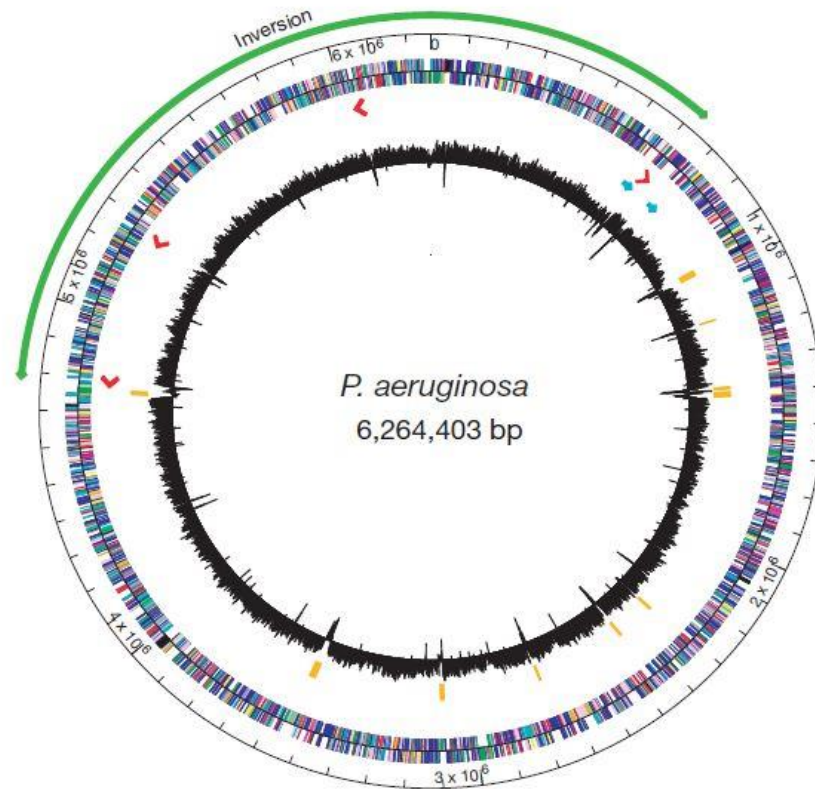


Figure 11 - Genome representation of PAO1. The outer circle is a base pair scale (each tick equivalent to 100,000 bp) that represents the chromosomal location. The colour distribution of the central circle represents genes according to its functional category. The arrow in the representation stands for the direction of transcription (the inner band represents the minus strand, the outer band represents the plus strand). Green arrow represents the inverted region resulting from homologous recombination event between *rrnA* and *rrnB*. Red arrows represent transcription direction and locations of rRNA genes. Blue arrows represents locations containing probable bacteriophages. The inner black band represents the G+C percentage schemed as the average for non-overlapping 1000 bp windows spanning one strand for the entire *P. aeruginosa* genome. Yellow bars represents genome regions of ≥ 3000 bp with G+C content of two standard deviations ($<58.8\%$) below the mean (66.6%). Adapted from Stover (2000) [19].

The full sequencing of the PAO1 make way for full genome sequencing of other *P. aeruginosa* strains central in laboratorial research (Table 2). The PA14 and LESB58 strains were the following *P. aeruginosa* strains genome to be fully sequenced, and alongside PAO1 strain they were used as laboratorial strain references for structural and functional studies, as well as pathogenic studies [76], [81], [82].

The PA14 was the next full sequenced genome of a *P. aeruginosa* strain after PAO1 sequencing. Alongside the PAO1 used as the main reference *P. aeruginosa* strain in laboratory, the PA14 has become to be used as a laboratory reference *P. aeruginosa* strain for studies of pathogenicity and virulence. The PA14 strain presents a substantial higher virulence than its counterpart, PAO1, displaying the capacity of infecting a broad cast of hosts, such as mammals, insects, nematodes and plants [76], [83]. The PA14 strain high virulence is correlated with particular sets of pathogenic genes within its genome. The full sequencing of its genome revealed two major sets of pathogenic genes defined as pathogenic islands and absent in the PAO1 genome. These two *Pseudomonas aeruginosa* pathogenic islands are PAPI-1 and PAPI-2 with 108 kb and 11 kb, respectively. They display high modular structures, mobile elements and complex derivations from other bacterial species.

Furthermore, a majority of its genes are homologous with genes in other human and plants pathogens. The virulent arsenal encoded by this PAPIs is one of the main sources for highly virulent *P. aeruginosa* strains [81], [84].

Table 2 - *Pseudomonas aeruginosa* fully sequenced genomes.

| Strain | Size (Mbp) | GC content (%) | Year | Genbank number | Reference |
|-----------------|------------|----------------|------|----------------|-----------|
| PA01 | 6.3 | 66.6 | 2000 | NC_002516 | [19] |
| PA14 | 6.5 | 66.3 | 2006 | NC_008463 | [83] |
| LESB58 | 6.6 | 66.3 | 2009 | NC_011770 | [82] |
| PA7 | 6.6 | 66.4 | 2010 | NC_009656 | [85] |
| M18 | 6.3 | 66.5 | 2011 | NC_017548 | [86] |
| NCGM2.S1 | 6.8 | 66.1 | 2011 | NC_017549 | [87] |
| DK2 | 6.4 | 66.3 | 2012 | NC_018080 | [88] |

The LESB58 is a high virulent *P. aeruginosa* strain first found in a Liverpool cystic fibrosis clinic facility for children in 1996, identified as Liverpool epidemic strain (LES). Its epidemic nature turn this strain famed for transfer between patients with cystic fibrosis to patients without cystic fibrosis, raising significant numbers of morbidity. In comparison to PA01, this strain shows a higher transmissible, an advanced aggressive feature, a superior virulence, a wider spectrum of antibiotic resistance and conceivably an enhanced aptness to cystic fibrosis lung patients. In infection context, the LESB58 strain persevered in the bronchial lumen while the PA01 and PA14 strain grew in macrocolonies after some days postinfection in the alveolar regions. Also, the LESB58 strain produce more biofilm than the PA01 and PA14 strain [81], [82]. The hyper virulence and the enhanced lung colonization feature of the LESB58 strain is attributable to pathogenic islands as in the PA14 strain, and also transcriptional variations at gene level expression. The genomic sequence of LESB58 exposed many large genomic islands (GI), counting 5 prophage clusters, 5 non-phage islands and 1 defective prophage cluster, some unique and others showing similarities with previous identified *P. aeruginosa* GIs [81], [82].

P. aeruginosa adaptable genome and its diversity of strains is a main issue concerning development, ecology and epidemiology of infectious diseases, which led efforts to establish links between distinct strains and search for better insights regarding infection process in the patient, aiming for improved prognostics and better patient care. Recently, in 2015, the International *Pseudomonas aeruginosa* Consortium (IPC) revealed a genomic study that allowed to group with an unmatched resolution the *P. aeruginosa* strains. This consortium is sequencing over a thousand genomes and developing an user-friendly analysis pipeline for the study of the *Pseudomonas* genome evolution [75].

Comparative genomic approaches led to identification of several changes in *P. aeruginosa* genome such as loss of virulence traits, improved antibiotic resistance, changes in surface antigens, increased production of alginate and modulation of metabolic pathways [89].

The evaluation of these changes is important to allow comparison of: virulence factors, shift of function mutations, antibiotic resistance genes, complete and accessory genomes. The IPC, aiming for fine-scale analyses to evaluate these changes, used 389 genomes and performed a phylogenetic analysis of the core genome of the *P. aeruginosa* strains. The results showed that the *P. aeruginosa* strains can be divided into 3 major groups and, subsequently, into further subgroups (Figure 12). The high number of strains and the extensive assortment of sources where these strains came from, such as clinical, environmental and animal strains, and also, the wide geographic distribution, suggests a tree arrangement where the group 1, which includes PAO1 and LESB58 strains, the most abundant group, followed by the group 2, which includes PA14 strain, and then the group 3 including the PA7 strain [75].

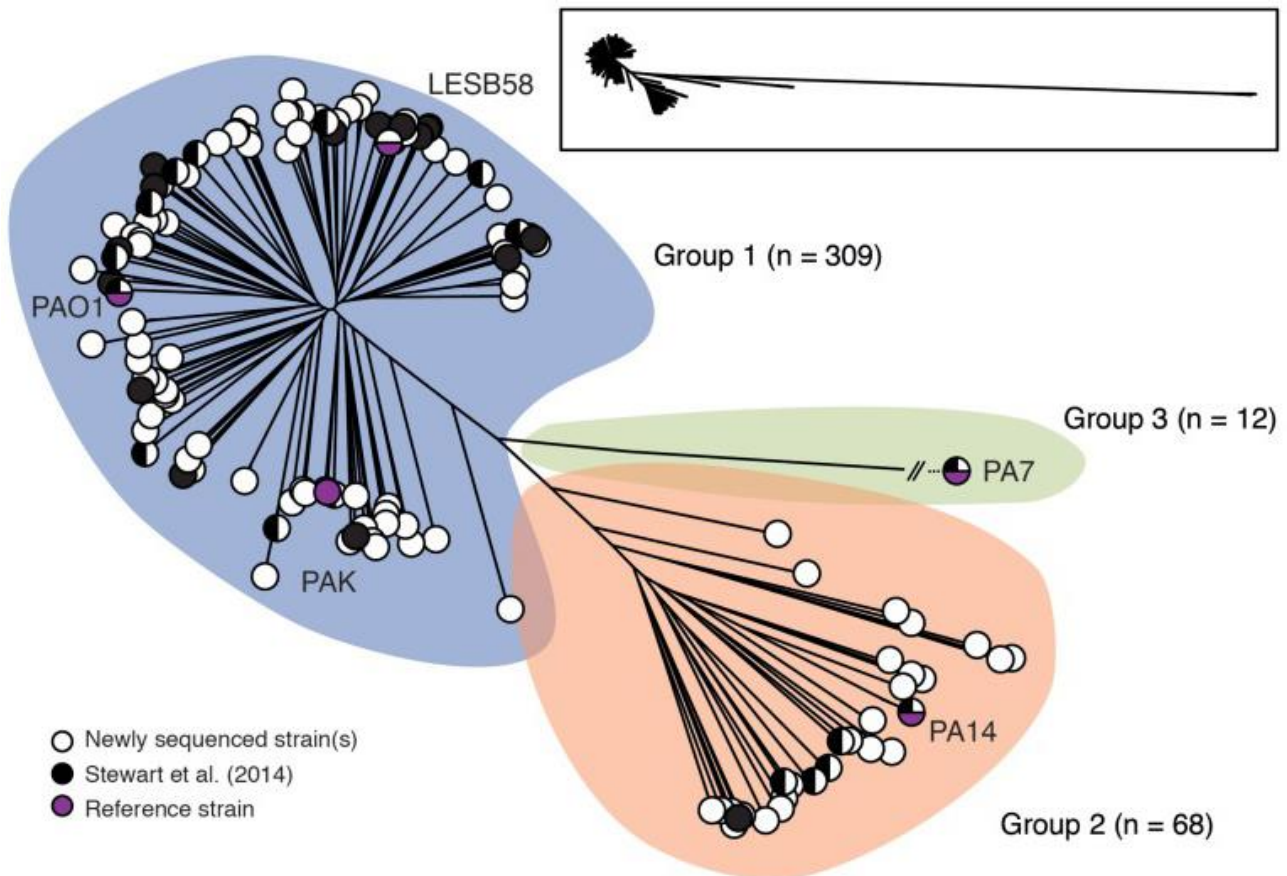


Figure 12 - *Pseudomonas aeruginosa* strains phylogenetic tree. The tree presented is an unrooted maximum likelihood tree representing 389 genomes of *P. aeruginosa* strains, based on SNPs within the core genome, using Harvest method (100 bootstraps). The tree is divided into three major groups of strains (group 1: blue, group 2: orange/pink, group 3: green). The strains distributed for each group are presented in circles. Black circles represent the strains already sequenced before the *Freschi et al.* study [75]; White circles represent one or more strains sequenced during *Freschi et al.* study [75]. The group 3 true appearance was contracted for visual proposes, the miniature of the tree true appearance is displayed in a framed miniature. Adapted from *Freschi et al.*, 2015 [75].

The data analysis of this genomic study revealed also that the core genome represents 17.5% of the average *P. aeruginosa* genome size, reflecting the high diversity of *P. aeruginosa* strains. Furthermore, the

identification of resistance genes in *P. aeruginosa* genome revealed that, approximately, 40% of the detected 73 resistance genes were spotted in a majority of strains, while, approximately, 60% of the resistance genes were discovered only in a restricted group of strains, underlining the pronounced variability of *P. aeruginosa* strains regarding the resistance genes [75].

1.3.1.1. Clinical isolates HB13 and HB15

The healthcare facilities are a fertile environment for the occurrence of a novel identifiable bacterial strains obtained under the form of clinical isolates. Every year in hospitals and clinics across the globe it is delivered numerous clinical isolates of *Pseudomonas aeruginosa* infections, where it is identifiable new strains or strain variants [90]–[93].

A partnership between the Centre of Molecular and Environmental Biology, University of Minho (CBMA – UM) and the Hospital of Braga, located in the city of Braga, north Portugal, handle about 500 clinical isolates of *P. aeruginosa* each year. The objective is a complete research methodology in order to obtain significant information and methods for genomic, functional and structural studies of these *P. aeruginosa* isolates [94].

The Pathology Service at the Hospital of Braga categorized the *P. aeruginosa* isolates into three classes according antibiotic susceptibility: pan-resistant isolates (displaying a broad resistance towards antibiotics and also are checked positive for metallo-beta-lactamases (MBLs)); multi-resistant isolates (displaying resistance toward at least 3 antibiotics and checked positive for MBLs); susceptible isolates (did not display an evident antibiotic resistance and checked negative for MBLs). The isolates susceptibilities towards antibiotics were accessed using the frequently third-generation cephalosporin Ceftazidime and β -lactams Imipenem and Piperacillin/Tazobactam, the aminoglycosides Tobramycin, Amikacin and Gentamicin and the fluoroquinolone Ciprofloxacin. Furthermore phenotypic studies and analysis were carry out in CBMA laboratories, for instance, motility assays (swarming, swimming and twitching), production of virulence factors (pigments, elastase, flagella and toxins), biofilm formation and exopolysaccharide production. Plus, virulence assays were performed with animal models (nematode *Caenorhabditis elegans* and the insect larvae *Galleria mellonella*) [94], [95].

Throughout a seasonal epidemiological survey carry out in the collaboration CBMA-UM/Hospital of Braga it was selected two particular isolates, the HB13 and the HB15 for further analysis (Table 3). These isolates were both collected from sputum of the lungs of pneumonic patients in the Hospital of Braga. The HB13 displayed an allelic representative type ST175 associated with multidrug resistance, it did not produce pigments, exhibiting a low level of virulence and demonstrated an antibiotic-panresistant phenotype. The HB15 displayed a rare allelic representative type ST560, it produced a large quantity of pyocyanin, exhibiting a high level of virulence and was susceptible to all antibiotics testes. Both HB13 and HB15 genomes were full sequenced revealing the estimated genome sizes, 6,357.409 bp and 6,813.259 bp, respectively, where is evident a

difference of about 0.5 Mbp between the two isolates. The GC content give roughly the same 66.2% for both isolates [94], [95].

A comparative genomic study on these strains revealed that the HB13 strain presented a genetic background more identical to the strains PAO1 and LESB58, with 98.8% pairwise identity, which is included in the group 1 of the *P. aeruginosa* strains. On the other hand, the HB15 strain presented more similarity with the PA14 strain, with 98.5% pairwise identity, putting it in the group 2 [75], [95].

Table 3 – Comparison summary of general features between the two clinical isolates HB13 and HB15.

| | HB13 | HB15 |
|------------------------------|------------------------------------|----------------|
| Allelic sequence type | ST175 | ST560 |
| Antibiotic resistance | Pan-resistant | Susceptible |
| Infection context | Pneumonia | Pneumonia |
| Infection type | Multi-infection (<i>E. coli</i>) | Mono-infection |
| Source | Sputum | Sputum |
| Pyocyanin production | Not detectable | Present |
| Genome size | 6,357.409 bp | 6,813.259 bp |
| Strain genomic group | Group 1 | Group 2 |

Further genomic comparative analysis revealed evidences of the accessory genomes of both isolates. In the HB13 isolate it is verified unique genes related with antibiotic resistance (for instance puromycin *N*-acetyltransferase-like gene), transposase elements and phages. In the HB15, instead, was verified unique genes for arsenic and chromate resistance and cell wall assembling (for instance glycosyltransferases) [94], [95].

The unique features of these clinical isolates and their infections context enlighten the importance of a complete and exploitative research, aiming for achieve relevant information regarding the pathogenic potential of these isolates and their impact in healthcare facilities. Pathogenicity studies relies frequently in host models to access levels of virulence of a determined microorganism.

1.4. Bacterial infection mechanisms and host models

The bacterial pathogenesis relies its harmfulness and capacity of host damage in a variety of infection mechanisms which can aid, both the pathogens in its way invading and binding to the host and in avoiding the host defence systems [1], [96]. Currently, significant evidences regarding the bacterial pathogenesis disclosed that many different pathogens share common infection strategies and mechanisms in order to harm the host and avoid its defences. Analogous infection mechanisms shared by different pathogens are associated with the acquirement of virulence genes from common bacterial ancestors. In turn, these virulence genes can be disseminated to other bacteria via horizontal transfer. Furthermore, horizontal transfer of virulence determinants is also responsible for pathogenic mechanisms common to different bacterial pathogens and directly associated to the onset of new pathogenic bacteria strains [1], [96].

There is a variety of mechanisms and process in which the bacterial pathogen can infect the host and evade its defences. In Figure 13, it is presented a summary of common infection mechanisms between bacterial pathogens. The bacterial pathogens infecting the host, may either induce several host responses and use its infection mechanisms to evade host defences, and/or adhere to the host surface in order to further invade host cell tissue, as well, invade the intracellular domain [1].

When encountering the host the bacterial pathogen use general processes, such as avoiding phagocytosis, prompting a septic shock by severe systemic inflammatory response, invading and damaging host cells and binding to host surface [1], [97].

One of the features of the bacterial pathogens responsible for evading host defences is the capsule. The bacterial capsule is a large structure enveloping the bacterial cell, characteristic of gram-positive bacteria. The capsule is constituted by a polysaccharide layer, also called exopolysaccharides (EPS), and it is consider a virulence factor because its ability of preventing the pathogen phagocytosis [98], [99]. Different species of bacteria may have the ability to use diverse types of sugar to produce the capsule. The capsule enables the bacterial pathogen to evade the host immune response, as well, protection from antibiotics. Moreover, some capsules displayed immunomodulatory effects on the host. In detail, the capsule avoid the pathogen to be phagocytosed by disabling the recognition of opsonising antibodies by phagocytic cells such as macrophages and neutrophils. This traduces in a “frustrated phagocytosis” that leads to a boosted inflammatory response, meanwhile, the phagocytic cells produces more cytokines in order to eliminate the bacteria, which by its turn, induces an increased tissue damaging, given the arriving of cumulative phagocytic cells into the infection site [1].

The bacterial cell wall is a rigid structure inclosing the cell membrane of the bacteria. It provides a structural and protection support to the bacteria, and acting as a pressure vessel disabling the over-expansion of the cell volume [100], [101].

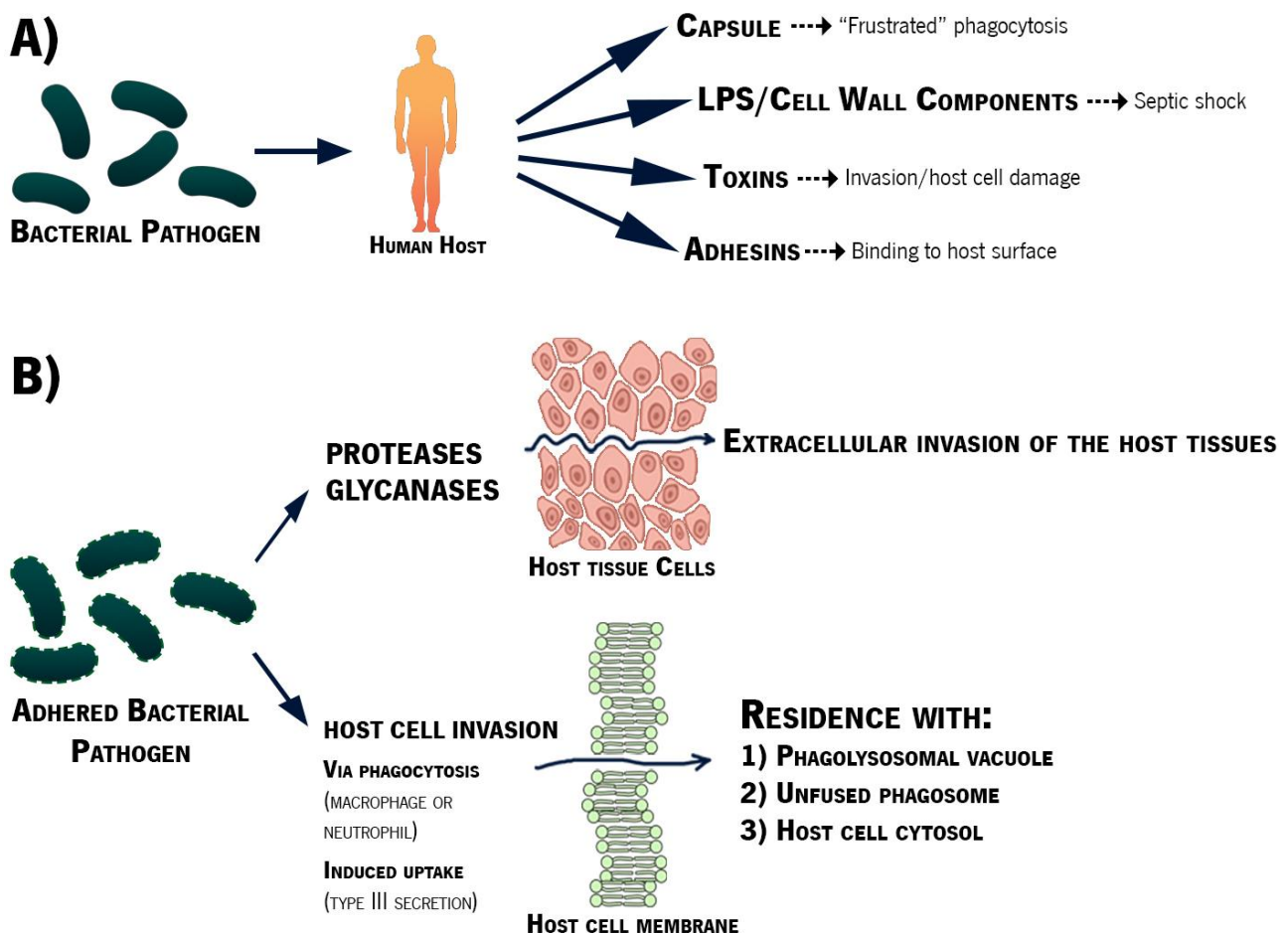


Figure 13 – Summary of the bacterial mechanisms for pathogenicity. (A) Bacterial pathogens finding a human host may induce a set of host responses and counter with several host defence evading mechanisms. The components from the pathogen that interact with the host include: (I) the capsule, which “frustrate” the phagocytic function and protect the pathogen from neutrophil and macrophage engulfment; (II) lipopolysaccharides (LPS) and cell wall components which may lead to septic shock; (III) toxins responsible for host cell damage and aiding in invasion; and (IV) adhesins that eases the binding of the pathogen with the host surface. In what level these mechanisms intervene in the pathogenesis of the infection is dependent of some factors such as bacterial species and strains, immune status of the host and pathogen entry site. (B) When the bacterial pathogen adheres to the host surface it can break into cell tissue by expressing and secreting proteases and glycanases that destroy the extracellular matrix. Furthermore, the pathogen invading cell tissue is also able to access intracellular domain. This process can be aided by action of natural phagocytosis mechanisms of macrophages and neutrophils or by action of an induced uptake where pathogen induce the host cell to engulf the adhered bacteria. One of the most common methods of the pathogens to induce uptakes is the type III secretion system which injects bacterial signalling proteins into the host cells. When inside the host cell, the pathogen can reside in the cell host cytosol or as a phagosome or even as a phagolysosome (a lysosome fused with hagosome). Adapted from Wilson *et al.*, 2002 [1].

The bacterial cell wall is mainly composed of peptidoglycan and its structure differs in gram-positive bacteria and gram-negative bacteria. The gram-positive bacteria cell wall is a thick layer, mainly composed with peptidoglycan and teichoic acid. In the other hand, the gram-negative bacteria cell wall is a relatively thin layer composed with a peptidoglycan layer surrounded with a second lipid membrane containing several components such as lipoproteins and lipopolysaccharides (LPS) [100], [102]. Much of these gram-negative cell wall components are strong virulence factors, playing effective roles in the bacterial septic shock, which may, easily, lead to a collapse of the circulatory system of the host and multiple organ failure. The bacterial virulence components of the cell wall are distinct structures, rarely secreted to the extracellular domain, until the bacteria

death and cell lysis. Paradoxically, the administration of antibiotics to treat the bacterial sepsis may lead to a release of virulence components of the cell wall which worsen the host convalescence [1].

The septic shock consists in an inflammatory mechanism mediated by cytokines, complement components, and the coagulation cascade. The realising of lipopolysaccharides (LPS) constituents of the bacterial cell wall is a major agent in triggering the inflammatory response leading to the septic shock. As described before, the LPS, also called endotoxins, are large amphophilic molecules located in the outer membrane of the bacterial cell wall, which activates inflammatory pathways leading to both innate and acquired host responses to infection [1], [100].

A battery of toxins are the arsenal of many bacterial pathogens in order to invade and cause damage to the host cells. Generally, the bacterial toxins are divide into proteinaceous, such as exotoxins and non-proteinaceous toxins, such as LPS. Regarding the proteinaceous toxins, they are generally enzymes which have the capacity to infect the host cell, either by secretion into the cell surrounding environment or by direct injection into the intracellular domain assisted with a delivery mechanisms, such as type III secretion system (TTSS). These toxins are common in several bacterial organisms and its function consists frequently in break down extracellular matrix and disruption of the cytoplasmic membrane. Furthermore, there are toxins that degrade immunoglobulins, such as immunoglobulin A, toxins that activate guanylate cyclase and toxins that affects the host cell cytoskeleton [1], [25], [38], [103].

Other important bacterial pathogen components in the infection context, is the adhesins. These components are cell surface appendages of the bacteria, which can be polypeptides or polysaccharides, and have the function of facilitating the adherence and binding of the pathogen to the host surface. Host surfaces may include, mucous membranes, deeper tissues and skin. Many host mechanical responses act against this bacterial adherence to the tissues, such as sneezing, coughing, mucous flow, blood flow, saliva production and gastric system movements. Although, bacterial pathogens developed a common trait where it expresses factors with the ability to bind to a variety of host tissues and promotes the resilience of the pathogen during the infection. When the pathogen is adhered to the host surface, it is triggered specific biochemical processes that will ultimately lead to bacterial proliferation, host cell invasion, toxin secretion and host cell signalling pathways [1], [104], [105].

When the pathogen adheres to the host surface, it becomes more accessible the infiltration of the pathogen further into the host cell tissue, leading to a higher endurance of the bacterial infection. Generally, the bacterial invasion of the host cell tissues can be classified as extracellular invasion or intracellular invasion. In extracellular invasion, the bacterial pathogens uses a set of enzymes that break down the host molecules and the host tissue barriers, leading to the advance of the pathogen further into the host extracellular domain while outside the host cells. The pathogen infiltration into the host tissues enables the pathogen to find niches in the tissues suitable for proliferation, evasion for other body parts, toxin secretion and trigger immuno-inflammatory

responses. In intracellular invasion, the pathogen is able to break into the cells of the host tissue. Many bacterial pathogens have been reported to break into host cells, both phagocytic and non-phagocytic cells. Bacterial pathogens lifecycle can be dependent of an intracellular residence, been obligated to invade a host cell in order to growth, as also, bacterial pathogens can be optionally intracellular, enter in the host cells as a mean to proliferate and invade other tissues. In addition to host intracellular invasion by phagocytosis of the pathogen, some bacterial pathogens are able to express molecular injection mechanisms, such as type III secretion system (TTSS). This mechanism injects into the cell proteins that triggers signalling pathways, ultimately leading to the incorporation of the pathogen in the intracellular domain, which often causes a disruption of the host cell cytoskeleton [1], [106], [107].

Bacterial pathogens residing within the host cell can be found in phagolysosomal vacuole, in a phagosome or living in the host cell cytosol. The phagolysosomal vacuole presents an acidic environment and hydrolytic functions. Some bacterial pathogens reside in this harsh vacuole environment and it is demonstrated that its low pH is required to trigger intracellular replication. The phagosome are frequently referred as a vacuole that was not fused with a lysosome. These vacuoles are occupied by pathogens, which leads to morphological differences from the other cellular vacuoles as also a characteristic set of surface markers. Some bacterial pathogens exhibits enzymatic mechanisms that digest the enveloping vacuole and allows it to proliferate into the host cell cytosol via cytoskeleton. The ability of bacterial pathogens to reside within the host cells may induce intracellular replication, which leads to proliferation in the infection area, as well, migration to other body parts [1], [107]–[110].

Comprehending the complexity of host-pathogen interaction require a wide range of possible host models and analytical methods. Through evolutionary course, certain virulence mechanisms and host responses have been conserved, enabling various organisms to be used as hosts for better understanding of infection mechanisms [111].

1.4.1. Infection host models

Several biological models are applicable to a variety of bacterial pathogens in order to study its infection mechanisms. The models for study *P. aeruginosa* infections mechanisms, as also, effects of virulence factors and lethality to the host, extends, not only, from animal models, such as mammals, fishes, insects, and nematodes (Table 4). But also, from mammalian cell lines, and even, plant models. These models beyond providing important resource for the development and experiment of new treatments, also offer important data about the beginning and development of the bacteria establishment and infection [112].

Mammal host models are the most widely and characterized models to study infection mechanisms leading to human disease. Unlike other models, mammals have both innate and adaptive immune systems, allowing an understanding of host-pathogen relationship at system level. One of the most important features of

the mammal host models is its route of infection which mimics the natural route of infection, since this would guarantee that the pathogen met proper barriers to infection. Models have been developed in sense of closely reflecting the natural routes of dissemination and infection [113].

Table 4 - Comparison between different animal host model features for studying infection mechanisms.

| PARAMETERS | Rodents | Zebrafish | <i>G. mellonella</i> | <i>D. melanogaster</i> | <i>C. elegans</i> |
|-------------------------------|-----------------|------------------|-----------------------------|-------------------------------|--------------------------|
| Size | 10 cm | 6.4 cm | 2 cm | 2.5 mm | 1 mm |
| Generation time | 10 weeks | 3-4 months | 30 days | 10 days | 4 days |
| Ease of handling | Difficult | Easy | Easy | Very easy | Very easy |
| Costs | High | Low | Low | Low | Low |
| Space requirements | Major | Minor | Minor | Minor | Minor |
| High throughput | No | Yes | Yes | Yes | Yes |
| Speed of outcome | Months | Days | Days | Days | Days |
| Temperature | 37°C | 29°C | 25-37°C | 18-29°C | 15-25°C |
| Immunity | Innate | Yes | Yes | Yes | Yes |
| | Adaptive | Yes | Yes | No | No |
| Biological relevance | Confirmed | Confirmed | Potential | Potential | Potential |
| Ethical considerations | Yes | Yes | No | No | No |

Rodent models became an election model to study lung infections caused by *P.aeruginosa*. One of the first models to be used was the rat model. In 1979, Cash inserted *P. aeruginosa* embedded in agar beads into the host rat, the mediation of agar beads or either agarose beads is essential to start the respiratory infection given the propriety of retaining physically the bacteria on the respiratory tracts and thus mimicking the bacterial biofilm present in airways tract infections such in the patients with cystic fibrosis [114]. Now it is evident that *P. aeruginosa* embedded in agar beads is more representative of the lung infection, although administration of the free-living bacteria cells may also reproduce relevant proceedings of a respiratory infection [112]. This procedure of agar bead model was then adapted for a new model using mice. Mice were modified genetically to simulating situations of fragile host system with susceptible respiratory functioning, such as in CF patients.

Other mammal models have been used for studies on respiratory tract infections and virulence potential caused by *P. aeruginosa*, given their lung size, architecture and function, more similar to the human. Ferrets have been used to test whether *P. aeruginosa* alginate stimulates secretion from mucous or serous cells in its trachea. Cat models was also used to study pulmonary infection using *P. aeruginosa* embedded in agar beads, the inflammation scenario in cat is very similar to the human case [112].

Even though the mammal model represent a valuable host model for human infection disease, there are several drawbacks in using this model that extends from ethical, social and scientific viewpoints to cost-effectiveness of the experiment. Many countries have tight regulations about animal experiments, leading many times to preclude the designated research. Also, the success of the usage of these models depends of a proper training of the staff, suitable experimental facilities and rigorous justification of the work. The animal species must be available, and ideally bred specifically for the infection research purpose, ensuring that the using model is free from pathogens which might be found in wild animals. Furthermore, despite of mammals being a finest host model, it is important to note that some mammalian used species may lack some of the human molecular features, such as cell surface receptors. These disadvantages of the mammalian host models led researchers to reduce, refine and replace these models for non-mammalian host model alternatives [113].

Non-mammalian host models represents many practical advantages over the mammal models, given the size of the models, cost-effectiveness, easy prolific reproduction, space confinement and maintenance [113].

One of the most well-established model of vertebrate cellular and genetic development in use is the Zebrafish (*Danio rerio*). This non-mammalian model combines the advantages of both invertebrate and rodent model, since this fish have about 6.4 cm in size and is relatively easy to handle and possesses both innate and adaptive immune systems. Zebrafish has been used as a model for *P. aeruginosa* infection, which was able to cause lethal infections in zebrafish embryos, influenced by inoculum size, presence of virulence determinants, the development stage of the zebrafish embryos, and the presence of immune cells [115]. Some of the main drawbacks of this model, may constitute the zebrafish inability to survive at 37°C, thus temperature regulated genes don't induce infection, the likelihood of zebrafish do not possess mammalian target receptors or organ, and zebrafish may not exhibit a complete immune response [113].

Insect models such as *Drosophila melanogaster* and *Galleria mellonella* have been chosen as fine models for infection mechanisms given its easy handling, maintenance and low cost. Insects have an innate immune system comprising cellular and humoral responses. Cellular response in insects involves production and mobilization of haemocytes that engulf bacteria, and the humoral response consists in the activation of Toll and Imd pathways ultimately leading to the expression of antimicrobial peptide genes [113].

Drosophila melanogaster is a fruit fly with an innate immune system that protects it from wide range of infections, in a multiple microorganism interaction environment through its lifetime. Intensive investigation has been conducted under the signal transduction cascade intrinsic to this system and these studies have revealed prominent resemblances to the mammalian innate immune response. Thus, this insect model is regarded as a good model organism to study complex interactions between *P. aeruginosa* virulence factors and host defenses motivated by human illnesses like pulmonary diseases [116]. One of the drawbacks of *D. melanogaster* as host model for study of human infectious diseases is the temperature of the infection assays (20 - 30°C) which is an obstacle to the study of temperature regulated virulence genes [113].

The greater wax moth, *Galleria mellonella*, has been a significant model to study human-pathogen interactions. The potential to explore aspects of mammalian innate immunity in the insect larvae combined with its low cost, easy maintenance and ethical acceptability, fixed *G. mellonella* larvae as an establish model. Many pathogens have been tested in this model, including the study of *P. aeruginosa* infection mechanism and their virulence factor mode of action such as the type III secretion system (TTSS) [117]. A great advantage compared to the *D. melanogaster* model and other invertebrate models is the fact that *G. mellonella* larvae grow at 37°C, thus enabling the study of temperature regulated virulence genes [113], [115].

Other well studied non-mammalian model is *Caenorhabditis elegans*. This organism is a bacteria-feeding nematode that lives in soil and can occasionally encounter *P. aeruginosa* in a host-pathogen skirmish in their own environment [118]. This nematode model is easily maintained in laboratory on agar plates, previously seeded with bacteria, such as *Escherichia coli* or *Bacillus subtilis*, have a rapid generation time, and, possesses an innate immune system that shows similarities with the mammal innate immune system [113], [115]. Concerning the *C. elegans* defense pathways, there is still a lack of knowledge about how it fights pathogenic microorganisms. It is also not well understood if *C. elegans* has an innate immune response similar to other models like insect and mammalian models [118]. Moreover, this model presents, also, as a disadvantage, several different development stages, including larval stages which may respond differently to different types of infection [113].

Plant models have been recently used as a reliable non-vertebrate host alternative of a human bacterial pathogen, much due to their Toll-like receptors, useful for analysis like *in vivo* high throughput screenings for virulence factors involved in mammalian pathogenesis [113], [115]. Virulence factors that play roles in animal diseases have been demonstrated to also play roles in plant diseases. Furthermore, some bacterial pathogens have evolved to cause disease both in mammalian and plants hosts [113].

Plant models have been used to bring more understanding about the infection mechanisms of *P. aeruginosa*. Pioneering studies on plant infection models have used clinical isolates of *P. aeruginosa*. It was demonstrated that human clinical isolates of *P. aeruginosa* were infectious in *Arabidopsis thaliana* model [113], [119]. Also, human clinical isolates were capable of causing soft-rot in plants like onion, tomato, lettuce and tobacco [120].

Pseudomonas aeruginosa utilizes a common set of virulence factors to infect both animals and plants pointing for a conserved universal mechanisms of pathogenesis through divergent evolutionary lines, ultimately leading to the usage of genetically tractable model hosts such plant models in development of therapeutics [119], [121].

Using plant models represents many advantages such as the cost-effectiveness of easily growing and handling the host and the high capacity of screening numerous bacterial strains in short time [121]. Although,

size and growth differences between individuals, and significant differences in the pathogenic potential of bacterial pathogens, such as *P. aeruginosa*, towards plants, constitutes major disadvantages of this host model.

These host models presented above represent whole systems models that provide the most information, but such models are unsuitable for more specialized analysis of bacterial virulence mechanisms [113].

1.4.1.1 Cell lines host models

Mammalian cell lines have shown a wide range of applications for numerous cellular function, morphological responses and pathogenicity studies. Robust and representative models of human cells and tissues are a pivotal for the interrogation of host-pathogen interaction. Cell line cultures represents a cost effective and a high-throughput experimental system which facilitates the dissection of pathogen interaction with a single cell type [113].

Cultured mammalian cells used for host-pathogen interaction studies comprise primary cells derived from a host, such as bone marrow-derived macrophages. Generally, these primary cells have a short life span, although they may be more representative of an *in vivo* response. Immortalized cell lines are also used for host-pathogen interaction studies, this type of cells proliferate indefinitely through random mutation or genetic modification. Different immortalized cell lines have advantages and disadvantages regarding their relevance and use as an infection model. For instance, these cell lines represent mammalian phagocytes cells, such as murine macrophage-like cell lines RAW264.1 and J774A.1, or human monocyte cell line THP-1. Furthermore, immortalized cell lines such as the monkey-derived COS-1 and the canine-derived MDCK are easily handled and they are promptly transfected for certain host-interaction studies, but, these cell lines may be less physiologically relevant to clinical infection than Hep-2 and HeLa cells. In the other hand, human cell lines such as the human colon epithelial T84 and CaCo2 cells are difficult to handle and to transfect, but, they are derived from human tissue and may be more physiological relevant for analysis of gastrointestinal pathogens that break through the gut wall [113], [122].

The monitoring of interactions between bacteria and culture cells have recurred mostly to three main approaches. The first approach comprise imaging the host-pathogen interactions using a range of microscopy methods. When cells are grown in an optical accessible surface it is possible to analyze specific interaction of the pathogen with the single cell type, such as cellular rearrangements. The imaging approach has been central to understanding of infection mechanisms of several pathogens. The second approach relies in measuring the host-pathogenic interaction by enumeration of bacteria stacks following a host-pathogen experiment designed to answer a specific question, such as, quantification of bacteria that have invaded or adhered to a cell monolayer, or quantification of bacteria that have survived within a macrophage monolayer. This type of approach is advantageous for studying the genetic basis of infection mechanisms, such as adhesion, invasion

and intracellular survival. The third approach involve analyzing inflammatory response driven by host-pathogen interaction, measuring cytokine and chemokine secretion profiles [113].

Thus far, cell culture-based infection models have been an election model to study *P. aeruginosa* cytotoxicity, for identifying important virulence factors and examine interactions with the epithelial barrier. The cell lines usually chosen to verify the pathogenicity of the *P. aeruginosa* are related with the tissues and organs that these bacteria typically infect, mostly regarding some cellular restraint given the cells susceptibility to the opportunistic feature of the *P. aeruginosa* [113], [115], [123].

A number of cell lines have been used to study the infection mechanisms of *P. aeruginosa*, such as, the human lung carcinoma A549 cell line, used to study effects of virulence factors, adhesion and invasion of respiratory tract cells, as also, alterations in gene expression in the host cell [115], [124], the CaCo-2 intestinal epithelial cells for studying *P. aeruginosa* interaction with the gastrointestinal tract [115], [125], the L929 mouse fibroblast, used in cytotoxicity assays and virulence factors processing studies [126], [127]. Also, the HeLa cervix epithelial cells [128], the MDCK canine kidney epithelial cells [129] and the CHO rodent ovary epithelial cells [130] and other cell lines have been used to study the host-pathogen interaction of *P. aeruginosa* [123].

Despite of the suitability of cell line host models for studying bacterial virulence mechanisms, major drawbacks of these models should be taken in account, such as, the lack of differentiation in phenotypes and absence of the complexity of intact organs, as well, the fact that hypothesis about host-pathogen interactions studied in this reductionist model should be verified in a whole system in order to validate the data in the context of infection [113], [115].

However, cell line host models maintain as a common choice for studying infection mechanisms due to their easier handling, cost-effectiveness, a more controlled condition status, the reaching of a more direct and objective study by specific conditions, observation of morphological changes at cellular level and the achievement of reproducible results [131]. Therefore, a cell culture-based infection system turn out to be the ideal model for evaluation of the pathogenic potential of *P. aeruginosa* strains, HB13 and HB15, in this thesis work [115], [132]–[135].

1.4.1.1.1 L929 and A549 cell lines

Given the wide range of tissues and organs that *P. aeruginosa* can infect, several types of cell lines can be used as models to give relevant data and understanding about *P. aeruginosa* infection mechanisms. The frequent cell lines used are derived from respiratory tracts, urinary tracts, cancer, skin and blood from mammalian animals [122]–[130], [136], [137]. In this thesis work it was chosen the fibroblast mouse L929 cell line and the lung carcinoma A549 cell line.

The cell line L929 are fibroblasts derived from the subcutaneous connective tissue of mice (Figure 14). This cell line is derivative from strain L of a NCTC 929 clone, from line CCL-1, a commercial source from ATCC

[138]. Fibroblasts are commonly defined as collagen producing cells and have a major role in production of the most extracellular matrix components. Characteristically they have the capacity to differentiate in specialized cells that possess a contractile phenotype with α -smooth muscle actin expression, called myofibroblasts. They have an important role in wound healing generating contractile forces that allow wound closure. Beyond the capacity of differentiation in myoblast, other differentiations into different lineages have been shown [139].

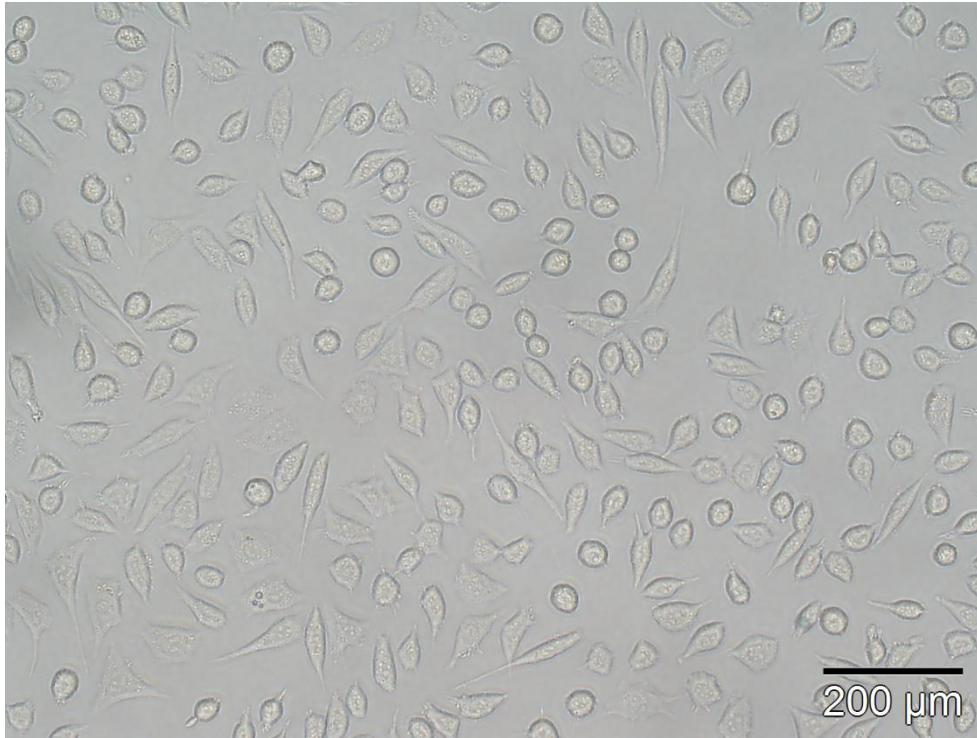


Figure 14 – L929 cells. Contrast phase microscope shot of L929 cell culture grown in 96 well plate at 24h endpoint. The image show abundant distinguishable fibroblasts with spindle and stellate shape. The scale bar is set for 200 μm .

This cell line is broadly used in several experimental procedures, from cell-to-cell interactions and cell-matrix interactions studies, to cytotoxic assays, cell death mechanistic studies and bacterial virulence studies [140]–[143].

L929 cell line was used earlier in *P. aeruginosa* to determine its pathogenicity and effects of singular virulence factors. Since skin wounds are a vehicle for most bacteria invasions including *P. aeruginosa* we take advantage of this host tissue susceptibility which make L929 a good model to study infection mechanisms of this pathogen [127], [144].

The A549 cell line is composed of adenocarcinoma cells from basal epithelia of the human lung alveoli (Figure 15). This cell line is hypotriploid with a modal chromosome number of 66 occurring in 24% of the cells, other modal chromosome numbers, 64 and 67, are also relatively common [145]. This cell line was first identified by Giard *et al.*, in 1972, through lung carcinomatous tissues explant culture from a Caucasian male 58 years old patient [146]. Attending its morphology, these cells present a squamous shape and are organized as an adherent monolayer *in vivo*. Analysis of antigen expression revealed that this cell line is positive for keratin

by immunoperoxidase staining. Metabolically, these cells produce lecithin and also showed high levels of unsaturated fatty acids essential for the phospholipid cell layer maintenance [145].

The A549 cell line is commonly exploited as a fine *in vitro* model of type II lung epithelial cells as transfection host and for analysis of drug metabolism [147].

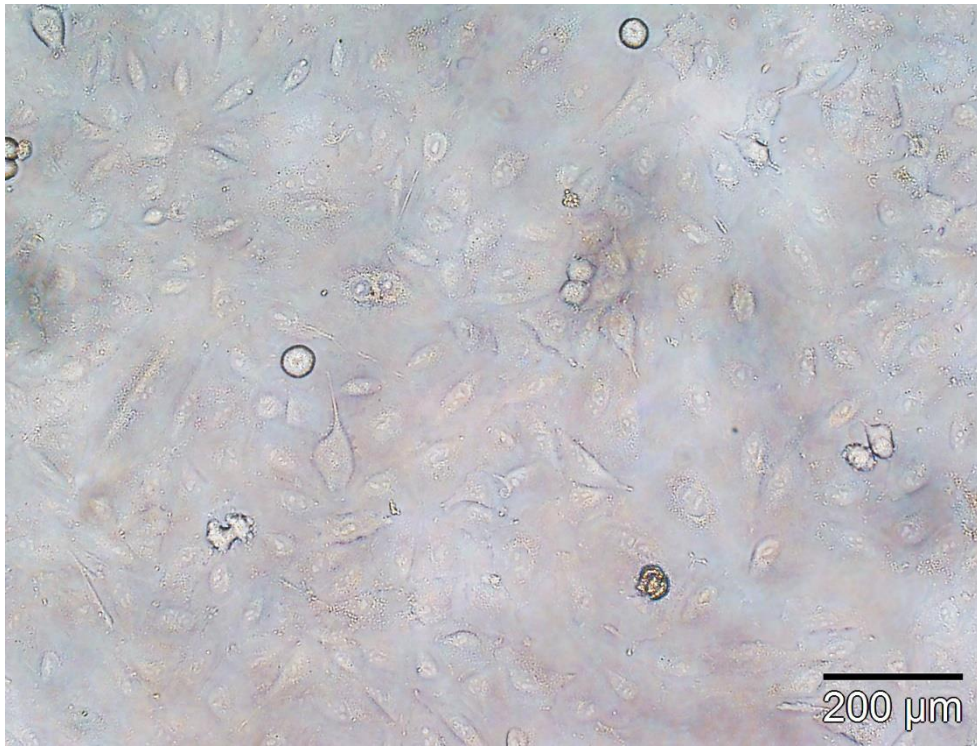


Figure 15 - A549 cells. Contrast phase microscope shot of A549 cell culture grown in 96 well plate at 24h endpoint. The image show abundant distinguishable fibroblasts with spindle and stellate shape. The scale bar is set for 200 μm .

Nowadays this cell line is widely used for diverse research concerning the pulmonary locus, homeostasis and function. It is suitable for studies of cellular processes related to the synthesis and secretion of saturated phosphatidylcoline [148]. Several studies has been performed with *P. aeruginosa* using the A549 cell line, analyzing cellular responses to the virulence factors, cellular apoptosis, oxidative stress, cellular adhesion, cytotoxicity, gene regulation and others [124], [149]–[153].

The characteristics and the former records of these two cell lines made them a suitable study model for the subsequent pathogenic studies in the *P. aeruginosa* strains, HB13 and HB15.

1.5. Objectives

This thesis work was conceived in the Laboratory of Molecular Biotechnology, the Laboratory of Animal Cells, and the Laboratory of Culture of Animal cells at the Molecular and Environment Biology Centre / Department of Biology of University of Minho, under supervision of Prof. Andreia Gomes, Prof. Pedro Miguel Santos and Prof. Isabel Alcobia (Faculdade de Medicina de Lisboa). It was performed in the scope of the of the 2nd year of the Master Degree in Applied Biochemistry in the specialisation area of Biomedicine, of the Department of Biology of University of Minho, and it aimed for the following main tasks:

- a) Performance of an initial screening of secreted virulence factors of the two clinical isolates, with different pathogenic features, obtained from Hospital of Braga's patients' sputum, classified later as *P. aeruginosa* strains HB13 and HB15, alongside with the PAO1 reference strain, in two different animal cell lines, L929 and A549.
- b) Characterization of the subsequent cytotoxicity of the PAO1, HB13 and HB15 strains on L929 and A549 cell lines.
- c) Characterization of the morphological alterations and oxidative stress induced by the *P. aeruginosa* strains, PAO1, HB13 and HB15, in the animal cell lines, L929 and A549.



2

Material and Methods

2.1. Biological Material

2.1.1. Bacterial species and strains

The bacterial species used in this thesis project was *P. aeruginosa*. In the context of a partnership between CBMA-UM and the Hospital of Braga, two different clinical isolates from the sputum of the patients infected with *P. aeruginosa*, classified as HB13 and HB15 [94], were available for this study. The strain HB13 does not produce pigments and evidenced resistance to a wide range of antibiotics. On the other hand, the strain HB15 produces a significant quantity of pyocyanin pigments and it is susceptible to antibiotics [94]. The *P. aeruginosa* strain PAO1 was used in this thesis work as a reference strain, as its genome is fully sequenced, extensively documented and is frequently studied in the scientific environment [19]. The strains used in this thesis work are identified in Table 5.

Table 5 - List of bacteria strains used in this thesis work.

| Strain | Information | Reference |
|---|--------------------------------|-----------|
| <i>Pseudomonas aeruginosa</i> HB13 | Pan-resistant clinical isolate | [94] |
| <i>Pseudomonas aeruginosa</i> HB15 | Susceptible clinical isolate | [94] |
| <i>Pseudomonas aeruginosa</i> PAO1 | All sequenced reference strain | [19] |

2.1.2. Bacterial culture media

The bacteria strains were cultivated in both liquid and solid medium (2% Agar medium supplement) of Lysogeny Broth (LB), with the Lennox formulation (LB-Lennox) composed with: 0.5% (w/v) Yeast extract, 1% (w/v) Tryptone and 0.5% (w/v) NaCl.

2.1.3. Animal cell lines maintenance

Two cell lines were used in this work in order to perform the studies of pathogenic potential of *Pseudomonas aeruginosa*: 1) L929 cell line, which are fibroblasts derived from the subcutaneous connective tissue from mice (*Mus musculus*). This cell line is a derivative from strain L of a NCTC 929 clone, from line CCL-1, commercially available from ATCC [154]. 2) A549 cell line, adenocarcinomic human alveolar basal epithelial cells with a triploid chromosomal feature. This cell line was initiated in 1972 by D.J. Giard, *et al.*, [155], through explant culture of lung carcinomatous tissues from 58-year-old Caucasian male [155]. Both L929 and A549 cells are adherent cells (Table 6).

Table 6 - Generic properties of the animal cell lines used in this work thesis.

| Cell Line | L929 | A549 |
|--------------------------------|------------------------|---------------------|
| Cell morphology | Fibroblast | Epithelial |
| Cell culture properties | Adherent | Adherent |
| Derivative tissue | Skin connective tissue | Lung |
| Species | <i>Mus musculus</i> | <i>Homo sapiens</i> |
| Age | 100 days | 58 years |
| Gender | Male | Male |
| Disease condition | None | Carcinoma |

2.1.4. Animal cell culture media

The animal cell cultures were both cultivated with Dulbecco Modified Eagle’s Medium (DMEM) with different formulations as shown in Table 7.

Table 7 - L929 and A549 cell culture medium formulation.

| L929 cell culture medium | A549 cell culture medium |
|--|--|
| 1.34% (w/v) DMEM (DMEM high glucose, Sigma-Aldrich “D5648” | 1.34% (w/v) DMEM (DMEM high glucose, Sigma-Aldrich “D5648” |
| 0.477% (w/v) HEPES | - |
| 0.15% (w/v) NaHCO ₃ | 0.37% (w/v) NaHCO ₃ |
| 10% (v/v) FBS | 10% (v/v) FBS |
| 1% (v/v) L-glutamine 200mM. | 1% (v/v) L-glutamine 200mM |
| 1% (v/v) Pre-set antibiotic mix: penicillin, streptomycin and amphotericin B | 1% (v/v) Pre-set antibiotic mix: penicillin, streptomycin and amphotericin B |
| 0.002% (v/v) Puromycin | 0.002% (v/v) Puromycin |
| pH range: 7.2 – 7.4 | pH range: 7.2 – 7.4 |

2.2. *Pseudomonas aeruginosa* virulence factors

2.2.1. Growth conditions of *Pseudomonas aeruginosa* strains

In order to obtain the virulence factors to be produced and secreted by *Pseudomonas aeruginosa* strains, bacterial culture growths were performed with two different time points of extraction.

The three *Pseudomonas aeruginosa* strains were cultivated in LB-Agar petri dishes and let to grow 8 hours at 37 °C. The cultures were then refreshed in new LB-Agar and grown overnight at room temperature.

An isolated colony forming-unit (CFU) was obtained from solid cultures and used to perform a pre-inoculum in liquid LB medium overnight at 37 °C. The optical densities (OD) of the pre-inoculi were measured at 600nm wavelength and an inoculi for the three strains were performed with a starting OD of 0.08. All the OD measures were performed with the equipment Genesys 20 Thermo Spectronic. Both pre-inoculi and inoculi liquid bacterial cultures were incubated at 37 °C with orbital shaking (200rpm) in an incubator Novotron HT Infors AG CH-4103 BOTT MINGEN.

The inoculi were grown for 24 hours and 48 hours to each strain at the pre-set conditions described above.

2.2.2. Bacterial culture supernatants extraction

After 24 hours or 48 hours of bacterial growth in LB liquid medium, the OD's were measured and the cultures submitted to a centrifugation at 11,000 rpm, during 10 minutes at 4 °C with an Eppendorf Centrifuge 5804 R.

The cultures supernatants were then extracted, filtered with a 0.22 µm filter and aliquoted. The total protein content of the supernatants was then quantified as described in the following section. The aliquots were kept at -80 °C until further use.

2.2.3. Total protein quantification

A fraction of the filtered *Pseudomonas aeruginosa* strains culture supernatants was used for the total protein quantification. The modified Lowry method was used for the quantifications. A BSA concentration gradient was used to obtain a calibration curve. The total protein concentration of the supernatants was then obtain by extrapolation of the calibration curve.

2.3. Virulence studies

2.3.1. *Pseudomonas aeruginosa* virulent factors testing concentrations

A gradient of 7 concentrations from the quantified total protein of *Pseudomonas aeruginosa* strains culture supernatants obtained at 24 and 48 hours of growth were set for the virulence potential studies. The concentration gradient started from the settled initial total protein concentration of 20.50 µg/ml and then 6 sequential dilutions, with a dilution factor of 6x, were performed according the follow table (Table 8).

Table 8 – Table of supernatant culture protein concentration gradient.

| Concentration | C1 | C2 | C3 | C4 | C5 | C6 | C7 |
|----------------------|-------------|------------|------------|------------|------------|-----------------------------|-----------------------------|
| | 20.50 µg/ml | 3.42 µg/ml | 0.57 µg/ml | 0.09 µg/ml | 0.02 µg/ml | 1.00x10 ⁻³ µg/ml | 1.00x10 ⁻⁴ µg/ml |

2.3.2. pH tests

Preparation of the gradient concentrations of total protein of *Pseudomonas aeruginosa* strains culture supernatants were set for pH measurement. Also, the initial concentrations of culture supernatants and bacterial culture medium LB was prepared for similar measurements.

The prepared samples were measured with a digital pHmeter, pHMeter pH 538 MultiCal ® WTW. The obtained pH values were annotated.

2.3.3. Cell lines growth conditions

The L929 and A549 cell lines were thawed and maintained growing in 4ml of the respective culture medium in a T25 flask at 37 °C and 5% CO₂ in a CO₂ incubator BINDER.

After reaching a confluence of 90%, the L929 cells are sub-cultivated to a new T25 flask with a starting cell density of 30,000 cells/ml. For the same condition, the A549 cells are sub-cultured to a new T25 flask with a starting cell density of 55,000 cells/ml. All procedures with animal cells lines were performed in sterile conditions in a laminar flux chamber (Telstar BIO IIA n°594).

2.3.4. Cytotoxicity tests

The cytotoxicity tests were achieved using MTT (3-(4,5-dimethylthiazol-2-yl)-2,5-diphenyltetrazolium bromide) assay. The L929 and A549 cells were seeded in 96 well plates (TTP® tissue culture plates) 12 – 16 hours before performing the assay itself.

The cells were left to grow until reaching 90% confluence. After removal of the culture medium and wash with sterile PBS 1x, cells were detached from the culture flask with 0.05% (v/v) Trypsin:EDTA for 5 minutes at 37 °C.

Fresh cell culture medium was added in order to inactivate the trypsin. The cell count for the suspension was performed with a *Neubauer* chamber.

For each experiment, the L929 cell suspension was added to each well of a 96 well plate in a total volume of 100µl with cell density of 55,000 cells/ml. For the A549 cells, 100µl of cell suspension was added to each well with a density of 100,000 cells/ml.

The culture plates of L929 and A549 were let grow 24 hours at 37 °C and 5% CO₂ with a BINDER incubator.

2.3.4.1. Incubations with virulent factors

After 24h of growth, the L929 cells, seeded in 96 well culture plates, were incubated with 50µl of the different concentrations of the *Pseudomonas aeruginosa* strains culture supernatants. Based on the results obtained with the L929 cell line, four concentrations were selected to incubate the A549 cell line 96 well culture plates, with the same procedure. The control set include a negative (-) control (only with cell line culture medium), a positive (+) control (containing 30% (v/v) DMSO) and bacterial culture medium (25% (v/v) LB and 7.5% (v/v) LB).

The incubations timepoints were defined for 24, 48 and 72 hours.

2.3.4.2. MTT assay

The MTT assay is a colourimetric assay that measures the cellular metabolic activity via NAD(P)H-dependent cellular oxidoreductases enzymes that reduce the MTT to purple formazan, reflecting the number of viable cells (Mosmann 1983; Berridge *et al.*, 2005). The cytotoxicity was obtained as percentage viability and calculated using the following formula:

$$\% \text{ Viability} = \frac{A(570\text{nm}) \text{ of the culture incubated with supernatant}}{A(570\text{nm}) \text{ of the control culture}} \times 100$$

The MTT assay was performed in 96 well culture plates after the referred incubation periods. After culture medium removal, cells were incubated with 100mM of MTT (3-(4,5-dimethylthiazol-2-yl)-2,5-diphenyltetrazolium bromide), dissolved in PBS 1x, for 90 minutes at 37 °C and 5% CO₂.

The resulting formazan crystals were dissolved with 200 µl of DMSO:Ethanol (1:1) solution. After dissolution, the absorbance of the formazan compound was read at 570 nm in a plate reader Molecular Devices Spectra Max Plus 384.

2.3.5. Cellular morphology observations

Cellular morphology alterations induced by the culture supernatants of the *Pseudomonas aeruginosa* strains were investigated by optical and fluorescence microscopy using an inverted microscope Olympus IX71 58F-3, equipped with a Olympus DP72 camera and fluorescent exciter X-Cite series 120Q EXFO.

In optical microscopy, cells were visualized directly in the 96 well plates destined to the MTT assay. In fluorescence microscopy, cells were visualized on coverslips from 24 well culture plate.

2.3.5.1. Sample preparation for fluorescence microscopy

In order to visualize cells by fluorescence microscopy, cells were grown in coverslips inside 24 well plates after preparation as described earlier.

The L929 cell suspension was added to each well in a total volume of 500 μ l with a density of 61,000 cells/ml. For the A549 cells, 500 μ l of cell suspension were added to each well with a density of 111,000 cells/ml.

2.3.5.2. Incubation with virulent factors

The L929 and A549 cell lines seeded in 24 well culture plates were incubated for 24 hours with 2 selected gradient total protein concentrations, 3.42 μ g/ml and 0.0026 μ g/ml, of the *Pseudomonas aeruginosa* strains culture supernatants from 24h and 48h of bacterial growth. The control set comprehends a life control, a death control (incubation with 30% DMSO) and culture medium control (incubation with 25% of LB medium).

2.3.5.3. Cytoskeleton and nucleus staining

After incubation, the cells were fixed with 3.7% formaldehyde solution for 10 minutes at room temperature.

The cells were then permeabilized with 0.1% Triton X-100 solution for 5 minutes.

Cytoskeleton actin was stained with Phalloidin linked to a fluorescent probe Alexa[®] Fluor 568 (Life Technologies) during 2 hours at room temperature.

Nucleus DNA was stained with a bis-benzimide (2'-[4-ethoxyphenyl]-5-[4-methyl-1-piperazinyl]-2,5'-bi-1H-benzimidazole trihydrochloride trihydrate) dye, Hoechst 34580 (Life Technologies) for 30 minutes at room temperature.

2.3.6. Oxidative stress tests

2.3.6.1. Sample preparation

The L929 cell suspension was added to each well in 24 well plates in a total volume of 500 μ l with cell density of 61,000 cells/ml. For the A549 cells, 500 μ l of cell suspension was added to each well with cell density of 111,000 cells/ml. Cultures were maintained in standard culture conditions for 24h to stabilize prior to incubation with virulence factors.

2.3.6.2. Incubation with virulent factors

The cell lines seeded in 24 well culture plates were incubated for 1 and 4 hours with 2 selected total protein concentrations from *Pseudomonas aeruginosa* strains culture supernatants. The control set was performed similarly to the control sets in the preceding tests with a hydrogen peroxide control (2mM H₂O₂).

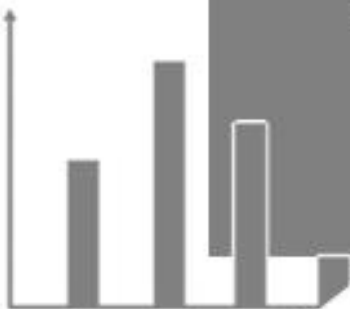
2.3.6.3. DCF assay

After incubation with the *Pseudomonas aeruginosa* strains supernatant cells were loaded with 200 μ l of 2',7' -dichlorofluorescein diacetate (DCFH-DA) 100mM and incubated at 37 ° C and 5% CO₂, in absence of light. The cells were later lysed with a solution of 90% DMSO – 10% PBS 1x.

The lysate was transferred to a 96 well black plate and the fluorescence intensity read in a fluorimeter FLuoroskan Ascent FL (Thermo Scientific) using an excitation wavelength of 485nm and emission wavelength of 538nm.

2.4. Statistical Analysis

All the experiments were repeated at least twice. Data were expressed as means with standard deviation for n independent experiments. A One way ANOVA analysis with post-hoc Tukey *test* was performed for multiple comparisons. A P -value of 0.05 was considered significant. GRAPHPAD PRISM 5 (GraphPad Software Inc., San Diego, CA) was used for the analysis.



3 Results and Discussion

3.1. Bacterial culture growth

The *Pseudomonas aeruginosa* strains PAO1, HB13 and HB15 were grown in LB-Lennox medium for 24 and 48 hours. For each strain and time point, the bacterial culture growths were prepared in duplicate. The OD of the respective bacterial cultures was measured at 600nm wavelength to assess the cell culture density. All the cultures started from an OD at 600nm of 0.08 (Table 9).

After 48 hours of culture growth there was a marked decay of optical density comparably to the 24 hours of culture growth. The accentuated reduction of optical density directly related with cell density is mainly due to the exhaustion of nutrients that happens through the decline phase of bacterial growth [158]. It is known that after 8 hours the bacterial growth of the reference strain (PAO1) reach a stationary phase with a constant OD>5 which indicates that the bacterial growth is already in a decline phase after 24 hours [159]. The selection of these two time setups of bacterial culture growth, was made in order to obtain a maximum of extracellular products, as also, verifying if through time there is any decadence of the secreted virulence factors.

The PAO1 and HB15 strain cultures have a higher cell density than HB13 strain culture at 24 hours of growth, however, at the end of 48 hours the HB13 strain culture has a higher density of cells than the PAO1 and HB15 strain. We can infer by the analysis of the results that PAO1 and HB15 strains have a higher growth rate which exhaust quicker the medium nutrients leading to a higher cell death at the end of 48h of bacterial growth, than the HB13. In the other hand the HB13 strain comparatively to the two strains above appears to have a lower growth rate because it shows a significant lower cell density after 24 hours and a higher cell density after 48h of bacterial growth. It is already reported that HB13 is a pan-resistant strain [94], and many studies point out that antibiotic resistant come with an effective biological fitness cost which is visible in these results [61], [160]–[162].

The performance of these bacterial cultures were essential to obtain supernatants with appropriate quantities of secreted virulence factors.

3.2. Virulence factors extraction

In order to evaluate the pathogenicity of the *Pseudomonas aeruginosa* strains conferred by the secreted virulence factors, the supernatants were isolated from the respective bacterial cultures. The supernatant of the *Pseudomonas aeruginosa* strains is composed of the consumed LB-Lennox medium and the bacteria secreted products which includes the virulence factors. In this framework, the cultures supernatants are a plentiful niche of secreted virulence factors produces by the *P. aeruginosa* strains. The isolation of the supernatant was obtained by centrifugation of the bacteria cultures and subsequent filtration to eliminate the remaining bacteria cells and cells debris.

3.3. Protein quantification of the supernatants

Total protein quantification was performed in order to assess the virulence factors secreted by the *Pseudomonas aeruginosa* strains. Since most of the secreted virulence factors are of protein nature [36], a protein quantification came out as a reliable method to estimate the amount of virulence factors.

To assess the protein levels the modified Lowry method was used. A calibration curve was drawn using serial dilutions of bovine serum albumin (BSA), with the mathematical equation $y = 0.0133x + 0.1119$ where Y is the absorbance and X the amount of protein. The resulting *Pearson* coefficient of determination was found acceptable.

Based on the calibration curve it was possible to determine the total protein concentration of the *Pseudomonas aeruginosa* strains supernatants showed in the table below (Table 9).

Table 9 – Optical densities of the culture growth and total protein determinations of the culture supernatants from the *Pseudomonas aeruginosa* strains. The table shows the optical densities (OD) of 24h and 48h bacterial culture growth from *P. aeruginosa* strains, and the subsequent protein concentration from its culture supernatants.

| STRAIN | Bacterial growth time | Bacterial culture OD | [Protein] µg/ml |
|---------------|------------------------------|-----------------------------|------------------------|
| PAO1 | t ₁ = 24h | 4.53 | 206 |
| | t ₂ = 48h | 1.15 | 310 |
| HB15 | t ₁ = 24h | 3.91 | 164 |
| | t ₂ = 48h | 0.94 | 303 |
| HB13 | t ₁ = 24h | 2.41 | 105 |
| | t ₂ = 48h | 1.79 | 158 |

The HB15 strain culture supernatant has almost the same quantity of protein as PAO1. In contrast, the HB13 strain culture supernatant has much less protein than the PAO1 and HB15 strains (Table 9).

The variation on the amounts of protein on the supernatants is related with pathogenic and metabolic features of each strain. Although each strain presented different amounts of protein, it is observable a noteworthy difference of protein quantity between the HB13 strain and the other two strains. We can relate this protein amount difference with the pathogenicity of the strains, it is already known that the HB13 is a lesser pathogenic

strain than the HB15 and PAO1, and that high pathogenic strains produce more extracellular proteins than low pathogenic strains [94], [163].

The assessment of the quantifications of the supernatant proteins were necessary for the subsequent pathogenic studies in this thesis work.

3.4. pH measurements of the supernatants concentrations of the *Pseudomonas aeruginosa* strains

The pH measures were made considering the protein concentrations from the 7 serial dilutions set of the supernatants from 24 and 48 hours (t_1 and t_2 , respectively) of bacterial growth, in duplicate, of the *Pseudomonas aeruginosa* strains used for the cytotoxicity screenings and the original concentration where the supernatants were obtained. The pH of the LB medium and DMEM medium used for the *P. aeruginosa* was also measured.

These measurements had as objective to verify if the pH of the chosen concentrations, and the media used, exhibited significant differences between each other which could lead to adulterated cytotoxicity results.

The results shows that it was not found any significant pH difference between the supernatant dilution concentrations with each other, and with the media, discarding possible adulterations in the cytotoxicity tests.

3.5. Cytotoxicity tests

Cytotoxicity is one of the main properties of pathogenic microorganisms that consists in the attribute of being toxic toward cells. The analysis of this property is a direct approach to study the *Pseudomonas aeruginosa* pathogenicity in the chosen cell models. The MTT assay was used in order to evaluate the cytotoxicity and consequent pathogenicity of the three *Pseudomonas aeruginosa* strains on the mammalian cell lines L929 and A549.

The serial range of total protein concentrations previously established were used to evaluate the cytotoxicity of the culture supernatants from the *Pseudomonas aeruginosa* strains at three time points, 24, 48 and 72 hours, of incubation with the mammalian cells.

A control set was performed with a negative control, with cells grown only in its proper medium and a positive control, where cells were incubated with 30% of DMSO.

Additionally to the negative and positive controls, two bacterial medium controls (7.5% and 25% of LB medium) were included. The purpose of these controls was to study the influence of the LB medium on the effective cytotoxicity caused by the secreted virulence factors.

3.5.1. Cytotoxicity of culture supernatants of the *Pseudomonas aeruginosa* strains in the L929 and A549 cell lines

The first cytotoxicity tests were performed on L929 cells incubated with the culture supernatants. The L929 cell line is an easy handling, valid and robust model, widely used in a variety of biological tests, which was the fundamental reason for using it to initiate the screening of cytotoxicity of supernatants and define concentration range for further experiments.

The L929 cells were incubated with two different type sets of culture supernatants concentrations of the *P. aeruginosa* strains. The sets represented the supernatants from two bacterial growth time points, t_1 (24 hours) and t_2 (48 hours). The utilization of these different timepoints was adequate to analyse the influence of different periods of bacterial growth on the associated cytotoxicity induced by the supernatants.

The results showed that there are no significant differences in cytotoxicity levels caused by the supernatants obtained from 24 or 48 h of bacterial culture growth. Figure 16 shows the concentration which presented the highest variance (3.42 $\mu\text{g/ml}$). A standard tendency is noted in which the supernatants from t_1 cause more cellular toxicity than t_2 . These observations might indicate that, after 24 hours of bacterial growth, the associated cytotoxicity decreases. Although, statistically, the results are not significant.

Other reports show that the secretion of several virulence factors is regulated in a growth-phase-dependent manner in gram-negative bacteria [164]. In studies by Bernardo *et al*, in 2004, it was demonstrated that production of exoproteins, in the gram-negative bacterium *Staphylococcus aureus*, were regulated in a

growth-phase-dependent-manner occurring mostly in the post-exponential growth phase [165]. Posteriorly, Sturm *et al.*, showed that the expression of the type three secretion system 3 (TTSS 3) in *Salmonella typhimurium* was increased in the beginning of the late logarithmic growth phase. Furthermore, at this growth phase, the increase of TTSS 3 expression would be related with growth-related environmental signals such as oxygen depletion, quorum signals, nutrient depletion and metabolites accumulation [166].

In 2005, studies performed by Kim *et al.*, showed that the *P. aeruginosa* type three system production was not active in the early adaptive-growth phase [167]. Anteriorly, it was already demonstrated that specific growth phases affected apoptosis induction and bacterial invasion ability in *P. aeruginosa* strains [168].

This previous knowledge of the influence of growth phases on the virulence mechanism in gram-negative bacteria, including *P. aeruginosa*, led us to search for visible effects on the associated cytotoxicity of the strains used in this work, between the two stipulated periods of growth. Based on that, in the above-described studies, the major influences of the growth phase were significant between exponential and stationary phase. In this work, the two selected timepoints already coincided with the death phase of *P. aeruginosa* culture growth. This might be the principal cause for the non-significant statistical results. Other timepoints from distinct bacterial growth phases, such as exponential and stationary growth phase, should have been selected in order to achieve significant results.

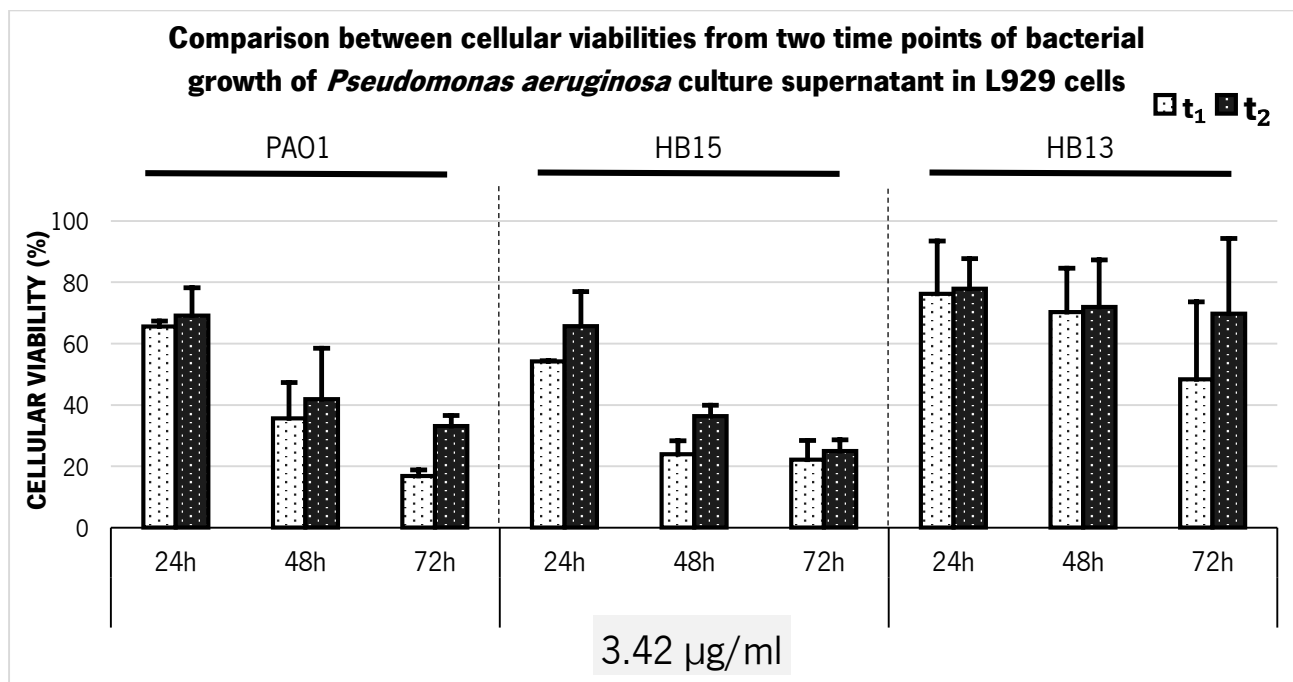


Figure 16 – Comparison between cellular viabilities from two time points of bacterial growth of *Pseudomonas aeruginosa* culture supernatant in L929 cells. The graphic displays the comparison of the cellular viabilities results in L929 cells from the MTT assay for each *Pseudomonas aeruginosa* strains (PAO1, HB15 and HB13) culture supernatants at the concentration 3.42 µg/ml, in all the 3 end times of incubation (24h, 48h, 72), between the bacterial growth periods t1 (24 hours of bacterial growth) and t2 (48 hours of bacterial growth). The resulting data was statistically analysed by a One-way ANOVA with Tukey test where the P value was set for: P < 0.05. Significant values comparing cellular viabilities between t1 and t2 were represented in the graphic as, * for P < 0.05, ** for P < 0.01 and *** for P < 0.001.

The cytotoxicity of the *P. aeruginosa* strains supernatants was measured in cellular viability compared to the negative control where the fibroblast cells simply grew in their culture medium.

In Figure 17 are shown the cellular viabilities for two concentrations of the supernatants used where the results were most significant. It is only shown the results from t₁ supernatants, since there were no significant differences between the cellular viabilities of supernatants from the two time points of the bacterial growth. Results of all the serial concentrations tested in appendix (Figure A 2, Figure A 3, Figure A 4). The results showed an effective cytotoxicity of the *P. aeruginosa* strains affecting these cells.

The strains led to different cellular viabilities, implying that they possess different cytotoxicity potential and therefore different pathogenicity.

At the concentration of 3.42 µg/ml, the cellular viability was affected significantly in the PAO1 and the HB15 strains, in all timepoints of incubation considered. In the HB13 strain, the viability was affected significantly only after 72h of incubation with the supernatants.

The strains from the clinical isolates studied here acted as expected, given previous evidences on their pathogenicity, in which the HB15 revealed a more aggressive infection potential than HB13. Previous studies performed by Soares-Castro *et al.* (2011) already indicated different levels of pathogenicity of these two strains. The HB15 demonstrated to possess unique genes that encode several virulence factors, contrary to the HB13 strain. Furthermore, the production of bacterial pigments, characteristic of virulent strains, was found dissimilar between these strains, where the HB15 strain was able to produce large amounts of pyocyanin pigment while in the HB13 strain its production was absent [94].

In the results displayed in Figure 17, the HB15 strain caused significant cytotoxicity, even more pronounced than the reference PAO1 strain after 24 and 48 hours of incubation with the supernatants. On other hand, the HB13 strain caused minor cytotoxicity. Another analysis of the results showed that, after 48h of incubation with the supernatants, the cellular viability values associated to the three strains were more disparate, with 24% of cellular viability for HB15 strain, 36% of cellular viability for PAO1 strain and 70% of cellular viability for HB13. It is possible to fit this finding in a cytotoxicity level ranking where apparently the HB15 strain is the most cytotoxic strain, with less than 1.5 times PAO1's cellular viability and almost less than 3 times HB13's cellular viability.

At the concentration of 20.50 µg/ml, six times the prior concentration, all strains severely affected cellular viability in L929 cells.

The results were all strongly significant with some values of 10% of cellular viability in the PAO1 and the HB15 strains, which was lesser than the positive control viability values (30% DMSO).

At this high concentration, the cytotoxicity variance between the strains was less prominent. Though, the HB15 strain apparently caused the highest cellular death compared with the other strains. And the HB13

strain despite of causing, in this concentration, significant cellular death, maintained itself as the less cytotoxic strain.

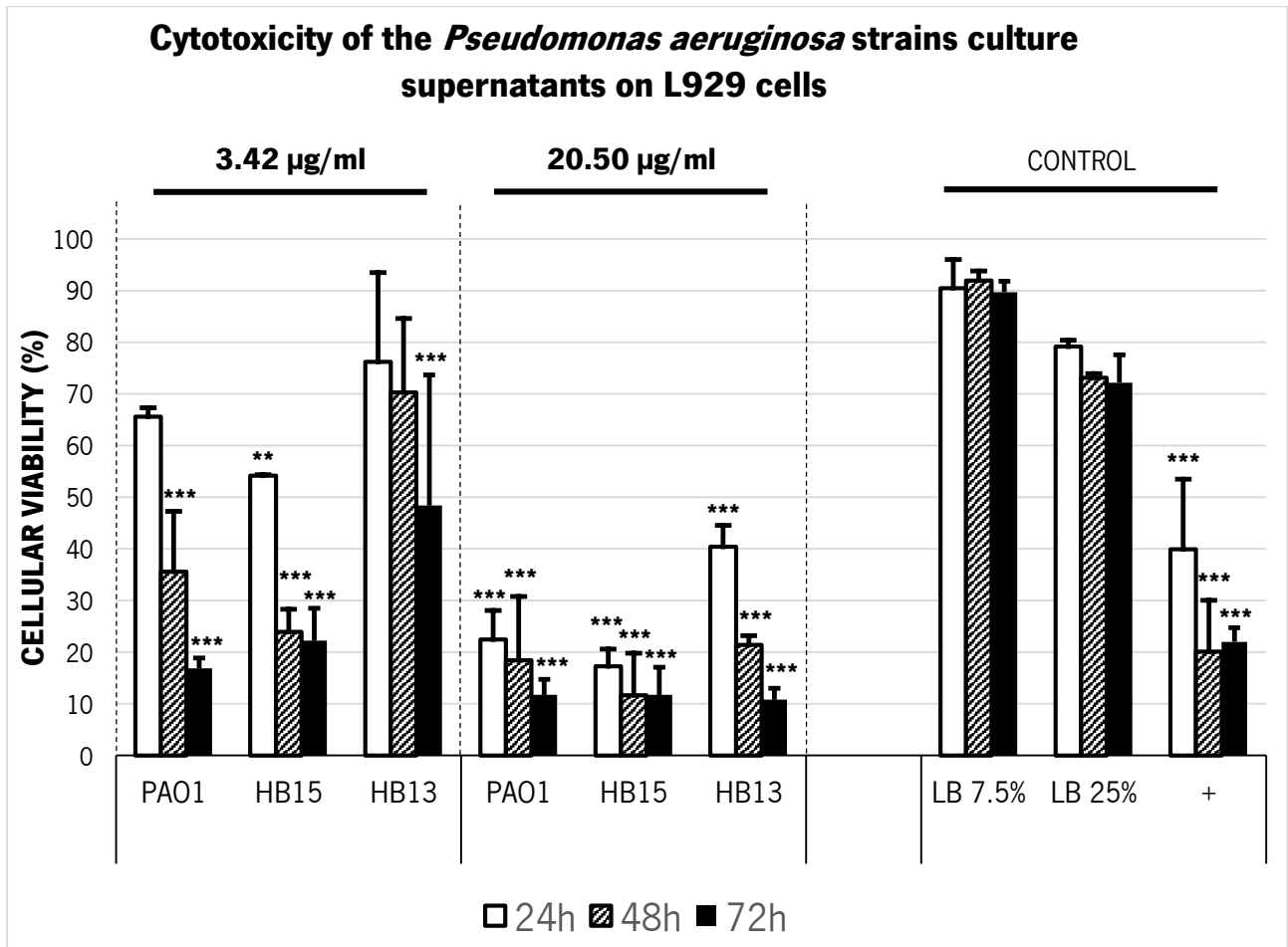


Figure 17 - Cytotoxicity of the *Pseudomonas aeruginosa* strains culture supernatants on L929 cells. The graphic displays the results of the MTT assay performed on L929 cells submitted to two total protein concentrations (3.42 µg/ml and 20.50 µg/ml) of the culture supernatants of the *Pseudomonas aeruginosa* strains (PAO1, HB15 and HB13) in cell viability percentage represented by bars with the respective standard deviation represented by vertical lines for a number of replicas n=2. The bar legend represents the end times of incubation (24h, 48h and 72h) with the supernatants. The full data is available in the appendix section of the thesis. The controls are presented in the graphic represented as "CONTROL". The negative control has the constant value of 100% of viability for each end times of incubation and not shown in the graphic. The positive control is represented as "+" on the graphic. The controls of the bacterial culture media (LB) are represented on the graphic as "LB 25%" and "LB 7.5%". The resulting data was statistically analysed by a One-way ANOVA with Tukey test where P value was set for: P <0.05. Significant values comparing to the negative control were represented in the graphic as, * for P <0.05, ** for P <0.01 and *** for P <0.001.

In the control set, the negative control value was assumed as 100% of cellular viability in all periods of incubation, in the MTT assay.

The positive control, as expected, caused high cellular toxicity in L929 cells. The DMSO used as control induces cell death by lethal membrane permeation [169], therefore its use was important to compare cytotoxicity levels associated to the supernatants.

The LB medium controls did not cause any significant effect on cellular viability. Therefore the LB medium present in the supernatants did not contribute significantly to the effective cytotoxicity of the secreted virulent factors in the supernatants.

The LB medium controls were performed in two different concentrations (7.5% and 25%) in order to evaluate the dilution effect of the medium components. Although it was not significant, there was a higher disturbance in cellular viability (values between 70% and 80% (v/v)) with the highest concentration of LB medium (25% (v/v)). These results indicated that the LB medium proper components may interfere with cell viability when cells are exposed to the supernatants. In fact, the LB medium contains, aside of the yeast extracts and tryptone, considerable concentrations of salts (NaCl). This concentration of salt might be inducing an osmotic shock when the LB medium is added to the L929 cells, causing some cell death. It is shown in the literature that the effect of osmotic stress causing effective damage in animal cells [170].

The cytotoxicity tests were continued on the A549 cell line. After the evaluation of the supernatants effect on L929 cells' viability showing an effective cytotoxicity, it became relevant to analyse the cytotoxicity level induced with the supernatants in this different cell line model.

The A549 cell line is a widely used *in vitro* model of pulmonary epithelia type II, responsible for the gas-exchange in the respiratory system. Therefore, this cell line mimics one of the cellular tracts most affected by *Pseudomonas aeruginosa* infections, instigating the relevance of studying the effect of the supernatants on this cell line.

As in the other cell line, the A549 cells were submitted to incubation with culture supernatants from two different timepoints of bacterial growth (t_1 and t_2). The analysis of the cellular viability results demonstrated that the supernatants from the timepoints of bacterial growth t_1 and t_2 caused similar cytotoxicity.

In Figure 18, it was selected the concentration (3.42 $\mu\text{g}/\text{ml}$) where the cellular viabilities differences between the t_1 and t_2 were most noticeable. The results shown a tendency where the t_1 supernatants induced more cellular death than the t_2 supernatants, however not as perceptible as in L929 cells, and still not significant.

The cytotoxicity of the *P. aeruginosa* strains supernatants on A549 cells was measured according as previous in L929 cells.

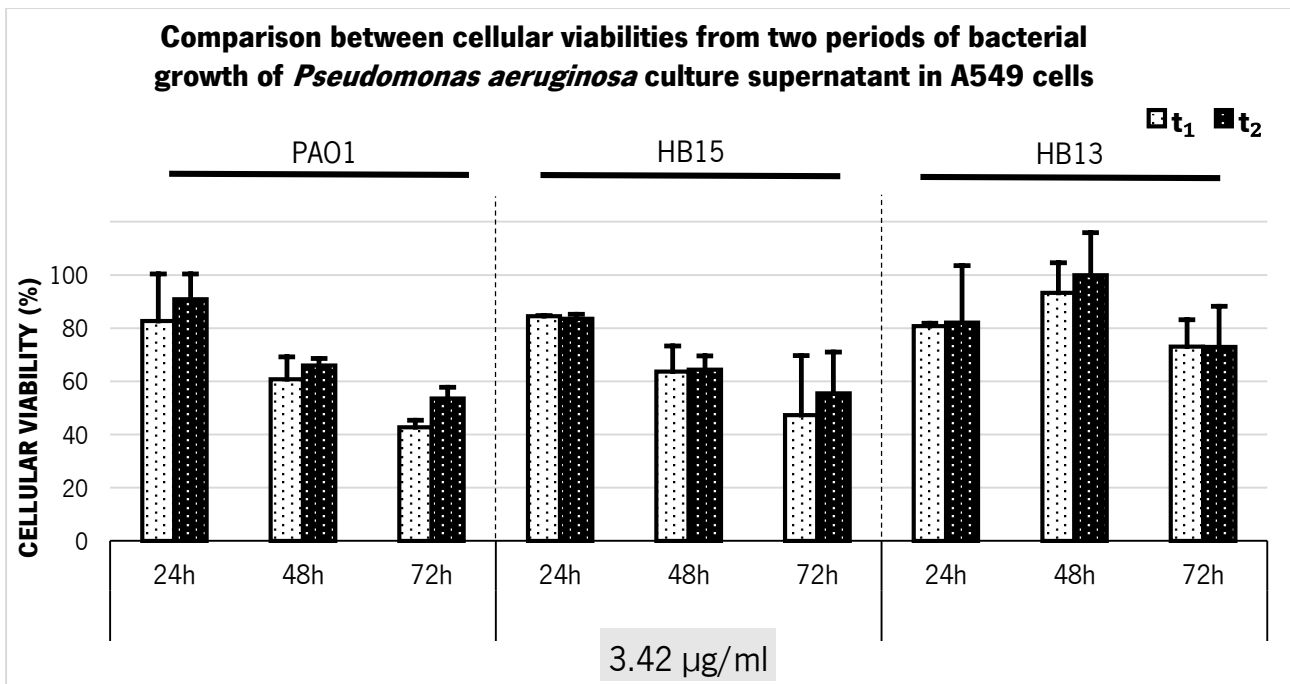


Figure 18 – Comparison between cellular viabilities from two periods of bacterial growth of *Pseudomonas aeruginosa* culture supernatant in A549 cells. The graphic displays the comparison of the cellular viabilities results in A549 cells from the MTT assay for each *Pseudomonas aeruginosa* strains (PAO1, HB15 and HB13) culture supernatants at the concentration 3.42 µg/ml, in all the 3 end times of incubation (24h, 48h, 72), between the bacterial growth periods t₁ (24 hours of bacterial growth) and t₂ (48 hours of bacterial growth). The resulting data was statistically analysed by a One-way ANOVA with Tukey test where P value was set for: P <0.05. Significant values comparing cellular viabilities between t₁ and t₂ were represented in the graphic as, * for P <0.05, ** for P<0.01 and *** for P<0.001.

In Figure 19 is shown that the cytotoxicity of the strains supernatants in cellular viability. The graphic shows the results for the two concentrations with the most significant results and give relevant information about the supernatant effect. Results of all the serial concentrations tested in appendix (Figure A 5, Figure A 6, Figure A 7). As before, it was only shown the results from t₁ supernatants since there were no significant differences between the two timepoints of bacterial growth.

At the concentration 3.42 µg/ml, the cytotoxicity of the supernatants demonstrated only significant effect on the A549 cells after 48h of incubation. In this situation, the HB13 strain was not able to produce any significant cellular death in all incubation times. The PAO1 strain and the HB15 strain supernatants led to similar cellular viability results.

The cytotoxicity of the supernatants at the concentration 20.50 µg/ml showed a significantly higher percentage of cellular death comparatively to the previous concentration (3.42 µg/ml). As in the L929 cells, at this concentration the PAO1 and HB15 strains showed a strong significant effect in the cellular viability in all periods of incubation. Contrarily, the HB13 strain at this concentration only induced a strong significant effect on cellular viability after 72 h of incubation, and yet, its cellular viability (40%) remained superior to the highest cellular viabilities of the PAO1 and HB15 strains (30% and 25%, respectively).

These results showed that the HB13 strain causes minor cytotoxic strain as previously has been demonstrated, comparatively to the other strains.

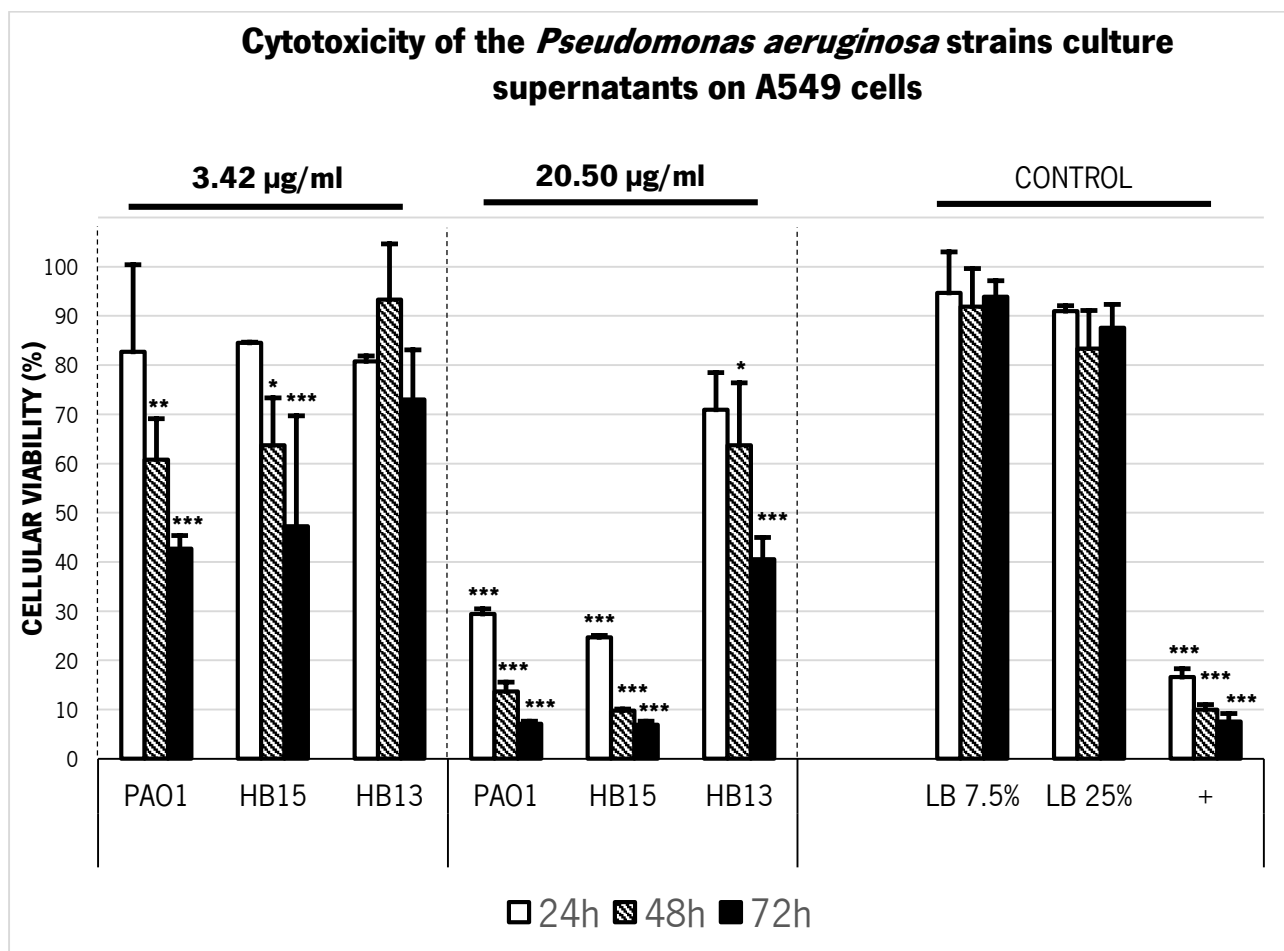


Figure 19 - Cytotoxicity of the *Pseudomonas aeruginosa* strains culture supernatants on A549 cells. The graphic displays the results of the MTT assay performed on A549 cells submitted to two total protein concentrations (3.42 µg/ml and 20.50 µg/ml) of the culture supernatants of the *Pseudomonas aeruginosa* strains (PAO1, HB15 and HB13) in cell viability percentage represented by bars with the respective standard deviation represented by vertical lines for a number of replicas n=2. The bar legend represents the end times of incubation (24h, 48h and 72h) with the supernatants. The full data is available in the appendix section of the thesis. The controls are presented in the graphic represented as “CONTROL”. The negative control has the constant value of 100% of viability for each end times of incubation and not shown in the graphic. The positive control is represented as “+” on the graphic. The controls of the bacterial culture media (LB) are represented on the graphic as “LB 25%” and “LB 7.5%”. The resulting data was statistically analysed by a One-way ANOVA with Tukey test where P value was set for: P <0.05. Significant values comparing to the negative control were represented in the graphic as, * for P <0.05, ** for P <0.01 and *** for P <0.001.

The control set was performed as previously and the results were similar as the obtained with the L929 cells as expected. This might indicate that A549 cells are more susceptible to DMSO than the L929 cells.

In all strains, the cellular viability presented high values comparatively to the previous results in L929 cells. These results indicate that the two cell line models in study possess different susceptibilities to the associated virulence of the *P. aeruginosa* strains.

3.5.2. Comparison of cytotoxicity in L929 and A549 cell lines exposed to culture supernatants from the *P. aeruginosa* strains

The cell lines used in this study displayed different susceptibilities to the associated cytotoxicity of the *P. aeruginosa* strains culture supernatants. In general, at the same concentrations, the supernatants cause more cytotoxicity in L929 cells than in the A549 cells.

In Figure 20 are shown the supernatant concentrations where the cellular viability variance between L929 cells and A549 cells was most noticeable.

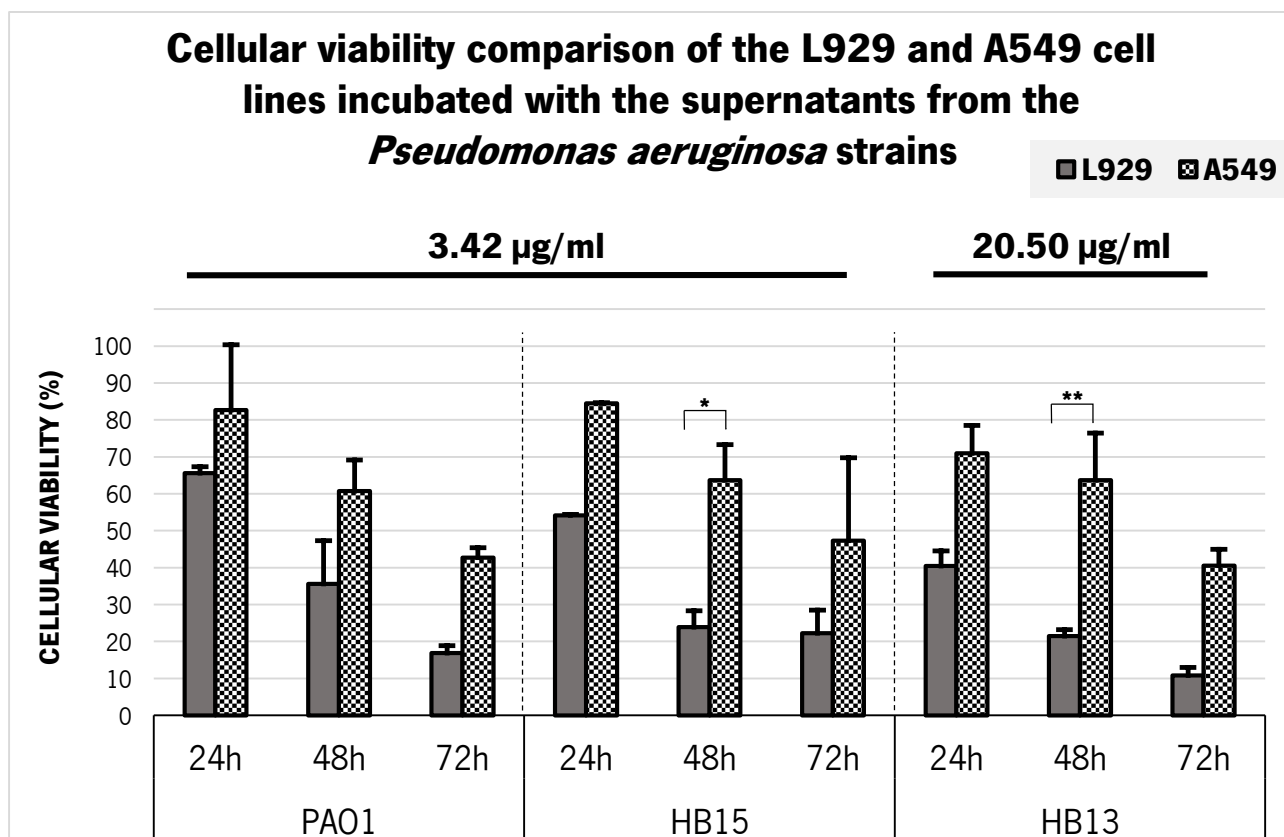


Figure 20 – Cellular viability comparison of the L929 and A549 cell lines incubated with the supernatants from the *Pseudomonas aeruginosa* strains. The graphic displays the comparison of the cellular viabilities results of the MTT assays performed between the two cell lines L929 and A549 incubated with two concentrations (3.42 µg/ml and 20.50 µg/ml) of culture supernatants of the *Pseudomonas aeruginosa* strains where the viability variance between cell lines were highest. The cellular viabilities are represented for all end time points of incubation with the supernatants. The full data is available in the appendix of the thesis. The graphic bars represents the cellular viability percentage and the respective vertical lines represents the standard deviation, for a number of replicas n=2. The resulting data was statistically analysed by a One-way ANOVA with Tukey test where p value was set for: P <0.05. Significant values comparing cellular viabilities of L929 cells and A549 cells were represented in the graphic as, * for P <0.05, ** for P <0.01 and *** for P <0.001.

The PA01 and HB15 strains supernatants lead to highest cellular viability variances between the two cell lines at 3.42 µg/ml. At this concentration, with the HB15 strain, the highest significant variance value reached 40% of viability, after 48 h of incubation.

On the other hand, the HB13 strain has the highest viability variances between the two cell lines at 20.50 µg/ml. At this concentration, the highest significant variance value reached 42% of viability, at 48 h of incubation.

The concentrations where the cellular viability variance between the two cell lines were more noticeable appears to be related with the cytotoxicity level. Either too high or too low supernatant concentrations cause cellular viability results in a stage of *plateau* where the concentration effect is constant. Given that, the cellular viability comparison between cell lines is not suitable at these concentrations. Concentration where effect is strictly dependent of concentration, such concentrations are near to a half maximum death concentration, are more likely to produce relevant information about different susceptibilities of two cell lines.

The appreciable cellular viability discrepancies between the two cell lines incubated with the supernatants demonstrate that these two cell models have different cellular features and mechanisms that provide more or less susceptibility to the virulence factors action which in consequence affect the cytotoxicity level. There is not, however, much information in literature about what molecular processes are responsible for the susceptibility level of the cell lines to the secreted virulence factors of the *P. aeruginosa* strains.

The pathogenic characterization of the *P. aeruginosa* strains here performed based in the cytotoxicity tests revealed significant and expected rates of cell death in the cell models employed. In order to support these results, cellular damage and stress levels were assessed.

3.6. Morphology alteration studies

The effects of bacterial pathogenicity at the cellular level can be analysed by direct microscopy observation. In the course of this thesis work, during the cytotoxicity tests, the cells incubated with the secreted virulence factors were firstly observed at the optical microscope in order to detect induced morphological alterations in the cells and/or evidences of apoptosis and necrosis, and therefore establish analytical associations with the results of the cytotoxicity tests.

Secreted virulence factors from *P. aeruginosa* had been reported to induce morphologic alterations in cell lines. Virulent factors such as elastases (LasA and LasB) induced the tissue elastin destruction [171], alkaline proteases (AprA) induced damage on basal laminin [38], the TTSS system responsible for secretion of exoenzymes causing cytoskeleton actin alteration [40] also associated surfactants as rhamnolipids exhibited interference with cell-to-cell communication and disrupting cellular tight junctions [43]. Cellular apoptosis induced by secreted virulence factors of the *P. aeruginosa* had been also reported in cell lines [172]–[177]. The exoenzyme ExoS secreted by T3SS caused the inhibition of the ERK1/2 and the p38 activation in HeLa cells, leading to the shutdown of the host cell survival signal pathways, subsequently leading to activation of proapoptotic pathways through elicitation of JNK1/2, and consequently lead to cytochrome c release and caspase activation [176]–[178]. The T3SS system had also been reported as an inducer of cellular apoptosis, not only by *P. aeruginosa* but also other several bacteria [174]. Pyocyanin produced by *P. aeruginosa* was also shown to induce apoptosis in neutrophils associated with consistent and swift generation of reactive oxygen intermediates and consequent reduction of intracellular cAMP [175]. Another cellular death form, necrosis, was verified in macrophages induced by *P. aeruginosa* secreted virulence factors such ExoU [174].

These previous findings supported the need to search for evidences of morphological disorders in the cells incubated with the *P. aeruginosa* supernatants that could correlate with the cytotoxicity tests described previously.

3.6.1. Cellular morphological changes in L929 cell line

The L929 cell line, as previously described, are fibroblast murine cells with a spindle shape form, occasionally presenting a stellate form. These adherent cells are robust and proliferate well in proper conditions and media. As described in the methods of this work thesis, the L929 cells were seeded in 96 well plates at an initial density of 55,000 cells/ml in purpose of performing the cytotoxicity tests. All wells seeded with L929 at the initial density were let grown through 24 hours before starting the incubations with the *P. aeruginosa* strains supernatants that ended then at 24h, 48h and 72h.

It is observable that the L929 cells grow well and reached a state of confluence at the time of 48h of the end points of the incubations with the supernatants. Cell culture growth through time are displayed in the appendix (Figure A 8).

The microscopy observations of L929 cells culture show the spindle and stellate shaped fibroblast cell population with presence of filopodia characteristic of the L929 cell line. It was also observable round shaped fibroblast cells, the emergence of this different shape dues to the entering of L929 cells in mitotic phase which confers round shape to the cell [179], [180].

The effect of *P. aeruginosa* virulence factors on these cells had induced noticeable morphological alterations at cellular level (Figure 21). All strains demonstrated to be able to cause morphologic disorders in the cells in a concentration- and time-dependent manner. Significant morphologic alterations in these cells were most noteworthy with the two highest concentrations (3.42 µg/ml and 20.50 µg/ml).

Cell density appears to decrease in function of time and through concentration increase. The direct observation and analysis of the cells incubated with the *P. aeruginosa* strains supernatants suggests a correlation between cell density and the previous cytotoxicity data results, with lower cell density the lower cellular viability. Although, cell density alone cannot make a direct relation with cellular viability since cells could maintain its structural integrity but lost its cellular functions and so, its cellular viability [181].

Aside cell density, significant cellular phenomena are observable in the cells incubated with the *P. aeruginosa* strains supernatants. One of the most noticeable morphological alterations in L929 cells incubated with the supernatants is the loss of its cellular spindle and stellate shape for a cellular round shape. All strains demonstrated to be able to cause cellular shape alteration, given that this feature is more distinct in the cells incubated with the strains PAO1 and HB15 (Figure 21), previously labelled has the most cytotoxic strains by the cytotoxicity tests results. The strain HB13, previously labelled as the less cytotoxic strain, was only capable of inducing a significant cellular shape alteration at the highest concentration after 72h of incubation (Figure 21). Although the presence of round shape L929 cells were referred above as cells that underwent mitosis in normal conditions, when incubated with the strains supernatants, the increasing appearance of round shape cells may be due to virulence factors of the strains, termed as cytopathic effect [182]. It was previously reported that HeLa cells under bacterial virulence factors lost their spindle shape to a round shape as also decrease the cell adherence [183]. Another study showed that L929 spindle cells underwent in a round shape after incubation with culture supernatant of *Mycobacterium ulcerans*. The alteration to a cellular round shape is attributed to the cytoskeleton rearrangement because of changes in the actin structure [182].

Morphologic alterations in L929 cells induced by PA strains

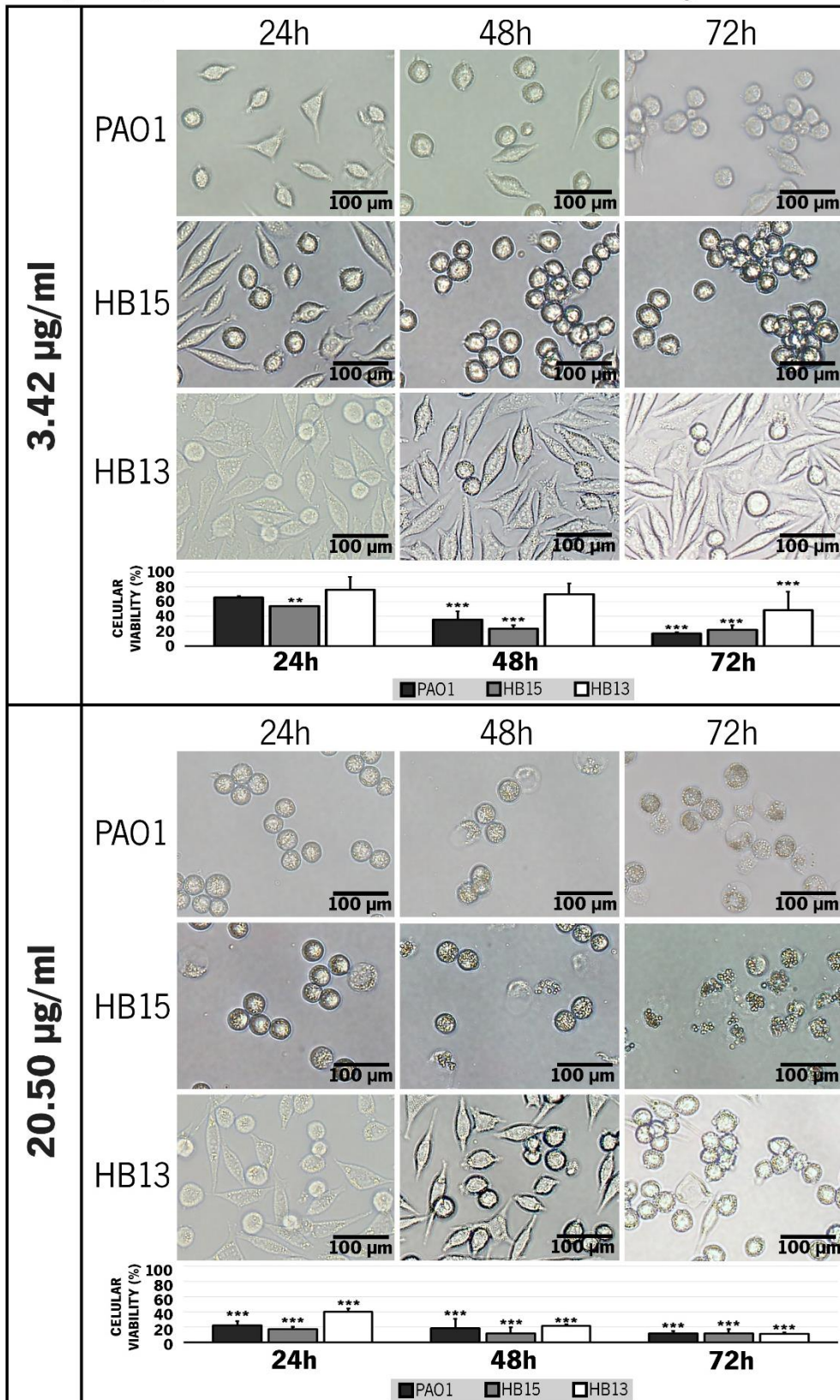


Figure 21 - Morphologic alterations in L929 cells induced by *Pseudomonas aeruginosa* strains culture supernatants.

The figure shows the L929 cells morphology alterations induced by *Pseudomonas aeruginosa* strains culture supernatants, cultured in 96 well plate, using phase contrast microscopy. The figure is divided in two sections, referring to morphologic alterations at 3.42 µg/ml and 20.50 µg/ml. The images of the cells are displayed by incubation times (24, 48 and 72 hours) horizontally and by *P. aeruginosa* strain (PAO1, HB15 and HB13) vertically. The scale bars represents 100µm length. Cytotoxicity data from previous results are shown to make relation between cellular viability and cellular morphology observations. Data represents the means ± SD, n=2 independent experiments. * for P < 0.05, ** for P < 0.01 and *** for P < 0.001.

Moreover, *P. aeruginosa* has been reported as being able to induce cytopathic effect on cells [184], [185]. In a study by Zanetti *et al.*, the multifactorial factor of the *P. aeruginosa* toxins in Hep-2 cells caused cytopathic effects [186]. Together with cell shape alteration, the cultured cells display agglutination clumps through the plate well surface, emerging in a time- and concentration-dependent manner of the strains supernatant. Above this feature, the more cytotoxic strains, PAO1 and HB15, are most noticeable. The L929 cell distribution under the influence of the strains supernatant begin to form visible cell clumps after 48h of incubation with 3.42 µg/ml and after 24h of incubation with 20.50 µg/ml of HB15 supernatant (Figure 21). For the PAO1 strain, distinct cell clumps begin to be visible only after 72h of incubation with 3.42 µg/ml (Figure 21). And for HB13 strain, there are no visible cell clumps at all times of incubation with 3.42 µg/ml, being only distinguishable after 72h of incubation with 20.50 µg/ml (Figure 21). Although there is not much information about cell agglutination caused by bacterial virulence factors, in particular with L929 cells and *P. aeruginosa* virulence factors, earlier observations have been described of cell clumps in animal cells caused by bacterial cell secreted products associated with apoptosis [187]. One of the most relevant morphologic alterations on the L929 cells induced by the supernatants of the *P. aeruginosa* strains observed by microscopy was cellular blebbing or zeiosis and formation of vesicles, much likely apoptotic bodies. Cell blebs are protuberances or bulges on the cytoplasmic membrane induced by localized disassembling of the cytoskeleton, associated to specific physiological functions including apoptosis [188], [189]. Apoptotic bodies are small vesicles derived from a cell undergoing in an apoptosis phase, frequently preceded by cell blebbing [190], [191]. Cellular vesicles were distinctly visible in the strains PAO1 and HB15 whereas in the strain HB13 presence of cellular vesicles is less distinguishable. In most cytotoxic strains, PAO1 and HB15, at the higher concentration after 48h of incubation, are visible isolated small vesicles, round cells presented abundant intracellular vesicles and blebs, and also cell lysis. These morphologic alterations are more accentuated in the HB15 strain, suggesting a more aggressive pathogenicity than its counterpart PAO1. After 72h of incubation, the majority of the cell were converted in small vesicles (apoptotic bodies) induced by HB15 strain whereas in the PAO1 there is still several cells with cytoplasmic membrane integrity. In the least cytotoxic strain, HB13, no significant formation of vesicles are observed with exception of the highest concentration (20.50 µg/ml) after 72h of incubation where traces of intracellular vesicle formation could be observed. Again it is observable for this morphologic alteration a time- and concentration-dependent relation, where the more the concentration and the time, the more is the cell blebbing and small cellular vesicles formation (apoptotic bodies). These observed morphologic alterations support the suggestion that these cells under influence of virulence factors of the *P. aeruginosa* strains underwent in apoptosis. It had already been previously stated the propensity of secreted virulence factors of *P. aeruginosa* to induce apoptosis in animal cells [174], [175]. Apoptotic features such as formation of apoptotic bodies has been reported in HeLa cells, and in other epithelia and fibroblast cells induced by *P. aeruginosa*

[178]. Furthermore has been reported formation of apoptotic bodies in endothelial cells induced by *P. aeruginosa* culture supernatants [192].

In order to enhance the observation of these morphologic changes at cellular level suggesting that L929 cells underwent an apoptotic phase induced the culture supernatant of the *P. aeruginosa* strains, a fluorescence microscopy assay was conducted.

The further microscopy fluorescence analysis of the intracellular morphological alterations of the L929 cells induced by the *P. aeruginosa* strains focussed on changes of the cytoskeleton and nucleus of the cells. In order to achieve both cytoskeleton and nucleus structure image representation, each organelle was labelled with fluorescence stains. The L929 cytoskeleton was label with the commercial probe Phalloidin Alexa Fluor 568, a high affinity F-actin probe, constituted with a bicyclic heptapeptide toxin, Phalloidin, which interacts with actin filaments preventing its depolymerisation, and a red dye, Alexa Fluor 568 [193], [194]. On the other hand, the L929 nucleus was labeled with the commercial dye Hoechst 34580, a bisbenzimidazole blue dye that binds to the DNA double strand minor groove [195].

Given the previous results, it was selected a specific concentration and incubation time to apply the fluorescence microscopy to. All L929 cell cultures samples were let grown in 24-well plates for 24 hours. In the positive control, L929 cells were let grown incubated with only DMEM medium. In the L929 cells incubated with the *P. aeruginosa* strains supernatants, the cells were incubated with 3.42 µg/ml of supernatant from each *P. aeruginosa* strain. After incubation, the samples were transferred into cover slips for microscope observation (Figure 22).

The obtained fluorescence microscopy images show distinct cytoskeleton and nucleus structures in all samples (Figure 22). In the control group, the cytoskeleton staining shows distinguishable actin filaments drawing the cellular shape. The L929 fusiform and stellate cell shape is also visible. The nucleus staining displays typical L929 uni-nucleated cells where the nucleus appears as a single integral organelle. In the samples of L929 cells incubated with *P. aeruginosa* strains supernatants morphological alterations were verified distinguishable. In the L929 cells incubated with 3.42 µg/ml of PAO1 strain supernatant it was verified cells developing cell blebs and nuclear fragmentation. In Figure 22 (PAO1), it is observable a cell exhibiting a bleb in its cytoplasmic domain traced by the phalloidin Alexa Fluor 568 stained cytoskeleton F-actin, pointed by white arrow. The cell blebbing phenomena observation at fluorescence microscopy with F-actin staining was been described, previously, as the emergence of the cellular bleb by initial F-actin rupture and hydrostatic pressure, the same F-actin promptly assemble at the bleb cortex, which became visible when using this technique [188]. In the same figure is visible a multi-nucleated cell with Hoechst 34580 stained six reduced nucleus indicating nuclear fragmentation. Nuclear fragmentation is one of the hallmarks of the apoptotic process [196], and it was previously reported in L929 cell line under virulence factors influence [197]. These findings, cell blebbing and

nuclear fragmentation, are in agreement with the above phase-contrast microscopy observations (Figure 21) and previous literature references, indicating that L929 cells enter an apoptotic phase.

In the cells incubated with 3.42 µg/ml of HB15 strain supernatant, concrete apoptotic hallmarks as in the cells incubated with PAO1 strain supernatant (Figure 22), were not visible which was expected based on similar observations given previous results. The fact of the technique used for this fluorescence microscopy required many steps and double staining procedure might produce undesired results if mismanaged, which in this circumstance is causing the unreliable results.

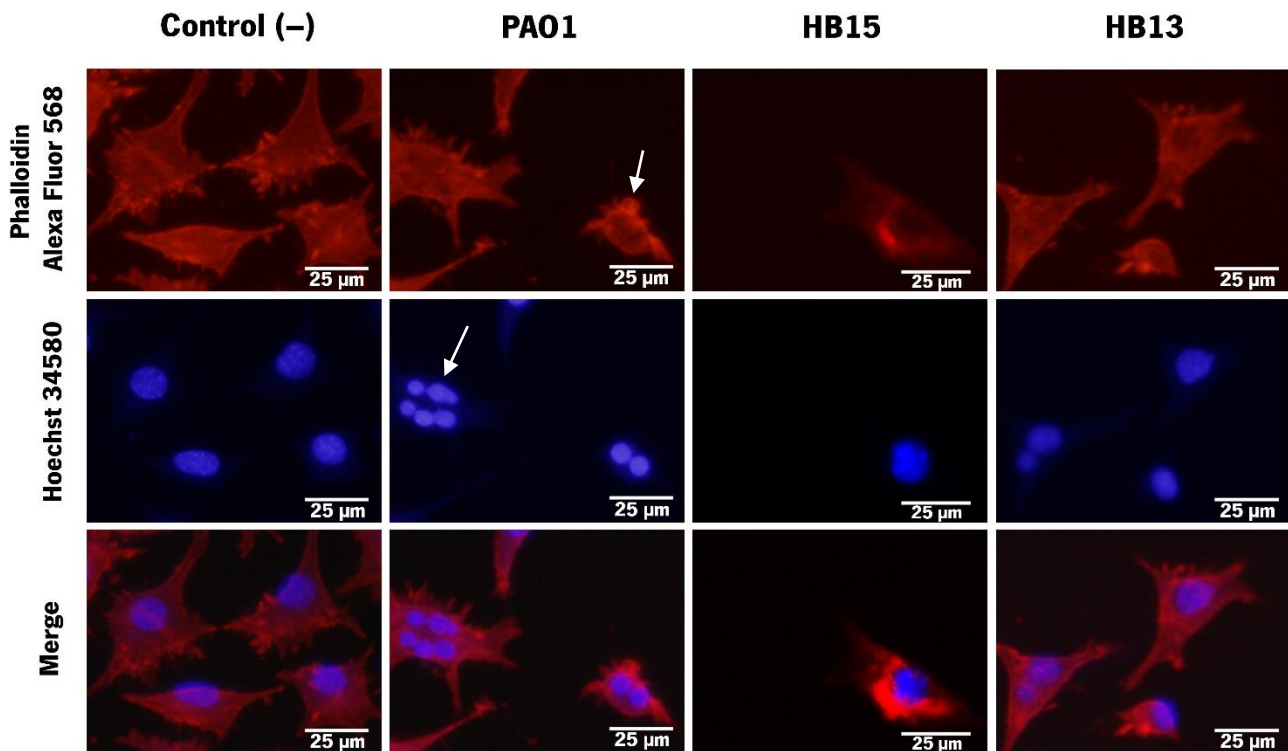


Figure 22 - Fluorescence microscopy of L929 cells to study morphological features induced by *Pseudomonas aeruginosa* strains. The cytoskeleton of the L929 cells are stained with the probe Phalloidin Alexa Fluor 568 (red) and the nucleus of the L929 cells are stained with the bisbenzimidazole dye Hoechst 34580 (blue). The merging of the individual stained components provides a composite image refining the cellular morphology observation. The L929 control cells cultured in DMEM medium, grown for 24h and transferred in cover slips for prior microscopy observation are represented as “Control (–)”. The L929 cells incubated with the supernatants of the *P. aeruginosa* strains are represented as “PAO1”, “HB15” and “HB13”. All cells were incubated with 3.42 µg/ml of *P. aeruginosa* strains supernatants during 24h, respectively and transferred in cover slips for prior microscopy observation. The white arrows points to noteworthy morphological features, in the up row (Phalloidin Alexa Fluor 568) indicates a visible cellular blebbing and in the middle row (Hoechst 34580) indicates a visible nuclear fragmentation. The scale bar represents 25 µm length.

In the cells incubated with 3.42 µg/ml of HB13 strain supernatant, there were no distinguishable noteworthy apoptotic hallmarks as in the PAO1 strain, which given the previous results, was expected because the HB13 strain was already classified as the less cytotoxic strain and L929 cells incubated at this concentration for 24 hours evidenced insignificant morphological alterations, furthermore presenting an high cellular viability (Figure 21).

In an overall analysis of fluorescence microscopy applied to the L929 cells, it was availed determining cellular structures remarks that corroborate with previous results and the indication of *Pseudomonas aeruginosa*

strains inducing apoptosis. Although the results did not show an high quantity of these apoptotic cellular structures and the preliminary procedural mismanagements of this technique on the cells incubated with HB15 strain supernatant avoided reliable results to use for strains effect comparison. Time and cost-effective limitation determined the use of a specific time/supernatant concentration (24h and 3.42 µg/ml) incubation of the cells, however, given the obtained results, using the higher concentration (20.50 µg/ml) of supernatant and the incubation times pre-defined previously (24h, 48h and 72h) would give an enhanced and more substantial results.

3.6.2. Cellular morphological changes in A549 cell line

Cellular morphological changes were analysed in A549 cells regarding the same microscopy procedure as in the analysis of cellular morphological changes in L929 cells. As already described, the A549 cell line are hypotriploid adenocarcinoma cells from basal epithelia of the human lung alveoli, these cells present a squamous shape and are organized as an adherent monolayer *in vivo*.

A549 cells were seeded in 96 well plates at an initial density of $1,0 \times 10^5$ cells/ml with the purpose of performing the cytotoxicity tests, as previously described in the methods of this work thesis. All wells seeded with A549 at the initial density were let grown through 24 hours before starting the incubations with the *P. aeruginosa* strains supernatants that ended then at 24h, 48h and 72h.

It is observable that the A549 cells grow well and reached a state of confluence at the time of 48h, the end points of the incubations with the supernatants. Cell culture growth over time is displayed in appendix (Figure A 9).

The microscopy observations made from the A549 cells culture grown with only the proper medium show the typical stellate shaped epithelial cells population cell. As in the L929 cell line culture, the presence of observable round shaped cells is due to the entering in mitotic phase of A549 cells which confers round shape to the cell [179], [198].

The A549 cells under the influence of the secreted virulence factors of the *P. aeruginosa* strains revealed significant morphological alterations at cellular level (Figure 23).

As in L929 cells, all strains demonstrated to be able to cause morphologic disorders in a concentration- and time-dependent manner. Significant morphologic alterations in these cells were most noteworthy in the two highest concentrations (3.42 µg/ml and 20.50 µg/ml).

As previously reported for L929 cells, one of the first morphological alterations observed in A549 cells incubated with *P. aeruginosa* virulent factors is the cell density decreasing in function of time and increasing concentration, which is one of the causes that lead to cellular unviability [181]. It is observable that there is a relation between cell density and cellular viability, while is observable in the Figure 23, that the least the cell density the least the cellular viability.

Morphologic alterations in A549 cells induced by PA strains

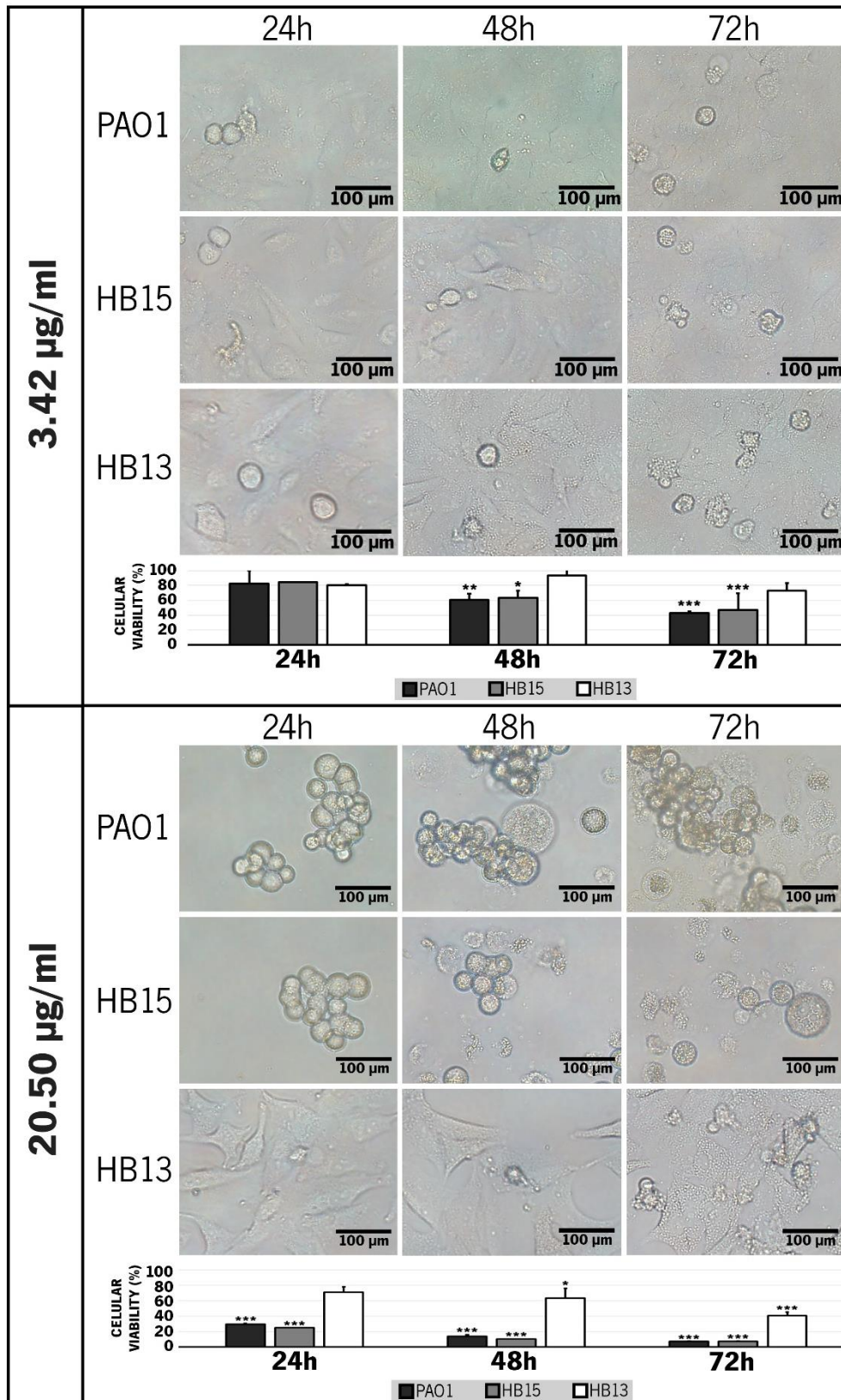


Figure 23 - Morphologic alterations in A549 cells induced by *Pseudomonas aeruginosa* strains culture supernatants.

The figure shows the A549 cells morphology alterations induced by *Pseudomonas aeruginosa* strains culture supernatants, cultured in 96 well plate, using phase contrast microscopy. The figure is divided in two sections, referring to morphologic alterations at 3.42 µg/ml and 20.50 µg/ml. The images of the cells are displayed by incubation times (24, 48 and 72 hours) horizontally and by *P. aeruginosa* strain (PAO1, HB15 and HB13) vertically. The scale bars represents 100µm length. Cytotoxicity data from previous results are shown to make relation between cellular viability and cellular morphology observations. Data represents the means ± SD, n=2 independent experiments. * for P < 0.05, ** for P < 0.01 and *** for P < 0.001.

One of the most noticeable morphological alterations in the A549 cells incubated with the *P. aeruginosa* supernatants is the change in cell shape and size. A general effect is observable with the virulent factors that cause A549 epithelial cellular shape to modify to a rounder shape and the independent appearance of some cells of odd size (Figure 23).

These alterations are more noticeable in cell cultures exposed to the supernatants from the PAO1 and HB15 strains, increasingly evident with concentration increase and longer incubation time. In cell cultures incubated with HB13 strain supernatant, this feature is not so noticeable. In fact only with the highest concentration (20.50 µg/ml) and after 72h of incubation time, the cell culture displays significant morphological alterations in cell shape. Again, the HB13 strain is the least pathogenic strain and, as observed in the L929 cells, it does not induce morphological alteration to the same extent as the other strains.

Changes in the original A549 cell shape to a round form under the effect of virulence factors have been described. It was reported that staurosporine from *Streptomyces staurosporeus* induced the A549 cells spindle and triangle shape to change to a round shape [199]. Another study reported *Pseudomonas aeruginosa* strains inducing cytopathic effects, such as cell rounding, in A549 cells [200].

The occurrence of cell agglutination clumps is observed in A549 cultures incubated with *P. aeruginosa* strains virulent factors, as previously observed in L929 cultures (Figure 23). Although the supernatants from HB13 strain did not induce any visible agglutination in A549 cells, the supernatants from PAO1 and HB15 strains had a significant impact in their highest concentration (20.50 µg/ml). The formation of agglutination clumps appears to be occurring in a time- and concentration-dependent manner, where the number of cell agglomerates grows along time. With the exception of the highest concentration of the supernatant of HB15 strain, where the damaging level caused by the virulent factors present in the supernatant appears to impair the formation of cell agglomerates. The agglutination clumps observed in A549 cells are more distinct and extended than in L929 cells, suggesting that in A549 cells cell-to-cell communication is more susceptible to the *P. aeruginosa* virulence factors.

One of the observed morphological alterations in A549 cells induced by the supernatants of the *P. aeruginosa* strains that stands out is cellular blebbing and formation of apoptotic bodies, and also cell lysis, in a time- and concentration-dependent manner (Figure 23). The cell blebs and apoptotic bodies are distinguishable in size and shape from the lamellar cell bodies of A549 cells, observable in Figure 23, where intracellular microvesicles, with function of storage of pulmonary surfactant, can be found [201]. Similar to what was observed in L929 cell cultures incubated with the supernatants of the *P. aeruginosa* strains, the emergence of cellular vesicles in A549 cells occurred in a time- and concentration-dependent manner, most evidently in the PAO1 and HB15 strains. These results, once more, correlate cytotoxicity of the strains with their level of effect on morphological alterations. The HB15 strain displayed the most aggressive morphological alteration in A549 cells, causing a substantial number of blebbing cells at the concentration 3.42 µg/ml after 72h of incubation,

and at the highest concentration (20.50 $\mu\text{g/ml}$) after 48h of incubation the A549 cell culture displayed an extensive number of blebbing and cells undergoing lysis.

As previously observed in L929 cells, these morphologic alterations support the suggestion that these cells also underwent apoptosis under influence of virulence factors of the *P. aeruginosa* strains, despite the number of cells killed through lysis. Evidences of *P. aeruginosa* inducing A549 cells to undergo apoptosis had been already reported [202], [203]. For instance, in 2013, it was reported that *P. aeruginosa*'s LPS induces A549 cells into apoptosis [151]. In order to strengthen the analysis of these morphological alterations in A549 cells, fluorescence microscopy was performed again on A549 cell cultures incubated with supernatants from the *P. aeruginosa* strains. The same staining procedure used in L929 cells was applied to the A549 cells. Concentration and incubation time was settled, as previously in L929 cells, and A549 cell culture were let grow in 24 well plates for 24h. The testing groups were incubated with 3.42 $\mu\text{g/ml}$ of the strains supernatants. After incubation, the samples were transferred into cover slips for observation under the microscope (Figure 24).

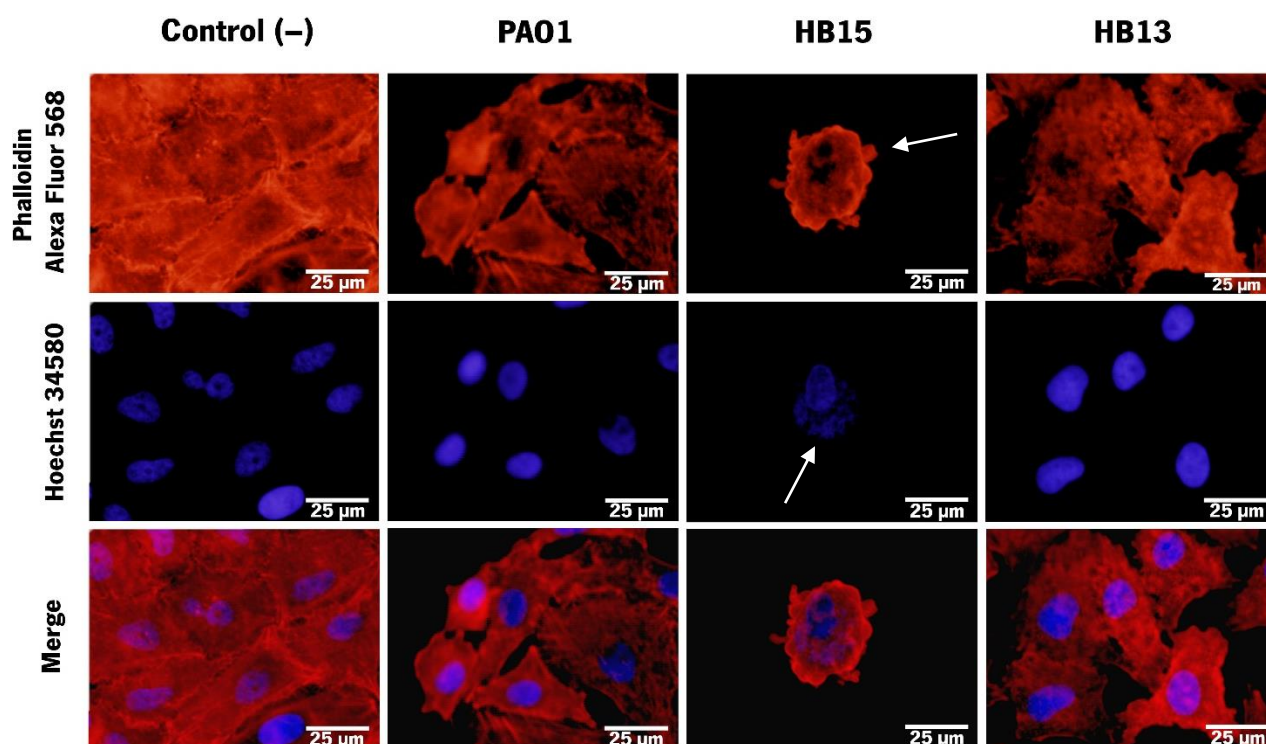


Figure 24 - Fluorescence microscopy of A549 cells to study morphological features induced by *Pseudomonas aeruginosa* strains. The cytoskeleton of the A549 cells are stained with the probe Phalloidin Alexa Fluor 568 (red) and the nucleus of the L929 cells are stained with the bisbenzimidazole dye Hoechst 34580 (blue). The merging of the individual stained components provides a composite image refining the cellular morphology observation. The A549 control cells cultured in DMEM medium, grown for 24h and transferred in cover slips for prior microscopy observation are represented as “Control (-)”. The A549 cells incubated with the supernatants of the *P. aeruginosa* strains are represented as “PA01”, “HB15” and “HB13”. All cells were incubated with 3.42 $\mu\text{g/ml}$ of *P. aeruginosa* strains supernatants during 24h, respectively and transferred in cover slips for prior microscopy observation. The white arrows points to noteworthy morphological features, in the up row (Phalloidin Alexa Fluor 568) indicates a visible cellular blebbing and in the middle row (Hoechst 34580) indicates a visible nuclear fragmentation. The scale bar represents 25 μm length.

The resulting images display A549 cells with distinct red stained cytoskeleton and distinct blue stained nuclei. In the control group are visible confluent cells exhibiting distinct actin filaments and single nuclei (Figure

24). The A549 cell cultures incubated with supernatants from the *P. aeruginosa* strains presented visible morphological alterations. In A549 cells incubated with 3.42 µg/ml of PAO1 strain supernatant is visible the reduction of F-actin density in some cells as well as actin cytoskeleton disorganization. Also cell-to-cell junctions appear diminished. Significant changes in the nucleus structure were not observable.

The A549 cells incubated with 3.42 µg/ml of HB15 strain supernatant display more conspicuous morphological alterations. There is less cell population density and the cells display cellular blebs and nuclear fragmentation, as indicated by white arrows in Figure 24. These are hallmarks of apoptosis, which indicates that HB15 secreted virulence factors is inducing it. In further literature, it was already described that *P. aeruginosa* virulence factors induce cytoskeleton reorganization, cellular blebbing, nuclear fragmentation and subsequently apoptosis in A549 cells [151]. These findings, once again, match the results obtained from the contrast-phase microscopy of the A549 cells incubates with the supernatants of the *P. aeruginosa* strains, indicating that the cells underwent apoptosis.

In A549 cells incubated with 3.42 µg/ml of HB13 strain supernatant the morphological changes were less significant than what was observed with the other two strains. However it can also be seen, in some cells, diminishing F-actin density as well as evidences of F-actin reorganization (Figure 24).

The visualization of these A549 cells with fluorescence microscopy showed to be a viable resource to confirm detailed cellular morphological evidences occurring during the incubation with secreted virulence factors from these three *P. aeruginosa* strains, translating into solid information about cellular processes during infection. Once again, time and cost-effective limitation barred the use of an extended time/concentration range which could provide more interesting results.

3.7. Final considerations and future perspectives

The exponential arising of new variants and strains of pathogenic bacteria has commanded researchers' attention towards the characterization of the pathogenic potential of these new threats. *Pseudomonas aeruginosa* specie has been considered as one of the most concerning nosocomial bacterial species, with a wide range of strains and variants comprehending high levels of pathogenicity and/or high levels of resistance [1].

The problematic of this thesis work results from an interlinked system between the model, the experiment and the output, in order to attempt answer the biological question posed.

Here, the characterization of the relatively recent *P. aeruginosa* clinical isolates, HB13 and HB15 strains, led this thesis work to converge its study focus to the pathogenic potential.

Therefore, the pathogenic potential characterization of these strains required a reliable design of a preliminary interface in order to produce a significant output that later help disclose sophisticated and complex molecular mechanism behind the infection mechanisms of these strains.

The HB13 and HB15 strains had been previously described to have significantly different features between them, regarding genomics, pathogenicity and antibiotic resistance [94], [204]. Thus, it became reasonable to invest in a close approach concerning their pathogenicity. Alongside, the introduction of the reference strain PAO1 served as a comparing rail in this thesis.

One of the main achievements of this thesis work was the performance of an initial concentration screening of the virulence factors from the *P. aeruginosa* strains on a cell culture. Without existing data about quantities of virulence factors that induce notable cellular damage, this procedure was suitable, not only to access the point where a concentration start to be toxic towards the cells, but also to give an initial insight on the evolution of toxicity dependent of the virulence factors' concentration.

The wide-known L929 and A549 cell line, used as host models for a variety of studies in *P. aeruginosa* [124], [127], [144], [149]–[153], in this thesis work were suitable models, not only to assess the HB13 and HB15 cytotoxicity, but also to examine different levels of cytotoxicity induced in cells from different tracts.

In the cytotoxicity tests, carried in these cell lines, it was possible to identify considerable differences between the HB13 and HB15 strains. It was stated that HB15 is significantly more cytotoxic than HB13, confirming previous literature referring the same divergences about pathogenicity of these strains [94], [204]. Nevertheless, the HB13 strain still showed considerable cytotoxicity, while possessing the feature of pan-resistance which places this strain as a dangerous resistant pathogen in hospital facilities. In both animal cell models, the concentrations obtained through dilutions of the original samples of the *P. aeruginosa* strains supernatants, revealed astonishing high cellular toxicity rates, sometimes even higher than the positive control (30% DMSO), which indicates the considerable pathogenicity of these strains, mainly the HB15 strain.

Pairing with the cytotoxicity tests, microscopy observations took place to inquire possible morphological alterations, which reveal considerable cell damaging, cell population organized in cell aggregates, loss of cellular shape, presence of cellular blebbing and evidences of formation of apoptotic bodies, as well as cytoskeleton disorganization and nuclear fragmentation confirmed by fluorescence microscopy. Here, the HB13 and HB15 displayed, also, significant differences regarding their capacity to induce morphological alterations. The HB15 strains revealed to easily induce drastic alterations in the cells morphology, whilst the HB13 strain didn't showed significant alterations, been only visible signs of loss of cellular shape and presence of cellular blebbing at the highest concentration after 72h of incubation. These findings helped to gain further insights into the biological processes behind the induced cytotoxicity in these cell lines. Cellular blebbing and formation of apoptotic bodies suggests that cellular death is the result of the tested cells undergoing apoptosis induced by the secreted virulence factors of the strains. Nevertheless, cellular death studies and apoptosis assays should be performed in order to better characterize the cell death process occurring here.

Regarding the intracellular processes that might be associated with the cytotoxicity levels, initiating steps during this thesis work have already been taken in order to ascertain if cellular oxidative stress is induced by the virulence factors of *P. aeruginosa* strains. One type of cellular response to pathogenic agents is the production of reactive oxygen species (ROS) causing cellular oxidative stress [151], therefore a dichlorofluorescein (DCF) assay was performed, as a straightforward and reliable means to assess cellular oxidative stress [205]. A549 cells were selected to perform the assay. The cells were incubated 1 hour and 4 hours with 3.42 µg/ml of culture supernatants from the *P. aeruginosa* strains, plus a negative control (A549 cells growing with only culture medium) and a H₂O₂ control (A549 cells incubated with 2mM of H₂O₂). The assay outcome was measured in relative fluorescence intensity, and it was evaluated comparing the relative fluorescence intensities of the cells incubated with the *P. aeruginosa* strains supernatants with the negative control, presented in appendix. In summary, the oxidative stress study was insufficiently designed though it gave availed results stating that in the early moments of the cells incubation with the secreted virulence factors the oxidative stress is enhanced, one of the causes that damage the cells and lead to cellular unviability, and further oxidative stress studies should be performed in order to obtain better results.

Regarding the experimental design of this thesis work, the pathogenicity of the HB13 and HB15 was accessed not from co-culture with the bacteria and the cell lines, but rather, incubation of the cells with supernatants from the bacterial culture. One of the problems of this experimental procedure is that virulence genes may not be expressed due to lack of an infection context. However, the results of this thesis showed that the bacterial culture of the *P. aeruginosa* strains in controlled conditions and medium in a laboratory flask for optimal growth, without any infection stimuli, which could provide a pathogenic response, still revealed an overwhelming abundant secretion of extracellular products which caused significant cellular damage in the tested cell lines, L929 and A549. These findings suggest that the bacterial species *P. aeruginosa* is capable of

displaying a battery of virulence factors without an infection context being absolutely required. Given the virulence factors are produced by bacteria to subvert the host defences, it is plausible to say that *P. aeruginosa* is always predisposed to subvert host defences even without effective contact with the host.

The strategy used in this thesis work to characterize the pathogenic potential of HB13 and HB15, had the main objective of using the initial concentration screening of virulence factors to assess the cytotoxicity and subsequent cell morphological alterations, in a very straightforward procedure comparing the two strains in his capacity of inducing cell damage. As this strategy consist in a simple and straightforward system, it revealed suitable for easily find concentrations of virulence factors toxic towards the cell, and so, establish a comparison reference between HB13 and HB15 pathogenicity. Although, a more refine set of concentrations is needed to answer significant biologic question such as the median lethal dose. More concentrations and a more narrow range in a concentration set should be applied in order to determine reliable and absolute values of lethality.

The output of the pathogenic studies in L929 and A549 cell lines revealed different levels of cell damaging. In general, the L929 cells were much more susceptible to the virulence factors from PAO1, HB13 and HB15 strains than the A549 cells. These findings may infer that skin infections could be more persistent than lung infections. However, it is needed more data about the molecular mechanisms underlying the host-pathogen interactions to inquire about the susceptibilities of the cell lines used.

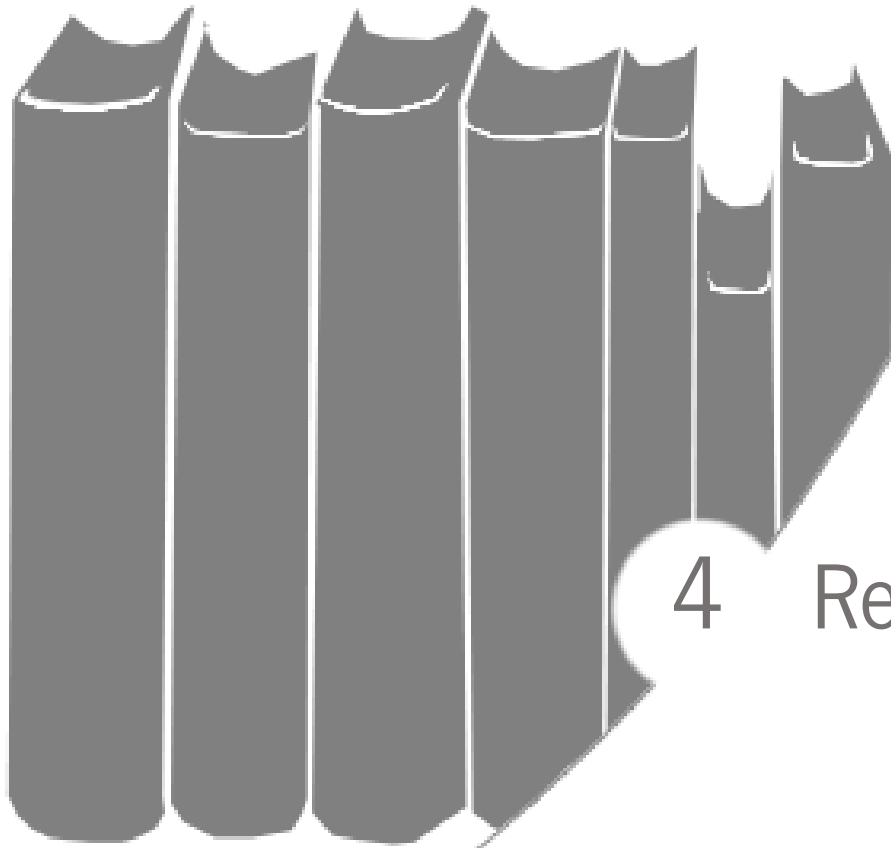
The L929 and the A549 cells morphologic alterations induced by HB13 and HB15 shed some insight iinto the possible infection mechanism of these strains. For instance, it is known that *P. aeruginosa* uses a variety of proteases, such as LasB, to disrupt the extracellular matrix, which in cell cultures causes cell dissociation. The HB15 strain induced noteworthy cellular dissociation unlike the HB13 strain, which suggest that HB13 may underexpress or even not express at all the LasB protease. Also, it is known that LasB mutants are less pathogenic than its counterparts [25], [38].

Other molecular machinery required for cell damaging and cell death may be underexpress or absent in HB13. In comparison with HB15 strain, HB13 didn't revealed significant intracellular morphologic changes, such as disruption of the cytoskeleton, which may be linked to an underexpression of the T3SS, or the set of exoenzymes. The disruption of the cytoskeleton may lead to programmed cell death, which also may explains the lower level of cytotoxicity by HB13.

These indications suggests an existence of different sets of virulence in each strain, HB13 and HB15. In future work, regarding comparative studies of these sets of virulence factors, a proteomic approach could give a deep insight in the molecular process behind the virulence expression pattern in these strains.

In general, this thesis work opened the way for insights into the pathogenicity of these strains. Although, further work should be conducted in order to achieve a fully understanding of the infection mechanisms behind the pathogenicity of HB13 and HB15. New cytotoxicity assays, oxidative stress tests, intracellular pH variations and nuclear fragmentation studies should be designed for further approaches. In the future, the possibility of an

integration of a whole system model should be envisaged for validation of the output in an actual infection situation.



4

References

- [1] J. W. Wilson, M. J. Schurr, C. L. Leblanc, R. Ramamurthy, K. L. Buchanan, and C. A. Nickerson, "Mechanisms of bacterial pathogenicity," *Postgraduate Medical Journal*, vol. 78, pp. 216–224, 2002.
- [2] World Health Organization - Media Centre - Fact sheet n° 310, "The top 10 causes of death," <http://www.who.int/>, 2014.
- [3] B. C. Millar, J. Xu, and J. E. Moore, "Molecular Diagnostics of Medically Important Bacterial Infections," *Current Issues in Molecular Biology*, vol. 9, pp. 21–40, 2007.
- [4] CDC, "Antibiotic resistance threats," *US Department of Health and Human Services - Centre for Disease Control and Prevention*, pp. 1–114, 2013.
- [5] A. Magiorakos, A. Srinivasan, R. B. Carey, Y. Carmeli, M. E. Falagas, C. G. Giske, S. Harbarth, and J. F. Hindler, "Multidrug-resistant, extensively drug-resistant and pandrug-resistant bacteria: an international expert proposal for interim standard definitions for acquired resistance," *Clinical Microbiology Infection*, vol. 18, pp. 268–281, 2012.
- [6] WHO, "Antimicrobial resistance Global Report," *WHO Library Cataloguing-in-Publication Data Antimicrobial*, pp. 1–256, 2014.
- [7] M. H. Kollef, L. M. Napolitano, J. S. Solomkin, R. G. Wunderink, I.-G. Bae, V. G. Fowler, R. a Balk, D. L. Stevens, J. J. Rahal, A. F. Shorr, P. K. Linden, and S. T. Micek, "Health care-associated infection (HAI): a critical appraisal of the emerging threat-proceedings of the HAI Summit," *Clinical Infectious Diseases*, vol. 47, pp. 55–99, 2008.
- [8] R. Laxminarayan and A. Malani, *Extending the cure : policy responses to the growing threat of antibiotic resistance*. 2007, pp. 1 – 192.
- [9] D. L. Paterson, "Resistance in gram-negative bacteria: enterobacteriaceae," *The American Journal of Medicine*, vol. 119, pp. 20–80, 2006.
- [10] V. Aloush, S. Navon-venezia, Y. Seigman-igra, S. Cabili, and Y. Carmeli, "Multidrug-Resistant *Pseudomonas aeruginosa* : Risk Factors and Clinical Impact," *Antimicrobial Agents and chemotherapy*, vol. 50, pp. 43–48, 2006.
- [11] ECDC, "Press release: Each day, one in 18 patients in European hospitals has a healthcare-associated infection: ECDC estimates," *ECDC press office*, vol. 46, pp. 1–2, 2013.
- [12] ECDC, *Antimicrobial resistance surveillance in Europe 2012*. 2013, pp. 1 – 218.
- [13] R. Gaynes and J. R. Edwards, "Overview of nosocomial infections caused by gram-negative bacilli," *Clinical Infectious Diseases*, vol. 41, pp. 848–854, 2005.
- [14] R. Hugh and E. Leifson, "The proposed neotype strains of *Pseudomonas aeruginosa* (Schroeter 1872) Migula 1900," *International bulletin of bacteriological nomenclature and taxonomy*, vol. 14, pp. 69–84, 1964.
- [15] M. Véron, "Sur l'opportunité de conserver le nom d'espèce *Pseudomonas pyocyanea* (Gessard 1882) Migula 1895," *International bulletin of bacteriological nomenclature and taxonomy*, vol. 15, pp. 187–190, 1965.

- [16] S. K. Green, M. N. Schroth, J. J. Cho, S. K. Kominos, and V. B. Vitanza-jack, "Agricultural plants and soil as a reservoir for *Pseudomonas aeruginosa*," *Applied microbiology*, vol. 28, pp. 987–991, 1974.
- [17] J. B. Goldberg, "*Pseudomonas*: global bacteria," *Trends in microbiology*, vol. 8, pp. 55–57, 2000.
- [18] A. J. Spiers, A. Buckling, and P. B. Rainey, "The causes of *Pseudomonas* diversity," *Microbiology*, vol. 146, pp. 2345–2350, 2000.
- [19] C. K. Stover, X. Q. Pham, a L. Erwin, S. D. Mizoguchi, P. Warrenner, M. J. Hickey, F. S. Brinkman, W. O. Hufnagle, D. J. Kowalik, M. Lagrou, R. L. Garber, L. Goltry, E. Tolentino, S. Westbrook-Wadman, Y. Yuan, L. L. Brody, S. N. Coulter, K. R. Folger, A. Kas, K. Larbig, R. Lim, K. Smith, D. Spencer, G. K. Wong, Z. Wu, I. T. Paulsen, J. Reizer, M. H. Saier, R. E. Hancock, S. Lory, and M. V Olson, "Complete genome sequence of *Pseudomonas aeruginosa* PAO1, an opportunistic pathogen," *Nature*, vol. 406, pp. 959–964, 2000.
- [20] E. Deligianni, S. Pattison, D. Berrar, N. G. Ternan, R. W. Haylock, J. E. Moore, S. J. Elborn, and J. S. G. Dooley, "*Pseudomonas aeruginosa* cystic fibrosis isolates of similar RAPD genotype exhibit diversity in biofilm forming ability in vitro," *BMC Microbiology*, vol. 10, pp. 1–13, 2010.
- [21] V. L. Kung, E. a Ozer, and A. R. Hauser, "The accessory genome of *Pseudomonas aeruginosa*," *Microbiology and molecular biology reviews: MMBR*, vol. 74, pp. 621–641, 2010.
- [22] L. Nicolle, "*Pseudomonas aeruginosa*: infections and Treatments," *New England Journal of Medicine*, vol. 332, pp. 616–617, 1995.
- [23] N. Mesaros, P. Nordmann, P. Plésiat, M. Roussel-Delvallez, J. Van Eldere, Y. Glupczynski, Y. Van Laethem, F. Jacobs, P. Lebecque, a Malfroot, P. M. Tulkens, and F. Van Bambeke, "*Pseudomonas aeruginosa*: resistance and therapeutic options at the turn of the new millennium," *Clinical microbiology and infection : the official publication of the European Society of Clinical Microbiology and Infectious Diseases*, vol. 13, pp. 560–578, 2007.
- [24] P. Tingpej, "Characterisation of genotypes and phenotypes of *Pseudomonas aeruginosa* infecting people with cystic fibrosis," University of Sydney, 2008.
- [25] H. B. Tang, E. DiMango, R. Bryan, M. Gambello, B. H. Iglewsky, J. B. Goldberg, and A. Prince, "Contribution of specific *Pseudomonas aeruginosa* virulence factors to pathogenesis of pneumonia in a neonatal mouse model of infection," *Infection and immunity*, vol. 64, pp. 37–43, 1996.
- [26] J. L. Veessenmeyer, A. R. Hauser, T. Lisboa, and J. Rello, "*Pseudomonas aeruginosa* Virulence and Therapy: Evolving Translational Strategies Jeffrey," *Critical Care Medicine*, vol. 37, pp. 1777–1786, 2009.
- [27] T. S. Cohen and A. Prince, "Cystic fibrosis: a mucosal immunodeficiency syndrome," *Nature Medicine*, vol. 18, pp. 509–519, 2012.
- [28] C. Van Delden and B. H. Iglewsky, "Cell-to-cell signaling and *Pseudomonas aeruginosa* infections," *Emerging infectious diseases*, vol. 4, pp. 551–560, 1998.
- [29] B. Prithviraj, H. P. Bais, T. Weir, B. Suresh, E. H. Najarro, V. Dayakar, H. P. Schweizer, J. M. Vivanco, and B. V Dayakar, "Down Regulation of Virulence Factors of *Pseudomonas aeruginosa* by Salicylic Acid

Attenuates Its Virulence on *Arabidopsis thaliana* and *Caenorhabditis elegans*," *Infection and immunity*, vol. 73, pp. 5319–5328, 2005.

- [30] L. I. N. Zeng, "Pseudomonas aeruginosa pathogenicity and antibiotic resistance," University of Florida, 2004.
- [31] I. Bucior, J. F. Pielage, and J. N. Engel, "Pseudomonas aeruginosa pili and flagella mediate distinct binding and signaling events at the apical and basolateral surface of airway epithelium," *PLoS pathogens*, vol. 8, pp. 1–18, 2012.
- [32] D. Kaiser, "Bacterial motility: How do pili pull?," *Current Biology*, vol. 10, pp. 777–780, 2000.
- [33] F. F. V Chevance and K. T. Hughes, "Coordinating assembly of a bacterial macromolecular machine," *Nature reviews. Microbiology*, vol. 6, no. 6, pp. 455–465, Jun. 2008.
- [34] G. B. Pier, "Pseudomonas aeruginosa lipopolysaccharide: a major virulence factor, initiator of inflammation and target for effective immunity," *International journal of medical microbiology*, vol. 297, pp. 277–295, 2007.
- [35] EMBL-EBI, "BioModels Database," <http://www.ebi.ac.uk/biomodels-main/>, 2012. .
- [36] J. B. Lyczak, C. L. Cannon, and G. B. Pier, "Establishment of Pseudomonas aeruginosa infection: lessons from a versatile opportunist," *Microbes and Infection*, vol. 2, pp. 1051–1060, 2000.
- [37] D. R. Galloway, "Pseudomonas aeruginosa elastase and elastolysis revisited: recent developments," *Molecular microbiology*, vol. 5, pp. 2315–2321, 1991.
- [38] R. Hoge, A. Pelzer, F. Rosenau, and S. Wilhelm, "Weapons of a pathogen: Proteases and their role in virulence of Pseudomonas aeruginosa," *Current Research, Technology and Education Topics in Applied Microbiology and Microbial Biotechnology*, vol. 45, pp. 383–395, 2010.
- [39] T. L. Pitt, "Biology of Pseudomonas aeruginosa in relation to pulmonary infection in cystic fibrosis," *Journal of the Royal Society of Medicine*, vol. 79, pp. 13–18, 1986.
- [40] J. Engel and P. Balachandran, "Role of Pseudomonas aeruginosa type III effectors in disease," *Current opinion in microbiology*, vol. 12, pp. 61–66, 2009.
- [41] H. Feltman, G. Schulert, S. Khan, M. Jain, L. Peterson, and a R. Hauser, "Prevalence of type III secretion genes in clinical and environmental isolates of Pseudomonas aeruginosa," *Microbiology*, vol. 147, pp. 2659–2669, 2001.
- [42] A. R. Hauser, "The Type III Secretion System of Pseudomonas aeruginosa: Infection by Injection," *Nature Reviews. Microbiology*, vol. 7, pp. 654 – 665, 2009.
- [43] L. Zulianello, C. Canard, T. Köhler, D. Caille, J.-S. Lacroix, and P. Meda, "Rhamnolipids are virulence factors that promote early infiltration of primary human airway epithelia by Pseudomonas aeruginosa," *Infection and immunity*, vol. 74, no. 6, pp. 3134–3147, 2006.
- [44] H. Anwar, J. L. Strap, and J. W. Costerton, "Establishment of Aging Biofilms: Possible Mechanism of Bacterial Resistance to Antimicrobial Therapy," *Antimicrobial agents and chemotherapy*, vol. 36, pp. 1347–1351, 1992.

- [45] B. S. Can Attila, "Identification of *Pseudomonas aeruginosa* Virulence Factors via a Poplar Tree Model," Texas A&M University, 2008.
- [46] D. V Mavrodi, R. F. Bonsall, S. M. Delaney, M. J. Soule, G. Phillips, and L. S. Thomashow, "Functional Analysis of Genes for Biosynthesis of Pyocyanin and Phenazine-1-Carboxamide from *Pseudomonas aeruginosa* PAO1," *Journal of Bacteriology*, vol. 183, pp. 6454–6465, 2001.
- [47] G. W. Lau, H. Ran, F. Kong, D. J. Hassett, and D. Mavrodi, "*Pseudomonas aeruginosa* Pyocyanin is Critical for Lung Infection in Mice," *Infection and immunity*, vol. 72, pp. 4275–4278, 2004.
- [48] M. Klausen, A. Heydorn, P. Ragas, L. Lambertsen, A. Aaes-Jørgensen, S. Molin, and T. Tolker-Nielsen, "Biofilm formation by *Pseudomonas aeruginosa* wild type, flagella and type IV pili mutants," *Molecular Microbiology*, vol. 48, pp. 1511–1524, 2003.
- [49] E. Werner, F. Roe, A. Bugnicourt, M. J. Franklin, A. Heydorn, S. Molin, B. Pitts, and P. S. Stewart, "Stratified Growth in *Pseudomonas aeruginosa* Biofilms," *Applied and environmental microbiology*, vol. 70, pp. 6188–6196, 2004.
- [50] K. Sauer, A. K. Camper, G. D. Ehrlich, J. William, D. G. Davies, and J. W. Costerton, "*Pseudomonas aeruginosa* Displays Multiple Phenotypes during Development as a Biofilm *Pseudomonas aeruginosa* Displays Multiple Phenotypes during Development as a Biofilm," *Journal of Bacteriology*, vol. 184, pp. 1140 – 1154, 2002.
- [51] D. Monroe, "Looking for chinks in the armor of bacterial biofilms," *PLoS Biology*, vol. 5, pp. 2458 – 2461, 2007.
- [52] A. B. T. Semmler, C. B. Whitchurch, and J. S. Mattick, "A re-examination of twitching motility in *Pseudomonas aeruginosa*," *Microbiology*, vol. 145, pp. 2863–2873, 1999.
- [53] R. Xu, "Spatial growth patterns of *Pseudomonas aeruginosa* biofilms," Montana State University, 2004.
- [54] E. Drenkard and F. M. Ausubel, "*Pseudomonas* biofilm formation and antibiotic resistance are linked to phenotypic variation," *Nature*, vol. 416, pp. 740–743, 2002.
- [55] von A. M. H. A. Ellah, "Environmental factors influence virulence of *Pseudomonas aeruginosa*," 2010.
- [56] J. P. Pearson, E. C. Pesci, and B. H. Iglewski, "Roles of *Pseudomonas aeruginosa* las and rhl quorum-sensing systems in control of elastase and rhamnolipid biosynthesis genes," *Journal of bacteriology*, vol. 179, pp. 5756–5767, 1997.
- [57] R. I. Aminov, "A brief history of the antibiotic era: lessons learned and challenges for the future," *Frontiers in microbiology*, vol. 1, pp. 1–7, 2010.
- [58] G. D. Wright, "Antibiotic resistance in the environment: a link to the clinic?," *Current opinion in microbiology*, vol. 13, pp. 589–594, 2010.
- [59] A. Giedraitienė A. Vitkauskienė R. Naginienė and A. Pavilonis, "Antibiotic Resistance Mechanisms of Clinically Important Bacteria," *Medicina (Kaunas)*, vol. 47, pp. 137–146, 2011.
- [60] S. Donadio, S. Maffioli, P. Monciardini, M. Sosio, and D. Jabes, "Antibiotic discovery in the twenty-first century: current trends and future perspectives," *The Journal of Antibiotics*, vol. 63, pp. 423–430, 2010.

- [61] J. L. Martinez, F. Baquero, and D. I. Andersson, "Predicting antibiotic resistance," *Nature Reviews Microbiology*, vol. 5, pp. 958–965, 2007.
- [62] P. A. Lambert, "Mechanisms of antibiotic resistance in *Pseudomonas aeruginosa*," *Journal of the Royal Society of Medicine*, vol. 95, pp. 22–26, 2002.
- [63] R. E. W. Hancock and D. P. Speert, "Antibiotic resistance in *Pseudomonas aeruginosa*: mechanisms and impact on treatment," *Drug resistance updates: reviews and commentaries in antimicrobial and anticancer chemotherapy*, vol. 3, pp. 247–255, 2000.
- [64] D. Ferguson, "A study of clinical strains of *Pseudomonas aeruginosa* and the investigation of antibiotic resistance mechanisms in the multidrug resistant strain PA13," Dublin City University, 2007.
- [65] M. D. Obritsch, D. N. Fish, R. MacLaren, and R. Jung, "Nosocomial infections due to multidrug-resistant *Pseudomonas aeruginosa*: epidemiology and treatment options.," *Pharmacotherapy*, vol. 25, pp. 1353–1364, 2005.
- [66] T. Strateva and D. Yordanov, "*Pseudomonas aeruginosa* - a phenomenon of bacterial resistance," *Journal of medical microbiology*, vol. 58, pp. 1133–1148, 2009.
- [67] D. M. Livermore, "Multiple mechanisms of antimicrobial resistance in *Pseudomonas aeruginosa*: our worst nightmare?," *Clinical infectious diseases: an official publication of the Infectious Diseases Society of America*, vol. 34, pp. 634–640, 2002.
- [68] T. Mah, B. Pitts, B. Pellock, G. C. Walker, P. S. Stewart, and G. A. O. Toole, "A genetic basis for *Pseudomonas aeruginosa* biofilm antibiotic resistance," *Nature*, vol. 426, pp. 306–310, 2003.
- [69] D. J. Brenner, J. T. Staley, and N. R. Krieg, "Classification of Prokaryotic Organisms and the Concept of Bacterial Speciation," in *Bergey's Manual of Systematic Bacteriology*, 2005, pp. 27–33.
- [70] F. C. Tenover, R. D. Arbeit, R. V. Goering, P. A. Mickelsen, B. E. Murray, D. H. Persing, and B. Swaminathan, "Interpreting Chromosomal DNA Restriction Patterns Produced by Pulsed-Field Gel Electrophoresis: Criteria for Bacterial Strain Typing," *Journal of Clinical Microbiology*, vol. 33, pp. 2233–2239, 1995.
- [71] L. Dijkshoorn, B. M. Ursing, and J. B. Ursing, "Strain, clone and species: comments on three basic concepts of bacteriology," *Journal of Medical Microbiology*, vol. 49, pp. 397–401, 2000.
- [72] NCBI, "*Pseudomonas aeruginosa*'s strains," *Taxonomy Browser*. [Online]. Available: <http://www.ncbi.nlm.nih.gov/Taxonomy/Browser/wwwtax.cgi?id=287>.
- [73] K. Mathee, G. Narasimhan, C. Valdes, X. Qiu, J. M. Matewish, M. Koehrsen, A. Rokas, C. N. Yandava, R. Engels, E. Zeng, R. Olavarietta, M. Doud, R. S. Smith, P. Montgomery, J. R. White, P. a Godfrey, C. Kodira, B. Birren, J. E. Galagan, and S. Lory, "Dynamics of *Pseudomonas aeruginosa* genome evolution," *Proceedings of the National Academy of Science*, vol. 105, pp. 3100–3105, 2008.
- [74] K. Shen, S. Sayeed, P. Antalis, J. Gladitz, A. Ahmed, B. Dice, B. Janto, R. Dopico, R. Keefe, J. Hayes, S. Johnson, S. Yu, N. Ehrlich, J. Jocz, L. Kropp, R. Wong, R. M. Wadowsky, M. Slifkin, R. a Preston, G. Erdos, J. C. Post, G. D. Ehrlich, and F. Z. Hu, "Extensive genomic plasticity in *Pseudomonas aeruginosa*

revealed by identification and distribution studies of novel genes among clinical isolates," *Infection and Immunity*, vol. 74, pp. 5272–5283, 2006.

- [75] L. Freschi, J. Jeukens, I. Kukavica-Ibrulj, B. Boyle, M.-J. Dupont, J. Laroche, S. Larose, H. Maaroufi, J. L. Fothergill, M. Moore, G. L. Winsor, S. D. Aaron, J. Barbeau, S. C. Bell, J. L. Burns, M. Camara, A. Cantin, S. J. Charette, K. Dewar, É. Déziel, K. Grimwood, R. E. W. Hancock, J. J. Harrison, S. Heeb, L. Jelsbak, B. Jia, D. T. Kenna, T. J. Kidd, J. Klockgether, J. S. Lam, I. L. Lamont, S. Lewenza, N. Loman, F. Malouin, J. Manos, A. G. McArthur, J. McKeown, J. Milot, H. Naghra, D. Nguyen, S. K. Pereira, G. G. Perron, J.-P. Pirnay, P. B. Rainey, S. Rousseau, P. M. Santos, A. Stephenson, V. Taylor, J. F. Turton, N. Waglechner, P. Williams, S. W. Thrane, G. D. Wright, F. S. L. Brinkman, N. P. Tucker, B. Tümmler, C. Winstanley, and R. C. Levesque, "Clinical utilization of genomics data produced by the international *Pseudomonas aeruginosa* consortium," *Frontiers in Microbiology*, vol. 6, pp. 1–8, 2015.
- [76] H. Mikkelsen, R. McMullan, and A. Filloux, "The *Pseudomonas aeruginosa* reference strain PA14 displays increased virulence due to a mutation in *ladS*," *PLoS one*, vol. 6, pp. 1–7, 2011.
- [77] Y. Wang, C. Li, C. Gao, C. Ma, and P. Xua, "Genome Sequence of the Nonpathogenic *Pseudomonas aeruginosa* Strain ATCC 15442," *Genome Announcements*, vol. 2, pp. 1–2, 2014.
- [78] W. Li, D. Raoult, and P.-E. Fournier, "Bacterial strain typing in the genomic era," *FEMS microbiology reviews*, vol. 33, pp. 892–916, 2009.
- [79] B. W. Holloway, "Genetic Recombination in *Pseudomonas aeruginosa*," *Journal of General Microbiology*, vol. 13, pp. 572–581, 1955.
- [80] J. Klockgether, A. Munder, J. Neugebauer, C. F. Davenport, F. Stanke, K. D. Larbig, S. Heeb, U. Schöck, T. M. Pohl, L. Wiehlmann, and B. Tümmler, "Genome diversity of *Pseudomonas aeruginosa* PAO1 laboratory strains," *Journal of bacteriology*, vol. 192, pp. 1113–1121, 2010.
- [81] I. Kukavica-Ibrulj, A. Bragonzi, M. Paroni, C. Winstanley, F. Sanschagrín, G. a O'Toole, and R. C. Levesque, "In vivo growth of *Pseudomonas aeruginosa* strains PAO1 and PA14 and the hypervirulent strain LESB58 in a rat model of chronic lung infection," *Journal of bacteriology*, vol. 190, pp. 2804–2813, 2008.
- [82] C. Winstanley, M. G. I. Langille, J. L. Fothergill, I. Kukavica-Ibrulj, C. Paradis-Bleau, F. Sanschagrín, N. R. Thomson, G. L. Winsor, M. a Quail, N. Lennard, A. Bignell, L. Clarke, K. Seeger, D. Saunders, D. Harris, J. Parkhill, R. E. W. Hancock, F. S. L. Brinkman, and R. C. Levesque, "Newly introduced genomic prophage islands are critical determinants of in vivo competitiveness in the Liverpool Epidemic Strain of *Pseudomonas aeruginosa*," *Genome research*, vol. 19, no. 1, pp. 12–23, 2009.
- [83] D. G. Lee, J. M. Urbach, G. Wu, N. T. Liberati, R. L. Feinbaum, S. Miyata, L. T. Diggins, J. He, M. Saucier, E. Déziel, L. Friedman, L. Li, G. Grills, K. Montgomery, R. Kucherlapati, L. G. Rahme, and F. M. Ausubel, "Genomic analysis reveals that *Pseudomonas aeruginosa* virulence is combinatorial," *Genome biology*, vol. 7, p. R90, 2006.
- [84] J. He, R. L. Baldini, E. Déziel, M. Saucier, Q. Zhang, N. T. Liberati, D. Lee, J. Urbach, H. M. Goodman, and L. G. Rahme, "The broad host range pathogen *Pseudomonas aeruginosa* strain PA14 carries two pathogenicity islands harboring plant and animal virulence genes," *Proceedings of the National Academy of Sciences of the United States of America*, vol. 101, pp. 2530–2535, 2004.

- [85] P. H. Roy, S. G. Tetu, A. Larouche, L. Elbourne, S. Tremblay, Q. Ren, R. Dodson, D. Harkins, R. Shay, K. Watkins, Y. Mahamoud, and I. T. Paulsen, "Complete genome sequence of the multiresistant taxonomic outlier *Pseudomonas aeruginosa* PA7," *PloS one*, vol. 5, pp. 1–10, 2010.
- [86] D.-Q. Wu, J. Ye, H.-Y. Ou, X. Wei, X. Huang, Y.-W. He, and Y. Xu, "Genomic analysis and temperature-dependent transcriptome profiles of the rhizosphere originating strain *Pseudomonas aeruginosa* M18," *BMC genomics*, vol. 12, pp. 1–17, 2011.
- [87] T. Miyoshi-Akiyama, T. Kuwahara, T. Tada, T. Kitao, and T. Kirikae, "Complete genome sequence of highly multidrug-resistant *Pseudomonas aeruginosa* NCGM2.S1, a representative strain of a cluster endemic to Japan," *Journal of Bacteriology*, vol. 193, p. 7010, 2011.
- [88] M. H. Rau, R. L. Marvig, G. D. Ehrlich, S. Molin, and L. Jelsbak, "Deletion and acquisition of genomic content during early stage adaptation of *Pseudomonas aeruginosa* to a human host environment," *Environmental Microbiology*, vol. 14, pp. 2200–2211, 2012.
- [89] J. Klockgether, N. Cramer, L. Wiehlmann, C. F. Davenport, and B. Tümmler, "*Pseudomonas aeruginosa* Genomic Structure and Diversity," *Frontiers in Microbiology*, vol. 2, pp. 1–18, 2011.
- [90] H. Pai, J. Kim, J. H. Lee, K. W. Choe, and N. Gotoh, "Carbapenem resistance mechanisms in *Pseudomonas aeruginosa* clinical isolates," *Antimicrobial Agents and Chemotherapy*, vol. 45, pp. 480–484, 2001.
- [91] S. Pournaras, A. Ikonomidis, A. Markogiannakis, N. Spanakis, A. N. Maniatis, and A. Tsakris, "Characterization of clinical isolates of *Pseudomonas aeruginosa* heterogeneously resistant to carbapenems," *Journal of Medical Microbiology*, vol. 56, pp. 66–70, 2007.
- [92] M. Gomila, M. Del Carmen Gallegos, V. Fernández-Baca, A. Pareja, M. Pascual, P. Díaz-Antolín, E. García-Valdés, and J. Lalucat, "Genetic diversity of clinical *Pseudomonas aeruginosa* isolates in a public hospital in Spain," *BMC Microbiology*, vol. 13, pp. 1–10, 2013.
- [93] L. V Silva, A. C. M. Galdino, A. P. F. Nunes, K. R. N. Dos Santos, B. M. Moreira, L. C. Cacci, C. L. Sodr e, M. Ziccardi, M. H. Branquinha, and A. L. S. Santos, "Virulence attributes in Brazilian clinical isolates of *Pseudomonas aeruginosa*," *International Journal of Medical Microbiology*, vol. 304, pp. 990–1000, 2014.
- [94] P. Soares-Castro, D. Marques, S. Demyanchuk, a Faustino, and P. M. Santos, "Draft genome sequences of two *Pseudomonas aeruginosa* clinical isolates with different antibiotic susceptibilities," *Journal of bacteriology*, vol. 193, p. 5573, 2011.
- [95] P. Soares-Castro, "Tailored strategies exploring genomic data from different *Pseudomonas* isolates," 2011.
- [96] C. Locht and M. Simonet, *Bacterial Pathogenesis: Molecular and Cellular Mechanisms*. 2012, p. 369.
- [97] P. Sudhakar and P. Subramani, "Mechanisms of Bacterial Pathogenesis and Targets for Vaccine Design," *Journal of young investigators*, vol. 13, pp. 1–12, 2005.

- [98] K. Yoshida, T. Matsumoto, K. Tateda, K. Uchida, S. Tsujimoto, and K. Yamaguchi, "Role of bacterial capsule in local and systemic inflammatory responses of mice during pulmonary infection with *Klebsiella pneumoniae*," *Journal of Medical Microbiology*, vol. 49, pp. 1003–1010, 2000.
- [99] J. Lengeler, G. Drews, and H. Schlegel, *Biology of the Prokaryotes*. 2009, p. 987.
- [100] A. L. Koch, "Bacterial Wall as Target for Attack: Past, Present, and Future," *Clinical Microbiology Reviews*, vol. 16, pp. 673–687, 2003.
- [101] N. A. Campbell, J. B. Reece, L. A. Urry, M. L. Cain, S. A. Wasserman, P. V. Minorsky, and R. B. Jackson, *Biology (8th edition)*. 2008, p. 118.
- [102] P. Hugenholtz, "Exploring prokaryotic diversity in the genomic era," *Genome biology*, vol. 3, pp. 1 – 8, 2002.
- [103] D. M. Monack and S. J. Hultgren, "The complex interactions of bacterial pathogens and host defenses," *Current opinion in microbiology*, vol. 16, pp. 1–3, 2013.
- [104] L. Coutte, S. Alonso, N. Reveneau, E. Willery, B. Quatannens, C. Loch, and F. Jacob-Dubuisson, "Role of adhesin release for mucosal colonization by a bacterial pathogen," *The Journal of experimental medicine*, vol. 197, pp. 735–742, 2003.
- [105] P. Klemm and M. A. Schembri, "Bacterial adhesins: function and structure," *International journal of medical microbiology*, vol. 290, pp. 27–35, 2000.
- [106] P. Cossart and P. J. Sansonetti, "Bacterial invasion: the paradigms of enteroinvasive pathogens," *Science*, vol. 304, pp. 242–248, 2004.
- [107] D. Ribet and P. Cossart, "How bacterial pathogens colonize their hosts and invade deeper tissues," *Microbes and Infection*, vol. 17, pp. 173–183, 2015.
- [108] A. P. Bhavsar, J. a. Guttman, and B. B. Finlay, "Manipulation of host-cell pathways by bacterial pathogens," *Nature*, vol. 449, pp. 827–834, 2007.
- [109] W. M. Bruckert, C. T. Price, and Y. A. Kwak, "Rapid nutritional remodeling of the host cell upon attachment of *Legionella pneumophila*," *Infection and Immunity*, vol. 82, pp. 72–82, 2014.
- [110] O. G. Baca, Y. P. Li, and H. Kumar, "Survival of the Q fever agent *Coxiella burnetii* in the phagolysosome," *Trends in microbiology*, vol. 2, pp. 476–480, 1994.
- [111] E. Pradel and J. J. Ewbank, "Genetic models in pathogenesis," *Annual review of genetics*, vol. 38, pp. 347–363, 2004.
- [112] I. Kukavica-Ibrulj and R. C. Levesque, "Animal models of chronic lung infection with *Pseudomonas aeruginosa*: useful tools for cystic fibrosis studies," *Laboratory animals*, vol. 42, pp. 389–412, 2008.
- [113] R. W. Tibal and O. L. Champion, "Models for Studying Bacterial Pathogenesis," in *Bacterial Pathogenesis: Molecular and Cellular Mechanisms*, C. Loch and M. Simonet, Eds. Caister Academic Press, 2012, p. 369.

- [114] H. Cash, D. Woods, B. McCullough, W. J. Johanson, and J. Bass, "A rat model of chronic respiratory infection with *Pseudomonas aeruginosa*," *The American review of respiratory disease*, vol. 119, pp. 453–459, 1979.
- [115] E. Papaioannou, P. Utari, and W. Quax, "Choosing an Appropriate Infection Model to Study Quorum Sensing Inhibition in *Pseudomonas* Infections," *International Journal of Molecular Sciences*, vol. 14, pp. 19309–19340, 2013.
- [116] D. A. D. Argenio, L. A. Gallagher, C. A. Berg, and C. Manoil, "Drosophila as a Model Host for *Pseudomonas aeruginosa* Infection," *Journal of bacteriology*, vol. 183, pp. 1466–1471, 2001.
- [117] S. Miyata, M. Casey, D. W. Frank, M. Frederick, and F. M. Ausubel, "Use of the *Galleria mellonella* Caterpillar as a Model Host To Study the Role of the Type III Secretion System in *Pseudomonas aeruginosa* Pathogenesis," *Infection and immunity*, vol. 71, pp. 2404–2413, 2003.
- [118] M. Tan and F. M. Ausubel, "*Caenorhabditis elegans*: a model genetic host to study *Pseudomonas aeruginosa* pathogenesis," *Current Opinion in Microbiology*, vol. 3, pp. 29–34, 2000.
- [119] L. G. Rahme, M.-W. Tan, L. Le, S. M. Wong, R. G. Tompkins, S. B. Calderwood, and F. M. Ausubel, "Use of model plant hosts to identify *Pseudomonas aeruginosa*," *PNAS*, vol. 94, pp. 13245 – 13250, 1997.
- [120] J. M. Plotnikova, L. G. Rahme, and F. M. Ausubel, "Pathogenesis of the human opportunistic pathogen *Pseudomonas aeruginosa* PA14 in Arabidopsis," *Plant physiology*, vol. 124, pp. 1766–1774, 2000.
- [121] M. Starkey and L. G. Rahme, "Modeling *Pseudomonas aeruginosa* pathogenesis in plant hosts," *Nature protocols*, vol. 4, pp. 117–124, 2009.
- [122] B. P. Hurley and B. a McCormick, "Translating tissue culture results into animal models: the case of *Salmonella typhimurium*," *Trends in Microbiology*, vol. 11, pp. 562–569, 2003.
- [123] I. Bucior, C. Tran, and J. Engel, "Assessing *Pseudomonas* Virulence Using Host Cells," *Methods in Molecular Biology*, vol. 1149, pp. 741–755, 2014.
- [124] E. Chi, T. Mehl, D. Nunn, and S. Lory, "Interaction of *Pseudomonas aeruginosa* with A549 Pneumocyte Cells," *Infection and immunity*, vol. 59, pp. 822–828, 1991.
- [125] R. S. Laughlin, M. W. Musch, C. J. Hollbrook, F. M. Rocha, E. B. Chang, and J. C. Alverdy, "The key role of *Pseudomonas aeruginosa* PA-I lectin on experimental gut-derived sepsis," *Annals of surgery*, vol. 232, pp. 133–142, 2000.
- [126] M. Ogata, V. K. Chaudhary, I. Pastan, and D. J. FitzGerald, "Processing of *Pseudomonas* exotoxin by a cellular protease results in the generation of a 37,000-Da toxin fragment that is translocated to the cytosol," *The Journal of biological chemistry*, vol. 265, pp. 20678–20685, 1990.
- [127] J. Morlon-Guyot, J. Méré, A. Bonhoure, and B. Beaumelle, "Processing of *Pseudomonas aeruginosa* exotoxin A is dispensable for cell intoxication," *Infection and immunity*, vol. 77, pp. 3090–3099, 2009.
- [128] M. Alaoui-El-Azher, J. Jia, W. Lian, and S. Jin, "ExoS of *Pseudomonas aeruginosa* induces apoptosis through a Fas receptor/caspase 8-independent pathway in HeLa cells," *Cellular microbiology*, vol. 8, pp. 326–338, 2006.

- [129] Y. Hirakata, B. B. Finlay, D. a Simpson, S. Kohno, S. Kamihira, and D. P. Speert, "Penetration of clinical isolates of *Pseudomonas aeruginosa* through MDCK epithelial cell monolayers," *The Journal of infectious diseases*, vol. 181, pp. 765–769, 2000.
- [130] A. J. Vallis, V. Finck-Barbançon, T. L. Yahr, and D. W. Frank, "Biological effects of *Pseudomonas aeruginosa* type III-secreted proteins on CHO cells," *Infection and immunity*, vol. 67, pp. 2040–2044, 1999.
- [131] P. Bourdeau, E. Somers, G. M. Richardson, and J. R. Hickman, "Short-term Toxicity Tests for Non-genotoxic Effects," 1990.
- [132] S. de Bentzmann and P. Plésiat, "The *Pseudomonas aeruginosa* opportunistic pathogen and human infections," *Environmental microbiology*, vol. 13, pp. 1655–65, 2011.
- [133] S. De Bentzmann, M. Polette, J. M. Zahm, J. Hinnrasky, C. Kileztky, O. Bajolet, J. M. Klossek, A. Filloux, A. Lazdunski, and E. Puchelle, "Airway Epithelial Wound Repair by Altering the Actin Cytoskeleton and Inducing Overactivation of Epithelial Matrix Metalloproteinase – 2," vol. 80, pp. 209–219, 2000.
- [134] G. S. El-housseiny, M. M. Aboulwafa, and N. A. Hassouna, "Adherence, Invasion and Cytotoxicity of Some Bacterial Pathogens," vol. 6, pp. 260–268, 2010.
- [135] J. C. Ramirez, S. M. J. Fleiszig, A. B. Sullivan, C. Tam, R. Borazjani, and D. J. Evans, "Traversal of multilayered corneal epithelia by cytotoxic *Pseudomonas aeruginosa* requires the phospholipase domain of exoU," *Investigative ophthalmology & visual science*, vol. 53, pp. 448–453, 2012.
- [136] J. Vranes, D. Tjesić-Drinković, I. Zulj, V. Kruzić, B. Turković, and S. Marić, "Adherence ability of *Pseudomonas aeruginosa* strains isolated from patients with cystic fibrosis to two different epithelial cell lines," *Collegium antropologicum*, vol. 28, pp. 675–680, 2004.
- [137] J. M. Buyck, P. M. Tulkens, and F. Van Bambeke, "Pharmacodynamic Evaluation of the Intracellular Activity of Antibiotics towards *Pseudomonas aeruginosa* PAO1 in a Model of THP-1 Human Monocytes," *Antimicrobial Agents and Chemotherapy*, vol. 57, pp. 2310–2318, 2013.
- [138] ATCC, "NCTC clone 929 [L cell, L-929, derivative of Strain L] (ATCC ® CCL-1™)," <https://www.lgcstandards-atcc.org> .
- [139] K. Theerakittayakorn and T. Bunprasert, "Differentiation Capacity of Mouse L929 Fibroblastic Cell Line Compare With Human Dermal Fibroblast," vol. 50, pp. 373–376, 2011.
- [140] N. Vanlangenakker, M. J. M. Bertrand, P. Bogaert, P. Vandenabeele, and T. Vanden Berghe, "TNF-induced necroptosis in L929 cells is tightly regulated by multiple TNFR1 complex I and II members," *Cell Death and Disease*, vol. 2, pp. 1–10, 2011.
- [141] D. Humphreys and M. Wilson, "Modes of L929 cell death induced by TNF-alpha and other cytotoxic agents," *Cytokine*, vol. 11, pp. 773–782, 1999.
- [142] C. Fady, A. Gardner, F. Jacoby, K. Briskin, Y. Tu, I. Schmid, and A. Lichtenstein, "Atypical Apoptotic Cell Death Induced in L929 Targets by Exposure to Tumor Necrosis Factor," *Journal of Interferon and Cytokine Research*, vol. 15, pp. 71–80, 1995.

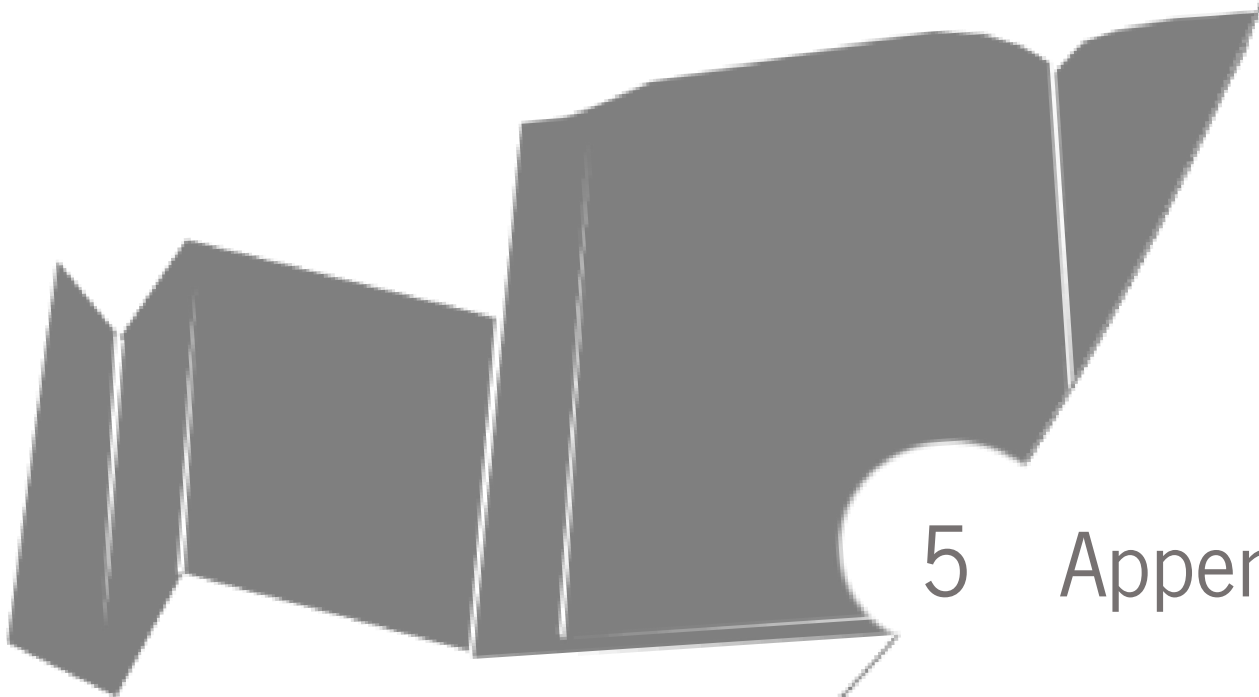
- [143] G. Bezanson, R. Fernandez, D. Haldane, S. Burbridge, and T. Marrie, "Virulence of patient and water isolates of *Legionella pneumophila* in guinea pigs and mouse L929 cells varies with bacterial genotype," *Canadian Journal of Microbiology*, vol. 40, pp. 426–431, 1994.
- [144] E. Biazar, Z. Roveimiab, G. Shahhosseini, M. Khataminezhad, and M. Zafari, "Biocompatibility evaluation of a new hydrogel dressing based on polyvinylpyrrolidone/polyethylene glycol," *Journal of Biomedicine and Biotechnology*, vol. 2012, pp. 1–5, 2011.
- [145] M. Lieber, B. Smith, A. Szakal, W. Nelson-rees, and G. Todaro, "A continuous tumor-cell line from human lung carcinoma with properties of type II alveolar," *International Journal of Cancer*, vol. 70, pp. 62–70, 1976.
- [146] D. J. Giard, S. A. Aaronson, G. J. Todaro, P. Arnstein, J. H. Kersey, and W. P. Parks, "In Vitro Cultivation of Human Tumors : Establishment of Cell Lines Derived From a Series of Solid Tumors," *Journal of the National Cancer Institute*, vol. 51, pp. 1417–1423, 1973.
- [147] H. Zanin, L. M. Hollanda, H. J. Ceragioli, M. S. Ferreira, D. Machado, M. Lancellotti, R. R. Catharino, V. Baranauskas, and a O. Lobo, "Carbon nanoparticles for gene transfection in eukaryotic cell lines," *Materials science & Engineering C*, vol. 39, pp. 359–370, 2014.
- [148] B. T. Smith, "Cell line A549: a model system for the study of alveolar type II cell function," *American journal of respiratory cell and molecular biology*, vol. 115, pp. 285–293, 1977.
- [149] N. a Hawdon, P. S. Aval, R. J. Barnes, S. K. Gravelle, J. Rosengren, S. Khan, O. Ciofu, H. K. Johansen, N. Høiby, and M. Ulanova, "Cellular responses of A549 alveolar epithelial cells to serially collected *Pseudomonas aeruginosa* from cystic fibrosis patients at different stages of pulmonary infection," *FEMS immunology and medical microbiology*, vol. 59, pp. 207–220, 2010.
- [150] F. H. Damron, J. Napper, M. A. Teter, and H. D. Yu, "Lipotoxin F of *Pseudomonas aeruginosa* is an AlgU-dependent and alginate-independent outer membrane protein involved in resistance to oxidative stress and adhesion to A549 human lung epithelia," *Microbiology (Reading, England)*, vol. 155, pp. 1028–1038, 2009.
- [151] X. Liu, K. Shao, and T. Sun, "SIRT1 regulates the human alveolar epithelial A549 cell apoptosis induced by *Pseudomonas aeruginosa* lipopolysaccharide," *Cellular physiology and biochemistry: international journal of experimental cellular physiology, biochemistry, and pharmacology*, vol. 31, pp. 92–101, 2013.
- [152] J. Wang, Y. Dong, T. Zhou, X. Liu, Y. Deng, C. Wang, J. Lee, and L.-H. Zhang, "*Pseudomonas aeruginosa* cytotoxicity is attenuated at high cell density and associated with the accumulation of phenylacetic acid," *PloS one*, vol. 8, p. e60187, 2013.
- [153] J. K. Ichikawa, a Norris, M. G. Bangera, G. K. Geiss, a B. van 't Wout, R. E. Bumgarner, and S. Lory, "Interaction of *Pseudomonas aeruginosa* with epithelial cells: identification of differentially regulated genes by expression microarray analysis of human cDNAs," *Proceedings of the National Academy of Sciences of the United States of America*, vol. 97, pp. 9659–9664, 2000.
- [154] M. H. Hutz, a M. Michelson, S. E. Antonarakis, S. H. Orkin, and H. H. Kazazian, "Restriction site polymorphism in the phosphoglycerate kinase gene on the X chromosome," *Human genetics*, vol. 66, pp. 217–219, 1984.

- [155] D. J. Giard, S. a Aaronson, G. J. Todaro, P. Arnstein, J. H. Kersey, H. Dosik, and W. P. Parks, "In vitro cultivation of human tumors: establishment of cell lines derived from a series of solid tumors," *Journal of the National Cancer Institute*, vol. 51, 1417–1423, 1973.
- [156] T. Mosmann, "Rapid colorimetric assay for cellular growth and survival: application to proliferation and cytotoxicity assays," *Journal of immunological methods*, vol. 65, pp. 55–63, 1983.
- [157] M. V Berridge, P. M. Herst, and A. S. Tan, "Tetrazolium dyes as tools in cell biology: new insights into their cellular reduction," *Biotechnology annual review*, vol. 11, pp. 127–152, 2005.
- [158] Jacques Monod, "The Growth of Bacterial Cultures," *Annual Review of Microbiology*, vol. 3, pp. 371–394, 1949.
- [159] J. Goldová, A. Ulrych, K. Hercik, and P. Branny, "A eukaryotic-type signalling system of *Pseudomonas aeruginosa* contributes to oxidative stress resistance, intracellular survival and virulence," *BMC genomics*, vol. 12, p. 437, 2011.
- [160] D. I. Andersson and B. R. Levin, "The biological cost of antibiotic resistance," *Current Opinion in Microbiology*, vol. 2, pp. 489–493, 1999.
- [161] D. I. Andersson, "The biological cost of mutational antibiotic resistance: any practical conclusions?," *Current opinion in microbiology*, vol. 9, pp. 461–465, 2006.
- [162] P. Sánchez, J. F. Linares, B. Ruiz-Díez, E. Campanario, A. Navas, F. Baquero, and J. L. Martínez, "Fitness of in vitro selected *Pseudomonas aeruginosa* nalB and nfxB multidrug resistant mutants," *Journal of Antimicrobial Chemotherapy*, vol. 50, pp. 657–664, 2002.
- [163] H. Zhu, S. J. Thuruthyil, and M. D. P. Willcox, "Determination of quorum-sensing signal molecules and virulence factors of *Pseudomonas aeruginosa* isolates from contact lens-induced microbial keratitis," *Journal of medical microbiology*, vol. 51, pp. 1063–1070, 2002.
- [164] M. Sandkvist, "Type II Secretion and Pathogenesis," *Infection and immunity*, vol. 69, pp. 3523–3535, 2001.
- [165] K. Bernardo, N. Pakulat, S. Fleer, A. Schnaith, O. Utermöhlen, O. Krut, M. Krönke, S. Mu, and M. Kro, "Subinhibitory Concentrations of Linezolid Reduce *Staphylococcus aureus* Virulence Factor Expression," *Antimicrobial agents and chemotherapy*, vol. 48, pp. 546–555, 2004.
- [166] A. Sturm, M. Heinemann, M. Arnoldini, A. Benecke, M. Ackermann, M. Benz, J. Dormann, and W.-D. Hardt, "The cost of virulence: retarded growth of *Salmonella Typhimurium* cells expressing type III secretion system 1," *PLoS pathogens*, vol. 7, p. e1002143, 2011.
- [167] J. Kim, K. Ahn, S. Min, J. Jia, U. Ha, D. Wu, and S. Jin, "Factors triggering type III secretion in *Pseudomonas aeruginosa*," *Microbiology*, vol. 151, pp. 3575–3587, 2005.
- [168] U. Ha and S. Jin, "Growth Phase-Dependent Invasion of *Pseudomonas aeruginosa* and Its Survival within HeLa Cells," *Infection and immunity*, vol. 69, pp. 4398–4406, 2001.

- [169] G. Da Violante, N. Zerrouk, I. Richard, G. Provot, J. C. Chaumeil, and P. Arnaud, "Evaluation of the cytotoxicity effect of dimethyl sulfoxide (DMSO) on Caco2/TC7 colon tumor cell cultures," *Biological & pharmaceutical bulletin*, vol. 25, pp. 1600–1603, 2002.
- [170] D. Kultz and M. Burg, "Evolution of osmotic stress signaling via MAP kinase cascades," *Journal of Experimental Biology*, vol. 201, pp. 3015–3021, 1998.
- [171] E. Kessler, M. Safrin, J. K. Gustin, and D. E. Ohman, "Elastase and the LasA protease of *Pseudomonas aeruginosa* are secreted with their propeptides," *The Journal of biological chemistry*, vol. 273, pp. 30225–30231, 1998.
- [172] C. L. Cannon, M. P. Kowalski, K. S. Stopak, and G. B. Pier, "*Pseudomonas aeruginosa*-induced apoptosis is defective in respiratory epithelial cells expressing mutant cystic fibrosis transmembrane conductance regulator," *American journal of respiratory cell and molecular biology*, vol. 29, pp. 188–197, 2003.
- [173] S. Rajan, G. Cacalano, R. Bryan, A. J. Ratner, C. U. Sontich, A. Van Heerckeren, P. Davis, and A. Prince, "*Pseudomonas aeruginosa* Induction of Apoptosis in Respiratory Epithelial Cells - Analysis of the Effects of Cystic Fibrosis Transmembrane Conductance Regulator Dysfunction and Bacterial Virulence Factors," *American journal of respiratory cell and molecular biology*, vol. 23, pp. 304–312, 2000.
- [174] A. R. Hauser and J. N. Engel, "*Pseudomonas aeruginosa* Induces Type-III-Secretion-Mediated Apoptosis of Macrophages and Epithelial Cells," *Infection and immunity*, vol. 67, pp. 5530–5537, 1999.
- [175] L. R. Usher, R. a. Lawson, I. Geary, C. J. Taylor, C. D. Bingle, G. W. Taylor, and M. K. B. Whyte, "Induction of Neutrophil Apoptosis by the *Pseudomonas aeruginosa* Exotoxin Pyocyanin: A Potential Mechanism of Persistent Infection," *The Journal of Immunology*, vol. 168, pp. 1861–1868, 2002.
- [176] A. Broquet and K. Asehnoune, "Apoptosis induced by *Pseudomonas aeruginosa*: a lonely killer?," *Microbial biotechnology*, vol. 8, pp. 49–51, 2014.
- [177] J. Jia, Y. Wang, L. Zhou, and S. Jin, "Expression of *Pseudomonas aeruginosa* toxin ExoS effectively induces apoptosis in host cells," *Infection and immunity*, vol. 74, pp. 6557–6570, 2006.
- [178] M. R. Kaufman, J. Jia, L. Zeng, U. Ha, M. Chow, and S. Jin, "*Pseudomonas aeruginosa* mediated apoptosis requires the ADP-ribosylating activity of exoS," *Microbiology*, vol. 146, pp. 2531–2541, 2000.
- [179] M. Théry and M. Bornens, "Get round and stiff for mitosis," *HFSP journal*, vol. 2, pp. 65–71, 2008.
- [180] D. A. A. Al-Samh and S. Al-Nazhan, "In vitro study of the cytotoxicity of the miswak ethanolic extract," *The Saudi Dental Journal*, vol. 9, pp. 125–132, 1997.
- [181] T. L. Riss, R. A. Moravec, A. L. Niles, H. A. Benink, T. J. Worzella, and L. Minor, "Cell Viability Assays," in *Assay Guidance Manual*, Bethesda, 2004.
- [182] K. M. George, L. P. Barker, D. M. Welty, P. L. C. Small, G. E. T. Al, and I. N. I. Mmun, "Partial Purification and Characterization of Biological Effects of a Lipid Toxin Produced by *Mycobacterium ulcerans*," *Infection and immunity*, vol. 66, pp. 587–593, 1998.
- [183] R. Chen, X. Fan, Y. Huang, N. Li, and C. Chen, "In vitro cytotoxicity of *Helicobacter pylori* on hepatocarcinoma HepG2 cells," *Chinese Journal of Cancer*, vol. 23, pp. 44–49, 2004.

- [184] I. A. Bnyan and H. Ahmed, "Effect of some factors on extracellular hemolysin filtrate from bacterial *Pseudomonas aeruginosa* isolated from burn infection in Hilla city," *Research in Pharmacy*, vol. 3, pp. 26–32, 2013.
- [185] H. Schmidt and M. Hensel, "Pathogenicity Islands in Bacterial Pathogenesis," *Clinical Microbiology Reviews*, vol. 17, pp. 14–56, 2004.
- [186] S. Zanetti, P. Cappuccinelli, and G. Fadda, "The cytopathic effect induced by strains of *Pseudomonas aeruginosa* producing hemolysin, leukocidin and proteases in Hep-2 cells," *Bollettino dell'Istituto Sieroterapico Milanese*, vol. 65, pp. 237–241, 1986.
- [187] Vi. Rambabu, S. Suba, P. Manikandan, and S. Vijayakumar, "Cytotoxic and apoptotic nature of migrastatin, a secondary metabolite from streptomyces evaluated on HepG2 cell line," *International Journal of Pharmacy and Pharmaceutical Sciences*, vol. 6, pp. 333–338, 2014.
- [188] O. T. Fackler and R. Grosse, "Cell motility through plasma membrane blebbing," *Journal of Cell Biology*, vol. 181, pp. 879–884, 2008.
- [189] K. Vermeulen, D. R. Van Bockstaele, and Z. N. Berneman, "Apoptosis: Mechanisms and relevance in cancer," *Annals of Hematology*, vol. 84, pp. 627–639, 2005.
- [190] J. D. Lane, V. J. Allan, and P. G. Woodman, "Active relocation of chromatin and endoplasmic reticulum into blebs in late apoptotic cells," *Journal of cell science*, vol. 118, pp. 4059–4071, 2005.
- [191] J. C. Mills, N. L. Stone, and R. N. Pittman, "Extranuclear apoptosis: The role of the cytoplasm in the execution phase," *Journal of Cell Biology*, vol. 146, pp. 703–707, 1999.
- [192] C. Curutiu, M. C. Chifiriuc, F. Iordache, C. Bleotu, V. Lazar, C. A. Mogoanta, C. R. Popescu, R. Grigore, and Ș. V. G. Bertesteanu, "Fluorescence analysis of apoptosis induced by *Pseudomonas aeruginosa* in endothelial cells," *Romanian journal of Morphology and Embryology*, vol. 55, pp. 313–317, 2014.
- [193] E. Wulf, A. Deboben, F. a Bautz, H. Faulstich, and T. Wieland, "Fluorescent phalloxin, a tool for the visualization of cellular actin," *Proceedings of the National Academy of Sciences*, vol. 76, pp. 4498–4502, 1979.
- [194] Life Technologies Data Sheet, "Phalloidin Alexa Fluor® 568." [Online]. Available: <https://www.lifetechnologies.com/order/catalog/product/A12380>.
- [195] Life Technologies Data Sheet, "Hoechst 34580," p. 34580.
- [196] S. Nagata, "Apoptotic DNA fragmentation," *Experimental cell research*, vol. 256, pp. 12 – 18, 2000.
- [197] K. M. George, L. Pascopella, D. M. Welty, and L. C. Small, "A *Mycobacterium ulcerans* Toxin, Mycolactone, causes Apoptosis in Guinea Pig Ulcers and Tissue Culture Cells," *Infection and immunity*, vol. 68, pp. 877–883, 2000.
- [198] M. Sasaki, K. Sugimoto, K. Tamayose, M. Ando, Y. Tanaka, and K. Oshimi, "Spindle checkpoint protein Bub1 corrects mitotic aberrancy induced by human T-cell leukemia virus type I Tax," *Oncogene*, vol. 25, pp. 3621–3627, 2006.

- [199] Y. Wang, H. Yang, H. Liu, J. Huang, and X. Song, "Effect of staurosporine on the mobility and invasiveness of lung adenocarcinoma A549 cells: an in vitro study," *BMC cancer*, vol. 9, p. 174, 2009.
- [200] J. Toska, Y. Sun, D. A. Carbonell, A. N. S. Foster, M. R. Jacobs, E. Pearlman, and A. Rietsch, "Diversity of virulence phenotypes among type III secretion negative *Pseudomonas aeruginosa* clinical isolates," *PLoS ONE*, vol. 9, pp. 1–8, 2014.
- [201] E. M. Messier, R. J. Mason, and B. Kosmider, "Efficient and rapid isolation and purification of mouse alveolar type II epithelial cells," *Experimental Lung Research*, vol. 38, pp. 363–373, 2012.
- [202] N. a Hawdon, P. S. Aval, R. J. Barnes, S. K. Gravelle, J. Rosengren, S. Khan, O. Ciofu, H. K. Johansen, N. Høiby, and M. Ulanova, "Cellular responses of A549 alveolar epithelial cells to serially collected *Pseudomonas aeruginosa* from cystic fibrosis patients at different stages of pulmonary infection," *FEMS immunology and medical microbiology*, vol. 59, pp. 207–220, 2010.
- [203] S. Worgall, K. Martushova, A. Busch, L. Lande, and R. G. Crystal, "Apoptosis induced by *Pseudomonas aeruginosa* in antigen presenting cells is diminished by genetic modification with CD40 ligand," *Pediatric Research*, vol. 52, pp. 636–644, 2002.
- [204] C. S. Mesquita, P. Soares-castro, and P. M. Santos, "*Pseudomonas aeruginosa* : phenotypic flexibility and antimicrobial resistance," *Microbial pathogens and strategies for combating them: science, technology and education*, pp. 650–665, 2013.
- [205] H. Wang and J. A. Joseph, "Quantifying cellular oxidative stress by dichlorofluorescein assay using microplate reader," *Free Radical Biology and Medicine*, vol. 27, pp. 612–616, 1999.
- [206] P. Li, J. Shi, Q. He, Q. Hu, Y. Y. Wang, L. J. Zhang, W. T. Chan, and W.-X. Chen, "*Streptococcus pneumoniae* Induces Autophagy through the Inhibition of the PI3K-I/Akt/mTOR Pathway and ROS Hypergeneration in A549 Cells," *Plos One*, vol. 10, pp. 1–15, 2015.
- [207] Y. Q. O'Malley, M. Y. Abdalla, M. L. McCormick, K. J. Reszka, G. M. Denning, and B. E. Britigan, "Subcellular localization of *Pseudomonas* pyocyanin cytotoxicity in human lung epithelial cells," *American journal of physiology. Lung cellular and molecular physiology*, vol. 284, pp. 420–430, 2003.
- [208] Y. Q. O'Malley, K. J. Reszka, and B. E. Britigan, "Direct oxidation of 2',7'-dichlorodihydrofluorescein by pyocyanin and other redox-active compounds independent of reactive oxygen species production," *Free Radical Biology and Medicine*, vol. 36, pp. 90–100, 2004.
- [209] L. Yin, R. Stearns, and B. González-Flecha, "Lysosomal and mitochondrial pathways in H₂O₂-induced apoptosis of alveolar type II cells," *Journal of Cellular Biochemistry*, vol. 94, pp. 433–445, 2005.
- [210] H. Ran, D. J. Hassett, and G. W. Lau, "Human targets of *Pseudomonas aeruginosa* pyocyanin," *Proceedings of the National Academy of Sciences of the United States of America*, vol. 100, pp. 14315–14320, 2003.
- [211] L. S. Gloyne, G. D. Grant, A. V. Perkins, K. L. Powell, C. M. McDermott, P. V. Johnson, G. J. Anderson, M. Kiefel, and S. Anoopkumar-Dukie, "Pyocyanin-induced toxicity in A549 respiratory cells is causally linked to oxidative stress," *Toxicology in vitro*, vol. 25, pp. 1353–1358, 2011.



5 Appendix

5.1. Appendix 1 – pH measurements of the supernatant concentrations of the *Pseudomonas aeruginosa* strains

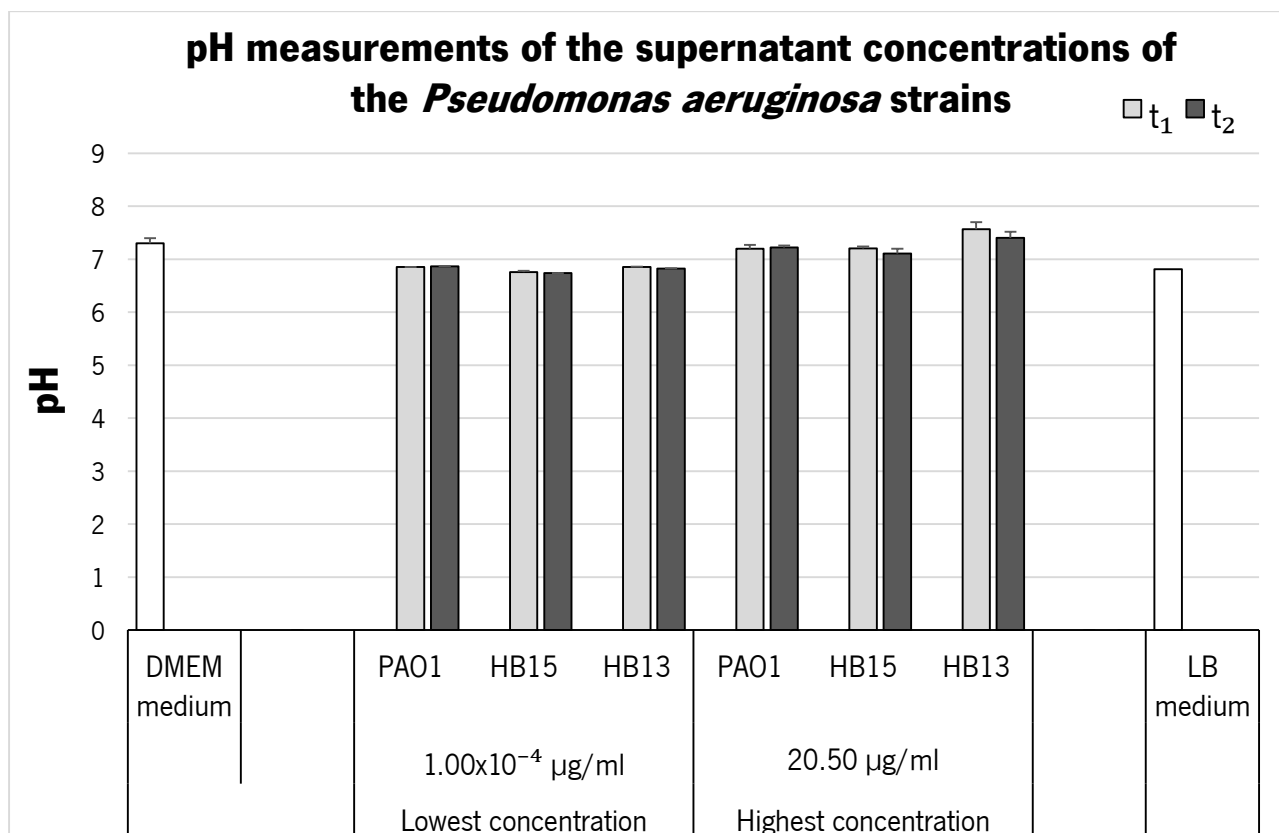


Figure A 1 - pH measurements of the supernatant concentrations of the *Pseudomonas aeruginosa* strains. The graphic exhibits pH measurements of the highest and lowest concentration of the supernatants of the *P. aeruginosa* strains, PAO1, HB15 and HB13, from the two time points of bacterial growth ($t_1 = 24h$, $t_2 = 48h$) from the serial dilutions made. Grey bars represent the supernatant *P. aeruginosa* strains dilution concentrations, light grey for the t_1 and hard grey for the t_2 . The pH measurements for the DMEM medium and LB medium are also shown represent by the white bars. The resulting data was statistically analysed by a One-way ANOVA with Tukey test where P value was set for: $P < 0.05$. Significant values comparing to the negative control were represented in the graphic as, * for $P < 0.05$, ** for $P < 0.01$ and *** for $P < 0.001$.

5.2. Annex 2 – Cytotoxicity of *Pseudomonas aeruginosa* strains in L929 cell availed in all concentrations tested

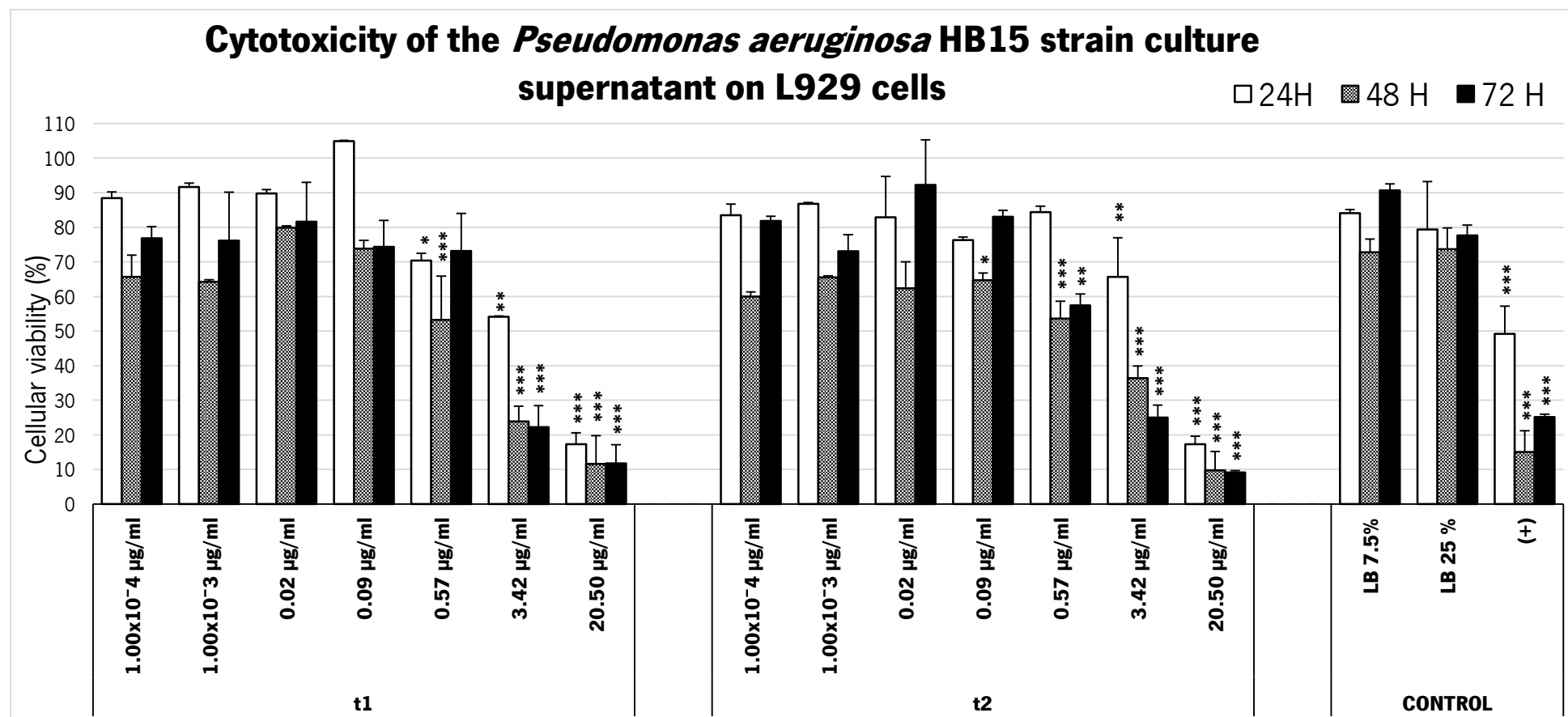


Figure A 2 - Cytotoxicity of the *Pseudomonas aeruginosa* HB15 strain culture supernatant on L929 cells. The graphic displays the results of the MTT assay performed on L929 cells submitted to a range of total protein concentrations of the culture supernatants of the *Pseudomonas aeruginosa* HB15 strain, grown in two different time setups, represented in the graphic as t₁ and t₂, respectively 24 hours of bacterial culture growth and 48 hours of bacterial culture growth, in cell viability percentage represented by bars with the respective standard deviation represented by vertical lines for a number of replicas n=2. The bar legend represents the end times of incubation (24h, 48h and 72h) with the supernatants. The controls are presented in the graphic represented as “CONTROL”. The negative control has the constant value of 100% of viability for each end times of incubation and not shown in the graphic. The positive control is represented as “+” on the graphic. The controls of the bacterial culture media (LB) are represented on the graphic as “LB 25%” and “LB 7.5%”. The resulting data was statistically analysed by a One-way ANOVA with Tukey test where P value was set for: P < 0.05. Significant values comparing to the negative control were represented in the graphic as, * for P < 0.05, ** for P < 0.01 and *** for P < 0.001.

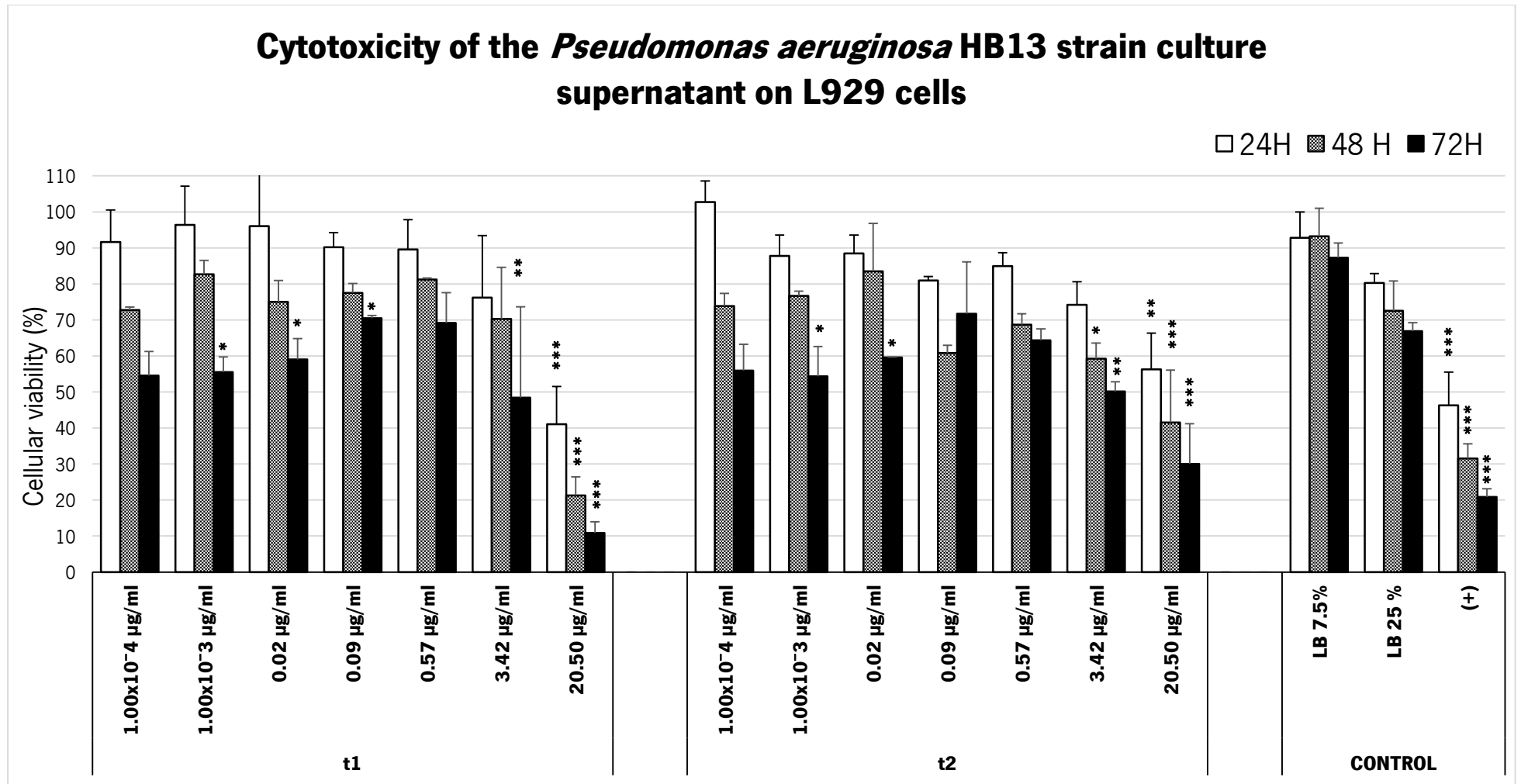


Figure A 3 - Cytotoxicity of the *Pseudomonas aeruginosa* HB13 strain culture supernatant on L929 cells. The graphic displays the results of the MTT assay performed on L929 cells submitted to a range of total protein concentrations of the culture supernatants of the *Pseudomonas aeruginosa* HB13 strain, grown in two different time setups, represented in the graphic as t₁ and t₂, respectively 24 hours of bacterial culture growth and 48 hours of bacterial culture growth, in cell viability percentage represented by bars with the respective standard deviation represented by vertical lines for a number of replicas n=2. The bar legend represents the end times of incubation (24h, 48h and 72h) with the supernatants. The controls are presented in the graphic represented as "CONTROL". The negative control has the constant value of 100% of viability for each end times of incubation and not shown in the graphic. The positive control is represented as "+" on the graphic. The controls of the bacterial culture media (LB) are represented on the graphic as "LB 25%" and "LB 7.5%". The resulting data was statistically analysed by a One-way ANOVA with Tukey test where P value was set for: P < 0.05. Significant values comparing to the negative control were represented in the graphic as, * for P < 0.05, ** for P < 0.01 and *** for P < 0.001.

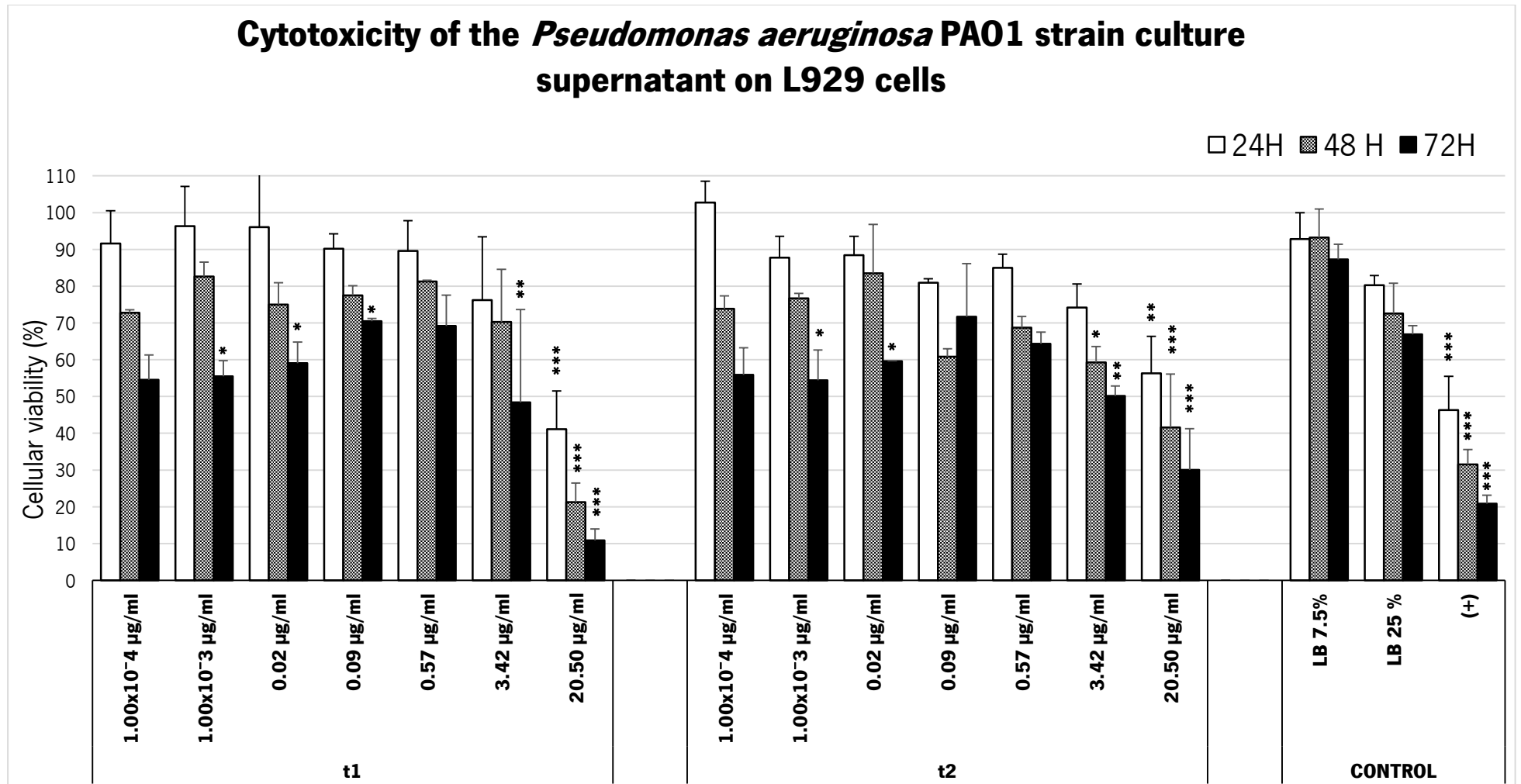


Figure A 4 - Cytotoxicity of the *Pseudomonas aeruginosa* PA01 strain culture supernatant on L929 cells. The graphic displays the results of the MTT assay performed on L929 cells submitted to a range of total protein concentrations of the culture supernatants of the *Pseudomonas aeruginosa* PA01 strain, grown in two different time setups, represented in the graphic as t₁ and t₂, respectively 24 hours of bacterial culture growth and 48 hours of bacterial culture growth, in cell viability percentage represented by bars with the respective standard deviation represented by vertical lines for a number of replicas n=2. The bar legend represents the end times of incubation (24h, 48h and 72h) with the supernatants. The controls are presented in the graphic represented as "CONTROL". The negative control has the constant value of 100% of viability for each end times of incubation and not shown in the graphic. The positive control is represented as "+" on the graphic. The controls of the bacterial culture media (LB) are represented on the graphic as "LB 25%" and "LB 7.5%". The resulting data was statistically analysed by a One-way ANOVA with Tukey test where P value was set for: P < 0.05. Significant values comparing to the negative control were represented in the graphic as, * for P < 0.05, ** for P < 0.01 and *** for P < 0.001.

5.3. Annex 3 – Cytotoxicity of *Pseudomonas aeruginosa* strains in A549 cell availed in all concentrations tested

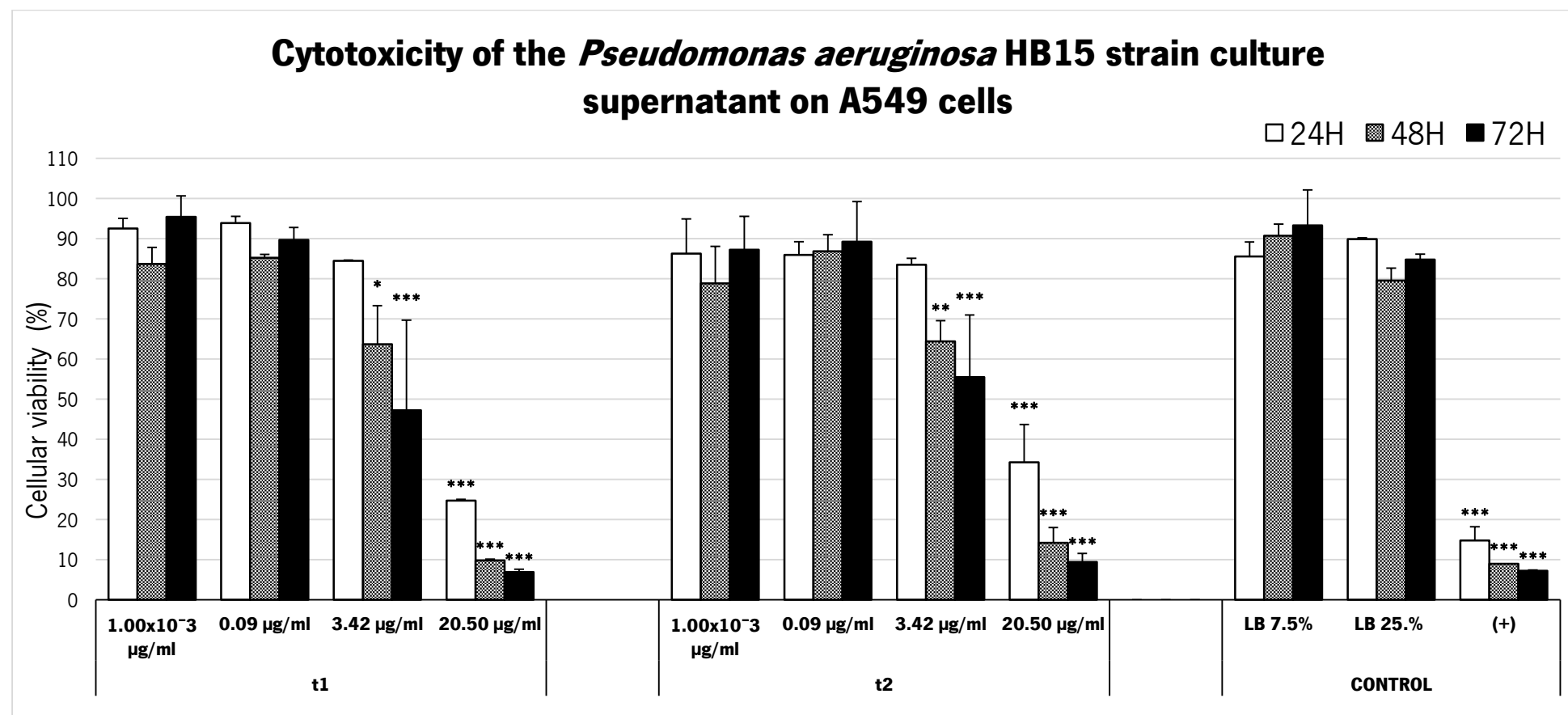


Figure A 5 - Cytotoxicity of the *Pseudomonas aeruginosa* HB15 strain culture supernatant on A549 cells. The graphic displays the results of the MTT assay performed on A549 cells submitted to a range of total protein concentrations of the culture supernatants of the *Pseudomonas aeruginosa* HB15 strain, grown in two different time setups, represented in the graphic as t₁ and t₂, respectively 24 hours of bacterial culture growth and 48 hours of bacterial culture growth, in cell viability percentage represented by bars with the respective standard deviation represented by vertical lines for a number of replicas n=2. The bar legend represents the end times of incubation (24h, 48h and 72h) with the supernatants. The controls are presented in the graphic represented as "CONTROL". The negative control has the constant value of 100% of viability for each end times of incubation and not shown in the graphic. The positive control is represented as "+" on the graphic. The controls of the bacterial culture media (LB) are represented on the graphic as "LB 25%" and "LB 7.5%". The resulting data was statistically analysed by a One-way ANOVA with Tukey test where P value was set for: P < 0.05. Significant values comparing to the negative control were represented in the graphic as, * for P < 0.05, ** for P < 0.01 and *** for P < 0.001.

Cytotoxicity of the *Pseudomonas aeruginosa* HB13 strain culture supernatant on A549 cells

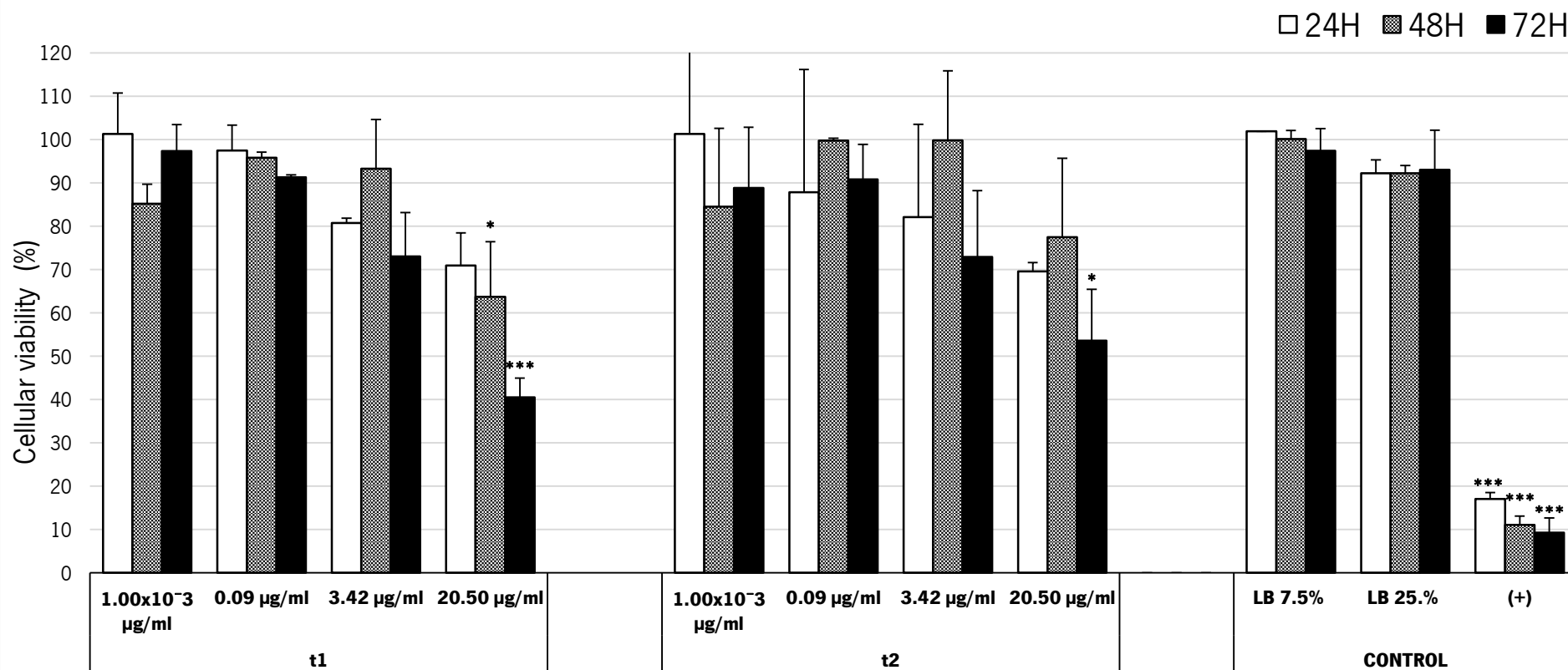


Figure A 6 - Cytotoxicity of the *Pseudomonas aeruginosa* HB13 strain culture supernatant on A549 cells. The graphic displays the results of the MTT assay performed on A549 cells submitted to a range of total protein concentrations of the culture supernatants of the *Pseudomonas aeruginosa* HB13 strain, grown in two different time setups, represented in the graphic as t₁ and t₂, respectively 24 hours of bacterial culture growth and 48 hours of bacterial culture growth, in cell viability percentage represented by bars with the respective standard deviation represented by vertical lines for a number of replicas n=2. The bar legend represents the end times of incubation (24h, 48h and 72h) with the supernatants. The controls are presented in the graphic represented as “CONTROL”. The negative control has the constant value of 100% of viability for each end times of incubation and not shown in the graphic. The positive control is represented as “+” on the graphic. The controls of the bacterial culture media (LB) are represented on the graphic as “LB 25%” and “LB 7.5%”. The resulting data was statistically analysed by a One-way ANOVA with Tukey test where P value was set for: P <0.05. Significant values comparing to the negative control were represented in the graphic as, * for P <0.05, ** for P <0.01 and *** for P <0.001.

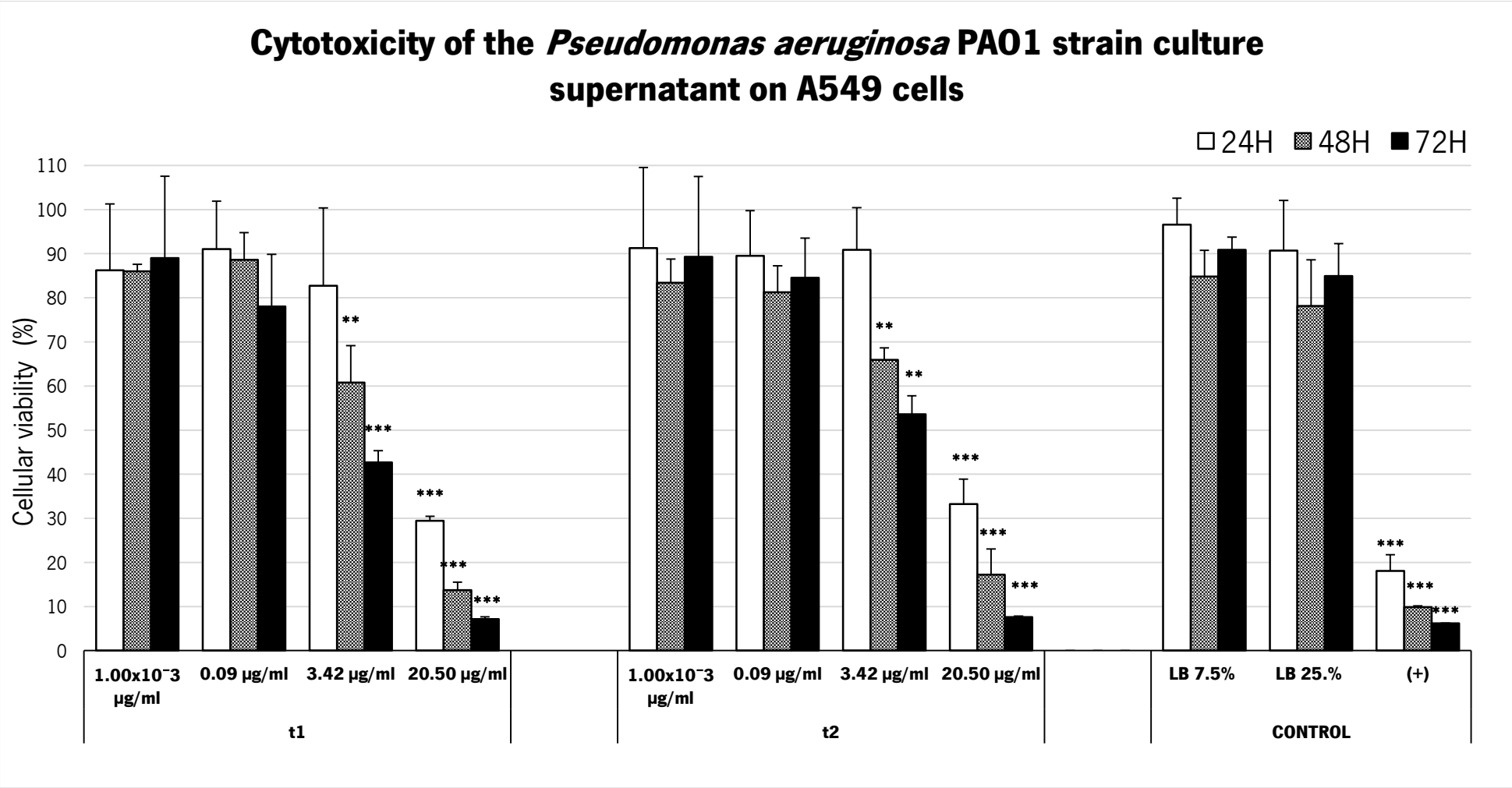


Figure A 7 - Cytotoxicity of the *Pseudomonas aeruginosa* PAO1 strain culture supernatant on A549 cells. The graphic displays the results of the MTT assay performed on A549 cells submitted to a range of total protein concentrations of the culture supernatants of the *Pseudomonas aeruginosa* PAO1 strain, grown in two different time setups, represented in the graphic as t₁ and t₂, respectively 24 hours of bacterial culture growth and 48 hours of bacterial culture growth, in cell viability percentage represented by bars with the respective standard deviation represented by vertical lines for a number of replicas n=2. The bar legend represents the end times of incubation (24h, 48h and 72h) with the supernatants. The controls are presented in the graphic represented as “CONTROL”. The negative control has the constant value of 100% of viability for each end times of incubation and not shown in the graphic. The positive control is represented as “+” on the graphic. The controls of the bacterial culture media (LB) are represented on the graphic as “LB 25%” and “LB 7.5%”. The resulting data was statistically analysed by a One-way ANOVA with Tukey test where P value was set for: P <0.05. Significant values comparing to the negative control were represented in the graphic as, * for P <0.05, ** for P <0.01 and *** for P <0.001.

5.4. Annex 4 - L929 and A549 cell line culture growth through time

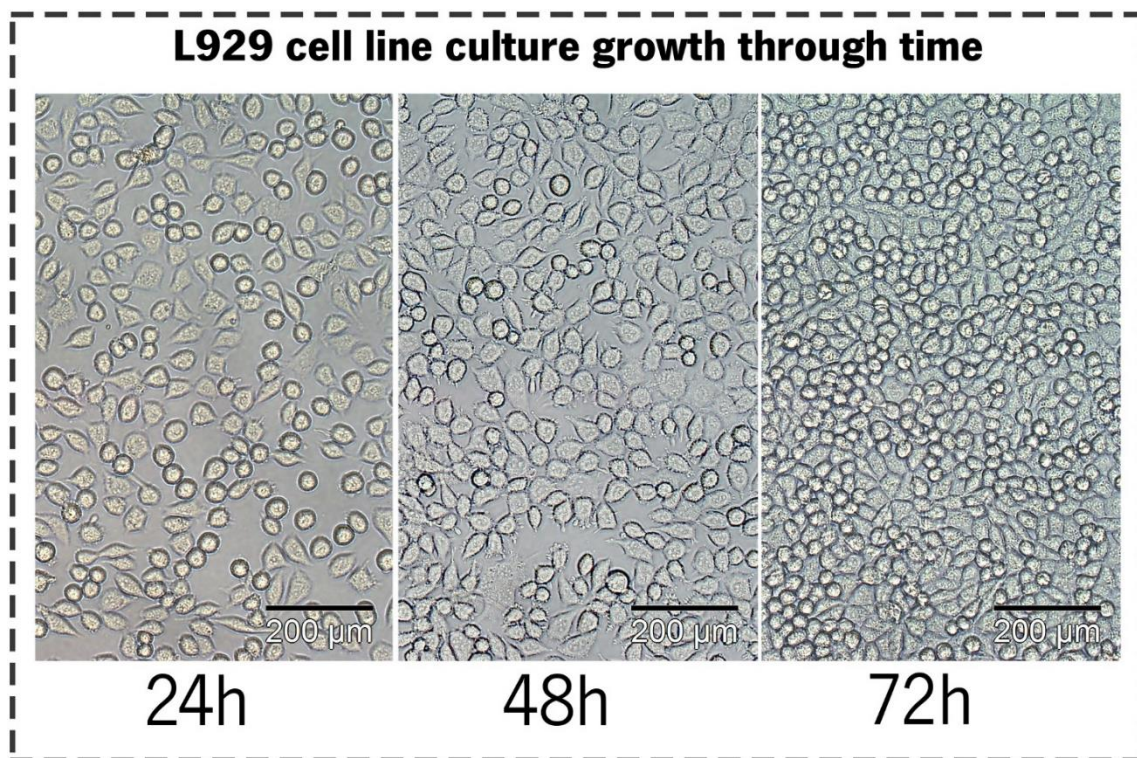


Figure A 8 - L929 cell line culture growth through time. Contrast phase microscope shot of L929 cell culture grown in 96 well plate at 24h, 48h and 72h. The image show abundant distinguishable fibroblasts with spindle and stellate shape and some round shape fibroblast. The scale bar is set for 200 μm .

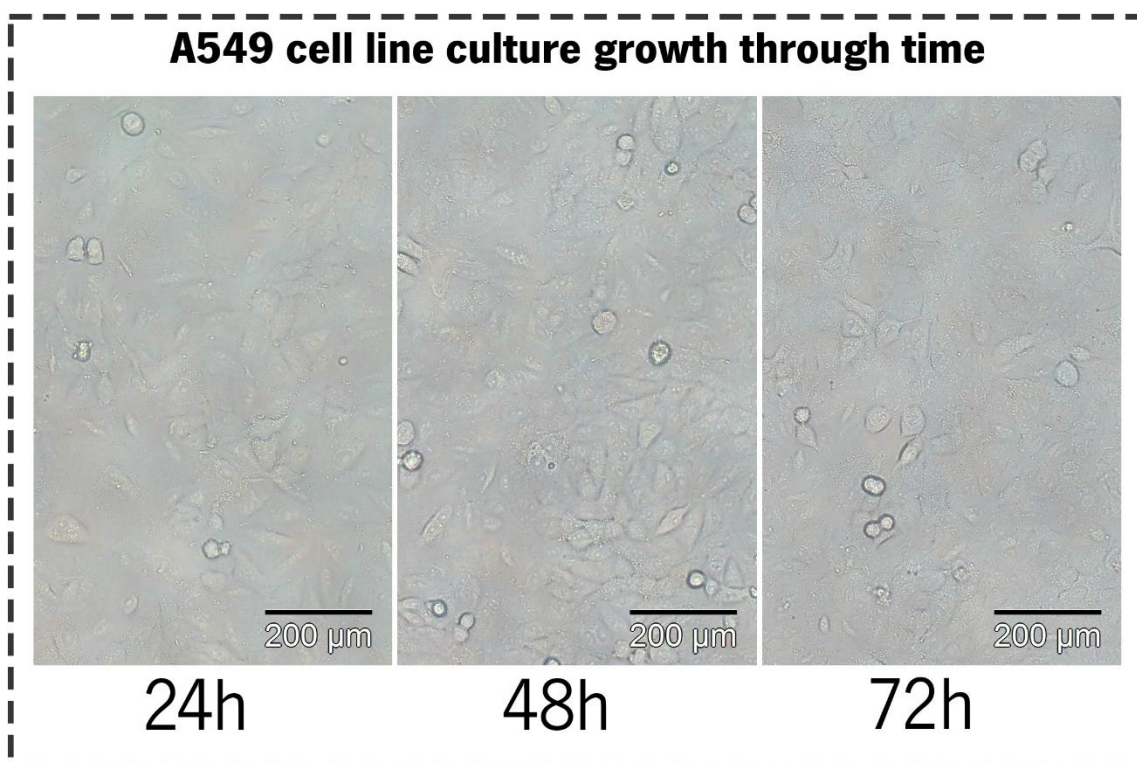


Figure A 9 – A549 cell line culture growth through time. Contrast phase microscope shot of A549 cell culture grown in 96 well plate at 24h, 48h and 72h. The image show abundant distinguishable fibroblasts with spindle and stellate shape and some round shape fibroblast. The scale bar is set for 200 μm .

5.5. Annex 5 - Oxidative stress induced by *Pseudomonas aeruginosa* strains culture supernatants

The DCF assay outcome, shows all the fluorescence intensities of the cells incubated 1 hour with *P. aeruginosa* strains supernatants superior to the negative control, indicating that *P. aeruginosa* strains supernatants are inducing oxidative stress in the cells. The H₂O₂ control exhibit an estimated 3 times fluorescence intensity than the fluorescence intensity in the negative control, establishing that the cells underwent oxidative stress in presence of a strong ROS. Fluorescence intensity caused by the *P. aeruginosa* strains supernatants didn't show considerable variances between each strain.

The fluorescence intensities of the cells incubated 4 hour with *P. aeruginosa* strains supernatants superior revealed no considerable differences with the negative control, plus, the H₂O₂ control exhibits also no considerable differences between the *P. aeruginosa* strains or the negative control fluorescence intensities.

Comparing the two incubation times (1h and 4h), it is observable a drop in fluorescence intensity after 4 hours of incubation in the *P. aeruginosa* strains group. In the negative control the fluorescence intensity raised after 4 hours of incubation, and in the H₂O₂ control decreased considerably (Figure A 10).

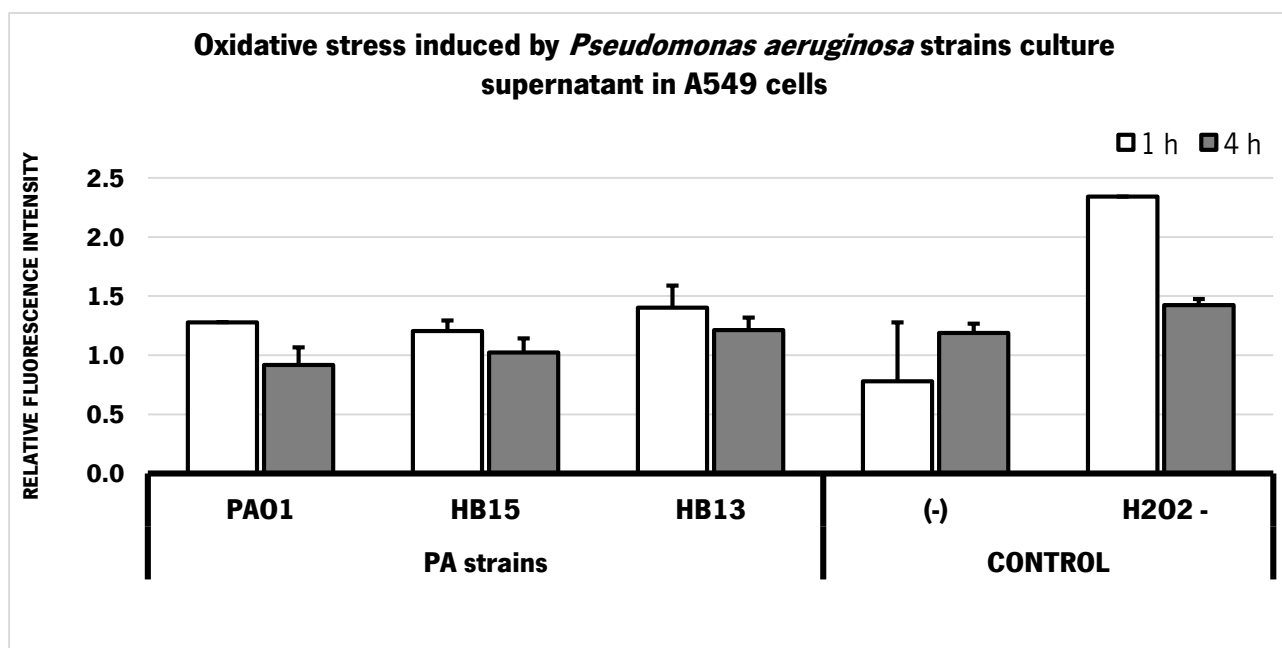


Figure A 10 – Oxidative stress induced by *Pseudomonas aeruginosa* strains culture supernatant in A549 cells. The graphic displays the results of the DCF assay performed on A549 cells submitted 3.42 µg/ml total protein of the culture supernatants of the *Pseudomonas aeruginosa* strains (PA01, HB15 and HB13) in fluorescence intensity (absolute units) obtained from fluorimetry using an emission wavelength of 538nm and excitation wavelength of 485nm, with the respective standard deviation represented by vertical lines for a number of replicas n=2. The bar legend represents the end times of incubation (white bar = 1h and grey bar = 4h) with the supernatants. The controls are presented in the graphic represented as “CONTROL”. The negative control represents the fluorescence intensity from the oxidative stress of the cells growing with only DMEM medium. The H₂O₂-control represent represents the fluorescence intensity from the oxidative stress of the cells growing with 2mM H₂O₂. The resulting data was statistically analysed by a One-way ANOVA with Tukey test where P value was set for: P <0.05, for n=2 independent experiments

The analysis of the DCF assay results suggests that oxidative stress was occurring in the cells incubated with the *P. aeruginosa* strains supernatants, though it was expected that the oxidative stress increased through time, not verified in the fluorescence intensity results after 4 hours of incubation. These incongruous results suggest that conceivably after 4 hours of incubation the cells are already in a death phase, which decreases the fluorescence signal given that there are fewer cells to do the intercellular hydroxylation and oxidization of the DCFH-DA species which then becomes fluorescent. In further literature, it is shown A549 cells incubated with pathogenic bacteria through shorter time lengths, where fluorescence intensity increases in a time-dependent manner until approximately 2 hours of incubation, after that the fluorescence intensity starts to drop [206]. Other literature refers short incubation times, around 1 hour of incubation, in A549 cells with virulent agents [207], [208]. Furthermore, the H₂O₂ control encompassing the testing groups, appears in literature with shorter incubation times also, lesser than 1 hour [209].

Analysing the DCF assay experiment design and the previous literature, it should be chosen shorter incubation times to evaluate the oxidative stress occurring in the A549 cells in order to achieve more significant results. Furthermore, time and cost-effective limitation restrained the use of the two cellular models (L929 and A549), thus the A549 cells were selected because it is a more recurrent model used to analyse oxidative stress on these conditions, there is also profuse literature concerning oxidative stress studies in A549 cells in bacteria infectious situation and it is a model more suitable to achieve relevant information regarding respiratory tract infection panorama caused by *Pseudomonas aeruginosa* [210], [211]. Also time and cost-effective limitation restrained the use of a more extended time/concentration range, which could provide more interesting results regarding the oxidative stress depending of concentration and incubation time. Nevertheless, this oxidative stress study findings indicates that oxidative stress is enhanced on the A549 cells in the early times prior incubation with the *P. aeruginosa* strains supernatants.

